

Analysis of matrilin function in knockout mice and knockdown zebrafish

Inaugural-Dissertation

zur Erlangung des Doktorgrades

der Mathematisch-Naturwissenschaftlichen Fakultät

der Universität zu Köln



vorgelegt von

Ya-Ping Ko

aus Ping-Tung, Taiwan

Mai 2005

Berichterstatter: Prof. Dr. Mats Paulsson

Prof. Dr. Thomas Langer

Tag der mündlichen Prüfung: July 11, 2005

Table of contents

Abstract.....	1
Zusammenfassung	3
1. Introduction	5
1.1. Extracellular matrix proteins	5
1.1.1. Proteoglycans.....	5
1.1.2. Collagens	7
1.1.3. Non-collagenous proteins	10
1.2. Matrilins.....	11
1.2.1. VWA domains	12
1.2.2. EGF-like domains	13
1.2.3. Coiled-coil domains.....	14
1.2.4. Matrilin-1	15
1.2.5. Matrilin-2	17
1.2.6. Matrilin-3	19
1.2.7. Matrilin-4	21
1.3. Model organisms.....	23
1.4. Zebrafish matrilins	23
1.4.1. Matrilin-1	27
1.4.2. Matrilin-3a	27

1.4.3.	Matrilin-3b	27
1.4.4.	Matrilin-4	28
1.4.5.	Sequence analysis	28
1.5.	Gene silencing methods	29
1.5.1.	RNAi	30
1.5.2.	Morpholino antisense oligonucleotides (morpholinos)	31
1.6.	The aims of the dissertation	36
2.	Materials and Methods	37
2.1.	Characterization of matrilin-3 deficient mice	37
2.1.1.	Genotyping by PCR	37
2.1.2.	Genotyping by Southern blot	39
2.1.2.1.	Dig-labeled probe for Southern blot	39
2.1.2.2.	Genomic DNA extraction	40
2.1.2.3.	Restriction enzyme digestion	40
2.1.2.4.	Southern blot	40
2.1.3.	Whole mount skeletal staining	41
2.1.4.	Immunohistochemistry	42
2.1.5.	Northern blot	43
2.1.6.	In situ hybridization	44
2.1.7.	Hematoxylin-eosin staining	44
2.1.8.	Van Kossa staining	45
2.1.9.	Safranin orange staining	45

2.1.10.	TRAP staining.....	46
2.1.11.	Glycosaminoglycan assay.....	47
2.1.12.	Cartilage extraction.....	48
2.1.13.	Western blot	48
2.2.	Characterization of matrilin-1/-3 double null mice	49
2.2.1.	Double fluorescence analysis for matrilin-4 and -1 in western blots of cartilage extracts	49
2.3.	Characterization of zebrafish matrilins.....	50
2.3.1.	Expression and purification of recombinant matrilin-1, -3a, -3b and -4 VWA1 domains.....	50
2.3.2.	Preparation of antibodies against matrilin-1, -3a and -4.....	52
2.3.3.	Determination of cross-reactivity of antibodies against each matrilin with the other matrilins	52
2.3.4.	Determination of cross-reactivity of the antibody against matrilin-3a with matrilin-3b	53
2.3.5.	Whole mount immunostaining.....	53
2.3.6.	Immunostaining on sections	54
2.3.7.	Temporal expression analysis by RT-PCR.....	55
2.3.8.	Whole mount skeletal staining.....	56
2.3.9.	Morpholino microinjection.....	57
3.	Results.....	58
3.1.	Matrilin-3 deficient mice	58
3.1.1.	Generation of matrilin-3 deficient mice.....	58
3.1.1.1.	Genotyping of offspring.....	60

3.1.2.	Gross morphology of the skeleton is normal in matrilin-3 deficient mice.....	61
3.1.3.	Matrilin-3-deficient mice show normal endochondral bone formation and intervertebral disk development.....	62
3.1.4.	Normal expression of other members of the matrilin family in matrilin-3-deficient skeletal tissues	68
3.1.5.	Biochemical analyses reveal no difference in matrix protein content in matrilin-3 null mice	72
3.1.6.	Summary	76
3.2.	Matrilin-1/matrilin-3 double deficient mice	76
3.2.1.	Summary	80
3.3.	Matrilins in zebrafish	80
3.3.1.	Generation of zebrafish-matrilin-specific antisera	81
3.3.2.	Matrilin expression during development	86
3.3.3.	Matrilins are differentially expressed	88
3.3.4.	Morpholino knockdowns of matrilins.....	92
3.3.4.1.	Specificity of morpholinos.....	92
3.3.4.2.	Matrilin knockdown phenotypes	93
3.3.4.3.	Matrilin-1 knockdown phenotype.....	95
3.3.4.4.	First characterization of matrilin-3a and matrilin-4 knockdown embryos.....	98
3.3.4.5.	Phenotype frequency and survival rate	98

4. Discussion	100
4.1. Mouse matrilins	100
4.1.1. Matrilin-3 is dispensable for mouse skeletal development.....	101
4.1.2. A biochemical phenotype in matrilin-1/matrilin-3 double deficient mice.....	101
4.1.3. Matrilins in disease	102
4.2. Zebrafish matrilins	104
4.3. Morpholino knockdowns of zebrafish matrilins.....	106
4.3.1. Matrilin knockdown phenotypes	106
4.3.2. Dose dependency of morpholino knockdown effects.....	107
4.3.3. Strength and limitations of morpholinos	108
4.3.4. Proper controls in morpholino experiments.....	109
4.4. The difference in phenotype between knockout mice and knockdown zebrafish.....	110
5. Perspectives	112
6. Bibliography.....	113
Abbreviations	125
Erklärung	127
Acknowledgements	128
Lebenslauf.....	130

Abstract

The matrilins are non-collagenous extracellular matrix proteins that form a subbranch of the superfamily of proteins containing VWA domains. Four matrilins are present in mammals, matrilin-1, -2, -3 and -4. The matrilins contain one or two VWA domains which are connected by a varying number of EGF-like domains, followed by a C-terminal α -helical coiled-coil domain. Matrilins serve as adaptors in the assembly of supramolecular structures in the extracellular matrix, but it is not known if this role is static or dynamic in nature. The *in vivo* functions of matrilins remain unclear and need to be elucidated in detail, in particular to understand the role of matrilins in inherited disease.

Mutations in the gene encoding human matrilin-3 lead to autosomal dominant skeletal disorders, such as multiple epiphyseal dysplasia (MED), which is characterized by short stature and early onset osteoarthritis, and bilateral hereditary microepiphyseal dysplasia, a variant form of MED characterized by pain in the hip and knee joints. In addition, a mutation in the first EGF-like domain of matrilin-3 has been linked to hand osteoarthritis in the Icelandic population.

Matrilin-3 null mice and matrilin-1/-3 double deficient mice were characterized. Homozygous matrilin-3 mutant mice appear normal, are fertile, and show no obvious skeletal malformations. Histological and ultrastructural analyses reveal an endochondral bone formation indistinguishable from that of wildtype animals. Northern blot, immunohistochemical, and biochemical analyses showed no compensatory upregulation of any other member of the matrilin family. In matrilin-1/-3 double null mice, biochemical analyses revealed a molecular phenotype in which the amount of matrilin-4 protein is increased and the band patterns of matrilin-3 and -4 are altered. The upregulation of matrilin-4 is likely to represent a compensatory mechanism. Altogether, the findings suggest functional redundancy among matrilins in mammals and demonstrate that the phenotypes of MED-like disorders are not caused by the absence of matrilin-3, but are likely to be due to dominant negative effects of the mutant proteins.

The zebrafish is a well established model organism for the study of vertebrate development. The matrilins are present in neither *Drosophila* nor in *C. elegans* and the zebrafish is therefore among the simplest organisms which express matrilins. Highly conserved orthologues, matrilin-1, -3a, -3b and -4, are present in zebrafish, while the matrilin-2 gene is missing. The temporal and spatial expression of zebrafish matrilins was characterized. Zebrafish matrilin-1 was found not only in skeletal tissue but also in notochord and intestine. Matrilin-3a expression is restricted to skeletal tissues, while the expression pattern of matrilin-3b has not yet been elucidated due to the lack of a specific antibody. Nevertheless, RT-PCR analysis reveals that matrilin-3b is expressed at 24 hpf and, interestingly, splice variants of matrilin-3b containing a proline- and serine/threonine-rich domain are found only in embryos but not in adult fish, indicating that this new domain probably has an important function during zebrafish development. Similar to in mammals, matrilin-4 is the earliest and most widely expressed matrilin in zebrafish. Matrilin-4 is strongly expressed already at 24 hpf and is present in the skeletal tissues, soft connective tissues and nervous tissues.

Morpholino antisense oligonucleotides were used to knockdown matrilins expressed in zebrafish. Malformations were seen at all the doses used and the phenotypes matched to the tissue distribution of the respective matrilin. Injection of matrilin-1 or matrilin-4 morpholinos give curled body shape, smaller eyes or a truncated body axis depending on dosage. The matrilin-3a knockdown embryos showed a serious skeletal phenotype.

Zusammenfassung

Die Matriline gehören zu den nicht-kollagenen Proteinen der extrazellulären Matrix, die einen Zweig der von Willebrandfaktor A Domänen (VWA) enthaltenden Proteinfamilie bilden. Bei Säugetieren gibt es insgesamt vier Matriline, Matrilin-1, -2, -3 und -4. Die Matriline enthalten ein oder zwei VWA Domänen, die durch eine unterschiedliche Anzahl von epidermalemem Wachstumsfaktor ähnlichen Domänen (EGF) verbunden sind, gefolgt von einer C-terminalen α -helikalen Coiled-Coil Domäne. Die Matriline dienen als Adaptorproteine bei der Verbindung von supramolekularen Strukturen in der extrazellulären Matrix, es ist aber noch unbekannt, ob die Matriline dabei eine statische oder dynamische Rolle spielen. Die genauen *in vivo* Funktionen der Matriline verbleiben unklar und müssen noch aufgeklärt werden, insbesondere die Rolle, die die Matriline bei der Entstehung von bestimmten Erbkrankheiten spielen.

Mutationen im menschlichen Matrilin-3 Gen führen zu autosomal dominanten Erbkrankheiten des Skelettsystems, wie z. B. der multiplen epiphysären Dysplasie (MED), die sich durch eine geringe Körpergröße und eine frühzeitig einsetzende Arthrose auszeichnen oder der bilateralen erblichen mikroepiphysären Dysplasie, einer Variante der MED, die durch Schmerzen in Hüft- und Kniegelenken charakterisiert ist. Außerdem wurde in der isländischen Bevölkerung eine Mutation in der ersten EGF Domäne von Matrilin-3 mit dem Vorkommen von Handarthrose in Verbindung gebracht.

Matrilin-3 defiziente und Matrilin-1/-3 doppeldefiziente Mäuse wurden untersucht. Die homozygoten, mutierten Matrilin-3 Mäuse sehen normal aus, sind fruchtbar und haben keinen offensichtlichen skeletalen Phänotyp. Histologische und ultrastrukturelle Untersuchungen zeigten eine endochondrale Knochenentwicklung, die sich von der vom Wildtyp nicht unterschied. Northernblot, Immunhistochemie und biochemische Analysen ergaben keine Hinweise auf eine Hochregulation der anderen Matriline, die das Fehlen von Matrilin-3 hätten kompensieren können. Bei der biochemischen Analyse der Matrilin-1/-3 doppeldefizienten Mäuse dagegen wurde ein molekularer Phänotyp entdeckt, in dem die Menge an Matrilin-4 erhöht war und sich das Bandenmuster von Matrilin-3 und -4 verändert hatte. Die Hochregulation von Matrilin-4 beruht wahrschein-

lich auf einem Kompensationsmechanismus. Insgesamt deuten die Ergebnisse auf eine funktionelle Redundanz der Matriline bei Säugetieren hin. Die Phänotypen der skeletalen Erkrankungen sind wahrscheinlich nicht durch das Fehlen von Matrilin-3 in der Matrix, sondern eher durch einen dominant negativen Effekt der mutierten Proteine zu erklären.

Der Zebrafisch ist ein gut eingeführter Modellorganismus bei der Untersuchung der Entwicklung von Wirbeltieren. Da die Matriline weder in *Drosophila* noch in *C. elegans* vorkommen, gehört der Zebrafisch zu den einfachsten Lebewesen, die Matriline exprimieren. Im Zebrafisch gibt es hoch konservierte orthologe Gene, die für Matrilin-1, -3a, 3b und -4 kodieren, während ein Matrilin-2 Gen fehlt. Die zeitliche und räumliche Expression von Matrilinen im Zebrafisch wurde untersucht. Zebrafisch Matrilin-1 konnte nicht nur in skeletalen Geweben, sondern auch im Notochord und Dünndarm nachgewiesen werden. Die Matrilin-3a Expression beschränkt sich auf skeletale Gewebe, während die Matrilin-3b Expression nicht untersucht werden konnte, da ein geeigneter Antikörper nicht zur Verfügung stand. Dennoch konnte mit Hilfe von RT-PCR bereits nachgewiesen werden, dass Matrilin-3b bereits 24 Stunden nach der Befruchtung exprimiert wird. Interessanterweise gibt es Spleißvarianten von Matrilin-3b, die eine an Prolin und Serin/Threonin reiche Domäne enthalten, welche nur in Embryos, aber nicht in erwachsenen Tieren vorkommt, was darauf hinweist, dass die Domäne möglicherweise eine Rolle während der Zebrafischentwicklung spielt. Wie bei Säugetieren ist Matrilin-4 beim Zebrafisch das am frühesten und breitesten exprimierte Matrilin. Matrilin-4 ist bereits 24 Stunden nach der Befruchtung stark exprimiert und kommt in skeletalen Geweben, weichen Bindegeweben und in Nervengeweben vor.

Morpholino Gegenstrangoligonukleotide wurden eingesetzt, um die Expression der Matriline im Zebrafisch zeitweilig zu unterbinden. Fehlbildungen wurden bei allen angewandten Dosierungen beobachtet und die Phänotypen passen zu der Gewebeverteilung der entsprechenden Matriline. Abhängig von der Dosis ergaben die Injektionen von Matrilin-1 bzw. Matrilin-4 spezifischen Morpholinos Tiere mit verdrehtem Körper, kleineren Augen oder gar einer verkürzten Körperachse. Die mit einem Matrilin-3a spezifischen Morpholino behandelten Tiere zeigten einen schweren skeletalen Phänotyp.

1. Introduction

1.1. Extracellular matrix proteins

The extracellular matrix (ECM) is a complex structural entity surrounding and supporting cells within tissues. The ECM has received considerable attention due to its importance in cell-cell interactions, signalling, wound repair, cell adhesion and tissue function.

The major constituents of the ECM are proteoglycans and collagens, which form a tissue-specific network providing the tensile strength and resilience required. A number of non-collagenous proteins are also found in the ECM and serve to regulate matrix assembly and cell adhesion.

1.1.1. Proteoglycans

Proteoglycans are complex macromolecules consisting of a central protein core to which a variable number of glycosaminoglycan (GAG) chains are covalently attached. Glycosaminoglycans are long, unbranched polyanionic carbohydrate chains consisting of repeating disaccharide units. There are four main classes of glycosaminoglycans: hyaluronic acid, the chondroitin sulphates (chondroitin 4-sulphate, chondroitin 6-sulphate, dermatan sulphate), keratan sulphate and the heparin-heparan sulphate class. As the glycosaminoglycans carry a large number of sulphate and carboxyl groups, the proteoglycans have a high negative net charge, which in turn results in an extended conformation due to electrostatic repulsion. Proteoglycans contribute about a third of the dry mass of a hyaline cartilage. At this high concentration, they are presumably kept in a compressed state by physical entrapment in the network of collagen fibers. The electrostatic repulsion between the fixed charged groups will be strong and any further compression will be resisted. Therefore, the proteoglycans contribute compressive

stiffness and elasticity to the cartilage.

Aggrecan is the most abundant proteoglycan in articular cartilage (Doege et al., 1994). The protein core is about 230 kDa in size (Watanabe and Yamada, 2002) and is heavily substituted with GAG chains. Cartilage matrix deficiency (*cmd*) in mice (Rittenhouse et al., 1978) is a natural functional knockout of the aggrecan gene, in which 7 bp in exon 5 were deleted resulting in severely truncated molecules (Watanabe et al., 1994). The homozygotes (*cmd/cmd*) are characterized by dwarfism, short limbs, a short trunk, tail and snout, as well as a protruding tongue and cleft palate and mice die shortly after birth due to respiratory failure (Rittenhouse et al., 1978; Watanabe and Yamada, 2002). Even though heterozygous mice appear normal at birth, dwarfism and age-associated spinal degeneration are observed while aging (Watanabe et al., 1997), indicating that aggrecan plays an important role in cartilage development and maintenance.

One subgroup of proteoglycans are the small leucine-rich proteoglycans (SLRPs) that share a multiple leucine-rich repeat (LRR) structural motif flanked by cysteine residues. The LRR domain is composed of ~10 repeats of 24 amino acid residues each, preferentially containing asparagin (N) and leucine (L) in conserved positions (LX₂LXLX₂NX(L/I)) (Iozzo, 1999). This motif is involved in many molecular recognition processes including cell adhesion, signal transduction, DNA repair and RNA processing (Kobe and Deisenhofer, 1994). SLRPs often interact with collagen, modifying the deposition and arrangement of collagen fibers in the extracellular matrix, but also with cells and with soluble growth factors (Ameye and Young, 2002). The interaction of SLRPs with cells and with growth factors like TGF- β may affect the cell proliferation in addition to modifying the extracellular environment (Ameye and Young, 2002).

The SLRP family is rapidly growing and more than 13 members are known including decorin, biglycan, asporin, fibromodulin, lumican, PRELP, keratocan, osteoadherin epiphican, mimican, opticin, chondroadherin and myctalopin (Ameye and Young, 2002).

Decorin is expressed throughout the body, stabilizes collagen fibrils and plays a

significant role in tissue development and assembly, as well as being involved in direct and indirect signaling (Reed and Iozzo, 2002). Mice harboring a targeted disruption of the decorin gene are viable but have fragile skin with markedly reduced tensile strength and irregular collagen fibril shape (Danielson et al., 1997; Reed and Iozzo, 2002).

Biglycan consists of a 45-kDa core protein made up almost entirely of leucine-rich repeats and is widely distributed in the extracellular matrices of bone and specialized, non-skeletal connective tissues. It was shown that biglycan-deficient mice develop age-related osteoporosis due to defects in bone marrow stromal cells (Chen et al., 2002).

Both decorin and biglycan bind to VWA domains in the N-terminal region of collagen VI and matrilins are in turn bound to these small leucine-rich proteoglycans (Wiberg et al., 2003).

1.1.2. Collagens

Collagens are the major proteins of the extracellular matrix, constituting 30% of the total protein mass. They play a dominant role in maintaining structures of various tissues and have been proven to have functions in cell adhesion, chemotaxis, migration and dynamic interplay between cells. In addition, collagens regulate tissue remodelling during growth, differentiation, morphogenesis and wound healing (Myllyharju and Kivirikko, 2004).

The primary feature of a typical collagen molecule is its long, stiff, triple-stranded helical structure, in which three collagen polypeptide α chains are wound around one another in a rope-like superhelix. An α chain is composed of a series of triplet Gly-X-Y sequences, in which X is commonly proline and Y often hydroxyproline. Therefore, collagens are extremely rich in proline and glycine and both amino acids are important in the formation of the triple-stranded helix. Proline stabilizes the helical conformation in each α chain because of its ring structure, while glycine is regularly spaced at every third residue throughout the central region of the α chain. The hydroxyl groups of hydroxyproline and hydroxylysine are thought to form interchain hydrogen bonds thus

helping to stabilize the triple helix.

Up to date, 28 members of the collagen family have been found (R. Wagener, personal communication, Myllyharju and Kivirikko, 2004). According to their assemblies, collagens can be divided into the following subgroups (Fig. 1-1): fibril-forming (type I, II, III, V, XI, XXIV and XXVII), fibril-associated collagens with interrupted triple helices (FACIT) (types IX, XII, XIV, XVI, XIX, XX, XXI, XXII and XXVI), hexagonal network forming (types VIII and X), beaded filament-forming (type VI), anchoring fibril-forming (type VII), collagens with transmembrane domains (types XIII, XVII, XXIII and XXV), nonfibril-forming (type IV), and multiplexin collagens (type XV and XVIII) (Myllyharju and Kivirikko, 2004).

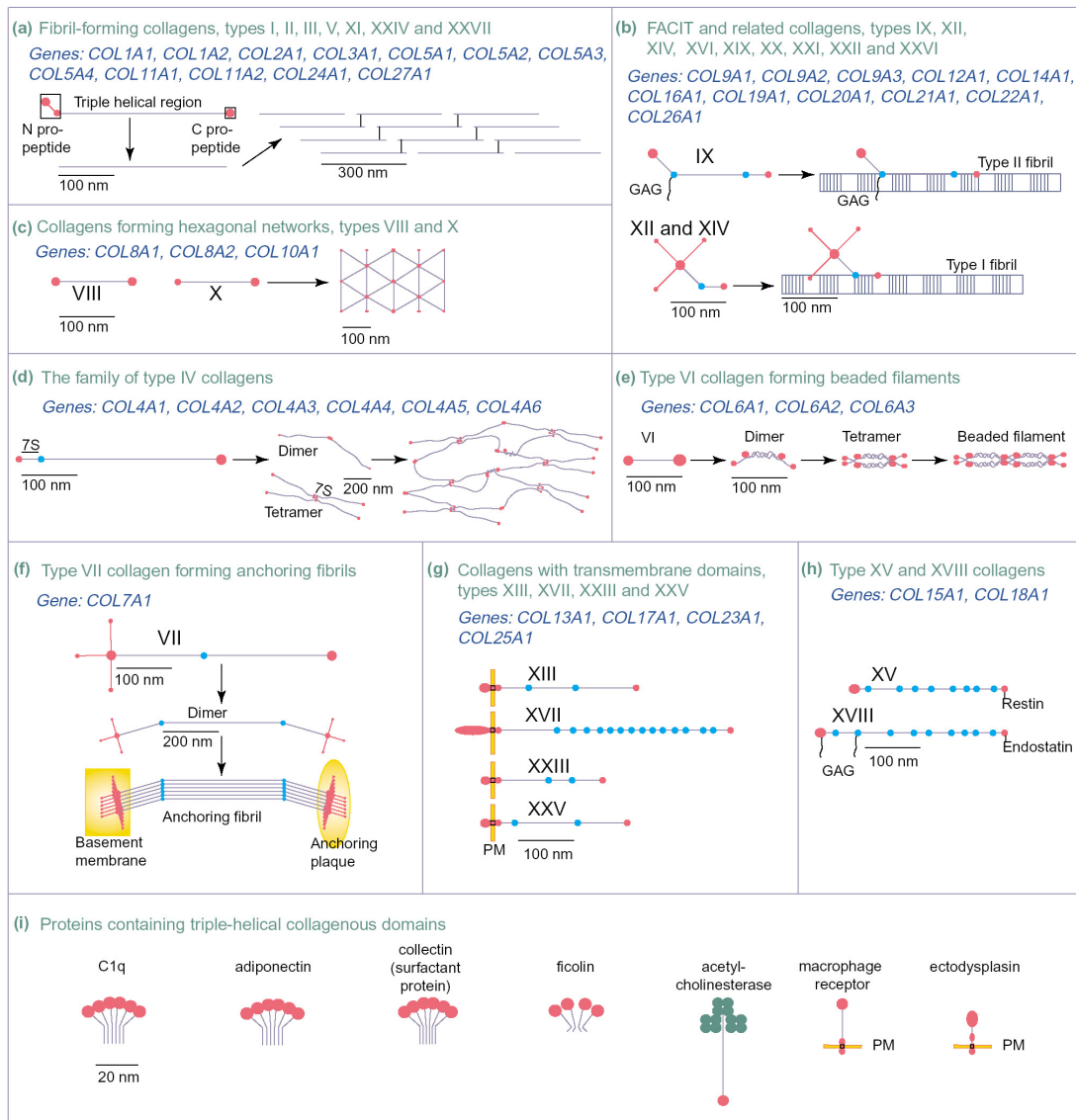


Fig. 1-1 Members of the collagen superfamily and their known supramolecular assemblies. The figure is from (Myllyharju and Kivirikko, 2004).

Among the collagens, collagen type II is cartilage-specific and the predominant collagen in cartilage, representing about 90% of the collagen content. It forms a firm network that provides tensile strength to the tissue. The fibres also contain type XI collagen which is a minor, cartilage-specific collagen representing only a few percent of the collagen content. Collagen type IX is associated with the collagen II/XI fibrils and has a positively charged domain protruding out from the fibrils that has been suggested to interact with proteoglycans. Collagen II/IX fibres form a fine network in the

superficial layer of adult articular cartilage. Collagen type X is mainly restricted to hypertrophic cartilage, but has also been shown to be present in the superficially layer of articular cartilage (Rucklidge et al., 1996). It has been suggested to have a role in endochondral ossification.

Collagens are known to mediate cell adhesion via integrin receptors. Previous studies have indicated the presence of a number of integrin recognition sites in collagens (Morton et al., 1994; Staatz et al., 1991). In addition, discoidin domain receptors (DDR), a subfamily of receptor tyrosine kinases, also act as receptors for collagens (Vogel et al., 1997) and the collagen binding sites in DDR2 have been identified (Leitinger, 2003). The activation of DDRs mediates cell proliferation, migration and motility. Moreover, it was demonstrated that DDRs influence the expression and activity of metalloproteinases (Leitinger et al., 2004).

A great many mutations in collagens have been identified and shown cause diseases including osteogenesis imperfecta, many chondrodysplasias, several subtypes of the Ehlers-Danlos syndrome, Alport syndrome, Bethlem myopathy, certain subtypes of epidermolysis bullosa, Knobloch syndrome and also some cases of osteoporosis, arterial aneurysms, osteoarthritis, and intervertebral disc degeneration (Myllyharju and Kivirikko, 2001).

1.1.3. Non-collagenous proteins

In addition to collagens and proteoglycans, many non-collagenous proteins are present in the ECM. However, in contrast to collagens and proteoglycans, which have been studied in detail since many years, the functions of many of the non-collagenous proteins are rather unclear.

Non-collagenous proteins typically contain multiple domains, each harbouring specific binding sites for other matrix macromolecules and for cell surface receptors. The first well characterized example was fibronectin, a large glycoprotein found both in blood plasma and in the extracellular matrix (Hynes and Yamada, 1982). Fibronectin was

shown to have multiple functions, affecting cellular adhesion, cell migration, cellular morphology and spreading, cytoskeletal organization, oncogenic transformation, phagocytosis, embryonic differentiation and wound healing (Hynes and Yamada, 1982). Fibronectin null mutant mice die early in embryogenesis because their endothelial cells fail to form proper blood vessels (George et al., 1993).

In addition to fibronectin, other proteins like osteonectin, tetranectin, tenascins, thrombospondins, laminins and matrilins also belong to the non-collagenous proteins.

The matrilins are widespread, but except for some information on their assembly with collagens and proteoglycans, their overall contribution to tissue function is not known.

1.2. Matrilins

The matrilins are a family of non-collagenous extracellular matrix proteins that form a subbranch of the superfamily of proteins containing VWA domains (for review, see (Whittaker and Hynes, 2002)).

The matrilin family consists of four members with a closely similar domain structure (Fig. 1-2). Two VWA domains are connected by a varying number of EGF-like domains. These are followed by a C-terminal α -helical coiled-coil domain, which allows the oligomerization of the single subunits in a bouquet-like fashion. Only matrilin-3 lacks the second VWA domain and here the EGF-like domains are directly connected to the coiled-coil domain. In addition, matrilin-2 and -3 contain a stretch of amino acid residues at the N-terminus with a high frequency of positively charged side chains. Uniquely, matrilin-2 contains a module between the second VWA domain and the oligomerization domain that has no homology to any other known protein sequence.

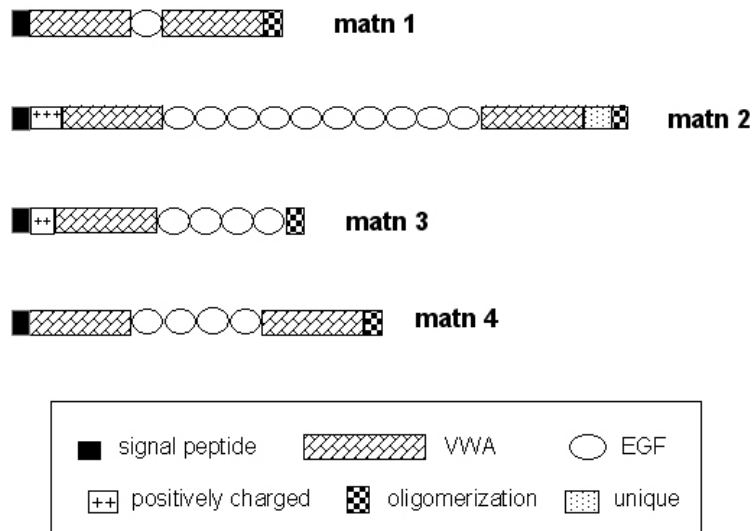


Fig. 1-2 Domain structure of mouse matrilins (modified from Wagener et al., 2005).

The matrilins are differentially expressed. Matrilin-1 and -3 are mainly present in skeletal tissues (Aszodi et al., 1996; Klatt et al., 2000), whereas matrilin-2 and -4 (Klatt et al., 2001; Piecha et al., 1999) are more widely distributed. It is thought that matrilins have an adapter function in the extracellular matrix, connecting macromolecular networks (Hauser et al., 1996). This role for matrilins was confirmed by recent results showing that matrilins-1, -3 and -4 are associated with collagen VI microfibrils extracted from rat chondrosarcoma tissue. The matrilins are here bound to the small leucine-rich repeat proteins biglycan and decorin, which in turn interact with the N-terminal globular domains of the collagen VI molecules (Wiberg et al., 2003).

1.2.1. VWA domains

The VWA domains of matrilins consist of about 200 amino acid residues in a classical Rossman fold with a central β -sheet surrounded by α -helices. A MIDAS (metal ion dependent adhesion site) motif (DXSXSX_nTX_nD), which may be involved in ligand binding, is perfectly conserved in nearly all matrilin VWA domains. The VWA domains of matrilins represent an own subgroup of the VWA domains of extracellular matrix

proteins (<http://www.ncbi.nlm.nih.gov/Structure/cdd/cdd.shtml>) (Marchler-Bauer et al., 2005). All matrilin VWA domains have higher identity to the members of the subgroup than to any other VWA domain, indicating that they originate from a common ancestor VWA domain (Deak et al., 1999). Phylogenetic studies assigned the first and the second VWA domains into two different groups, of which each splits into a matrilin-1/3 and a matrilin-2/4 subbranch (Deak et al., 1999). Among other VWA domain family members, the VWA domains of different collagens, vitrin, $\alpha 1$ integrin, WARP and AMACO have the highest identity (approx. 30%). It is probable that the VWA domains are the principal interaction modules of matrilins, since matrilin-1 and -3 splice variants that lack all EGF domains exist in zebrafish (Ko et al., 2005).

VWA domains are found not only in the matrilins, but also in a large number of other extracellular proteins (for review see (Whittaker and Hynes, 2002)) such as von Willebrand factor, collagens type VI, VII, XII, XIV, XXI and XXII, complement factors B and C2, the H2 and H3 subunits of the inter- α -trypsin inhibitor, the α and β -chains of integrins and putative transmembrane proteins of lower eukaryotes (Whittaker and Hynes, 2002). Recently, also intracellular proteins like copines were identified as members of the family (Tomsig and Creutz, 2002; Whittaker and Hynes, 2002).

1.2.2. EGF-like domains

Except for some splice variants in zebrafish which lack EGF-like domains, all other matrilins contain at least one such domain, the highest number being in a splice variant of zebrafish matrilin-4 where 12 EGF domains are present (Ko et al., 2005). EGF domains contain 40-50 amino acid residues, including six conserved disulphide bonds. The structure shows a two stranded β -sheet and often EGF domains are present in multiple copies (Rao et al., 1995). The function of the EGF domains of matrilins is still not clear. A comparison of the matrilin EGF domains with the key residues of the calcium-binding motifs in calcium binding EGF domains (Handford et al., 1991; Rao et al., 1995) showed no match with the consensus sequence. Neither was a non-canonical calcium binding site (Malby et al., 2001) detected in matrilin EGF domains.

Moreover, even though matrilin EGF domains show an overall structural similarity to epidermal growth factor, there is no evidence that they retain growth factor activity. It is more likely that they serve as spacers between VWA domains, which in many other proteins show ligand binding activities.

Database searches show that EGF domains of scube proteins, fibulins and fibrillins have the highest homologies to matrilin EGF domains (Wagener et al., 2005).

1.2.3. Coiled-coil domains

The matrilins contain a C-terminal α -helical coiled-coil domain that allows oligomerization of the subunits in a bouquet-like fashion. Coiled-coil domains are characterised by heptad repeats (a-g) of amino acid residues that typically have non-polar amino acids at position a and d. The coiled-coil domains of matrilins contain 4.5 heptad repeats, showing the least perfect match with the consensus sequence for matrilin-3. Nevertheless, by SDS-PAGE and electron microscopy of full-length proteins, it has been shown that matrilin-1 and -4 form homo-trimers (Hauser and Paulsson, 1994; Klatt et al., 2001), whereas matrilin-2 and -3 form homo-tetramers (Klatt et al., 2000; Piecha et al., 1999). The oligomerization was also studied by using recombinantly expressed coiled-coil domains (Frank et al., 2002). The analysis of oligomerization in mixtures of isolated coiled-coil domains showed a broad range of interactions and the only hetero-oligomers not found were those containing matrilin-2 and -3 or matrilin-3 and -4 (Frank et al., 2002). In contrast, here the coiled-coil domain of matrilin-2 formed only trimers. It could well be that the oligomerization is influenced by the unique domain adjacent to the coiled-coil domain of matrilin-2. Hetero-oligomeric forms of matrilin-1 and -3 have been isolated from fetal human and calf cartilage (Klatt et al., 2000; Kleemann-Fischer et al., 2001; Wu and Eyre, 1998). There is no conclusive evidence for natural occurrence of other hetero-oligomers, but a SDS-PAGE band from an extract of newborn mouse epiphyseal cartilage was shown by peptide mass fingerprinting to contain both matrilin-1 and matrilin-4 (G. Sengle, unpublished results).

1.2.4. Matrilin-1

Matrilin-1, which was first purified from bovine cartilage, is the prototype member of the family and was originally called "cartilage matrix protein" or CMP (Paulsson and Heinegard, 1979). It is an abundant protein in many forms of cartilage. The single subunit has a molecular weight of 52,000 Da and contains 3.9% carbohydrate, probably in the form of N-linked glycans (Paulsson and Heinegard, 1981). In electron microscopy matrilin-1 shows the typical bouquet-like structure where the single VWA domains of the subunits are not resolved, indicating an interaction between VWA1 and VWA2 (Hauser and Paulsson, 1994) (Fig. 1-3). The solution structure of the oligomerization domain of matrilin-1 has been determined by heteronuclear NMR spectroscopy. As predicted, the domain folds into a parallel, disulfide-linked, three-stranded, α -helical coiled coil, spanning five heptad repeats in the amino acid sequence (Dames et al., 1998).

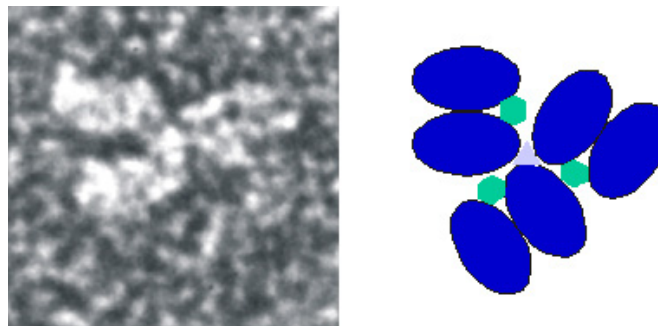


Fig. 1-3 Oligomerization of matrilin-1 visualized by electron microscopy. The figure is modified from (Hauser and Paulsson, 1994). In the schematic drawing the VWA domains are in dark blue, the EGF-like domains are in green and the coiled-coil domain is in light blue.

In the mouse, matrilin-1 can be detected by antibody labeling in myocardium at 9.5 days p.c. (Segat et al., 2000). This expression is however transient and of unknown physiological significance. More lasting expression is seen for both matrilin-1 and -3 in the condensing mesenchyme at day 12.5 p.c.. Matrilin-1 expression is restricted to

certain types of cartilage. In the mouse tibial growth plate, matrilin-1 is abundant in resting, proliferating and hypertrophic cartilage (Klatt et al., 2002), but it is not present in articular and intervertebral disc cartilages (Aszodi et al., 1996; Aszodi et al., 1994). Moreover, in situ hybridization analysis of matrilin-1 mRNA showed a downregulation concomitant with the progress of hypertrophy at later stages of chondrogenesis (Aszodi et al., 1996).

Matrilin-1 is abundantly expressed in tracheal, nasal septum, auricular, and epiphyseal cartilages (Paulsson and Heinegard, 1982), and continued expression of matrilin-1 is seen in tissues that remain cartilaginous during the whole lifespan, e.g. in costal cartilage and in the nasal septum (Klatt et al., 2002).

The genetic basis for matrilin-1 gene expression has been studied in some detail in the chicken system. A minimal promoter has been defined that functions both in chondrocytes and fibroblasts (Goetinck et al., 1990). An enhancer exerts a chondrocyte-specific stimulation on the promoter activity and a silencer inhibits activity both in chondrocytes and fibroblasts. The enhancer is independent of the developmental stage of the chondrocytes, while promoter upstream control regions appear to restrict the promoter activity to certain chondrocyte developmental stages (Muratoglu et al., 1995). Transgenic experiments with the chicken matrilin-1 promoter in mouse have indicated that the tissue specific control elements are divided between the promoter upstream and intronic regions in a manner similar to that of the *Coll1a2* gene (Karcagi et al., 2004).

Matrilin-1 was first recognized as a protein tightly bound to aggrecan and which copurified with aggrecan in a variety of separation methods (Paulsson and Heinegard, 1979). The bound matrilin-1 molecules with time become covalently crosslinked to the aggrecan core protein, with at least some of the crosslinks not being sensitive to reduction (Hauser et al., 1996). In addition, an interaction was found between matrilin-1 and cartilage collagen fibrils (Winterbottom et al., 1992) and between matrilins and other non-collagenous molecules, in particular COMP and decorin (Mann et al., 2004). Furthermore, matrilin-1 has the ability to enhance the adhesion of chondrocytes via integrin $\alpha_1\beta_1$ (Makihira et al., 1999). However, two different strains of mice lacking

matrilin-1 show normal skeletal development (Aszodi et al., 1999; Huang et al., 1999). Nevertheless, in one of the two strains the mice have alterations in type II collagen fibrillogenesis and fibril organization (Huang et al., 1999).

Matrilin-1 is a potential autoantigen able to trigger the tissue-specific immune response, as seen both in patients and in animals, resulting in relapsing polychondritis and related autoimmune diseases (Buckner et al., 2000; Hansson et al., 1999; Hansson et al., 2001; Hansson and Holmdahl, 2002). It has also been reported that the expression of matrilin-1 is enhanced in knee osteoarthritic cartilage and in knee or hip rheumatoid arthritic cartilage (Okimura et al., 1997). In addition, elevated serum levels of matrilin-1 were detected in patients with active rheumatoid arthritis (Saxne and Heinegard, 1989). Matrilin-1 also showed an increased expression in specimens from arthritic condylar cartilage of temporomandibular joints (Ohno et al., 2003).

1.2.5. Matrilin-2

Matrilin-2 is the largest matrilin with a calculated molecular weight of 104,300 Da and also carries N-linked glycans (Piecha et al., 1999). A 3.9-kilobase matrilin-2 mRNA was detected in a variety of mouse organs, including calvaria, uterus, heart, and brain, as well as fibroblast and osteoblast cell lines (Deak et al., 1997). Similar to matrilin-1, in electron microscopy the two VWA domains appear to bind to each other causing the subunit to form a loop extending from the central coiled-coil (Fig. 1-4). Both recombinant matrilin-2 and the protein detected by immunoblot in tissue extracts are often degraded and actually seen as a ladder of bands in SDS-PAGE. This is most likely due to proteolytic processing.

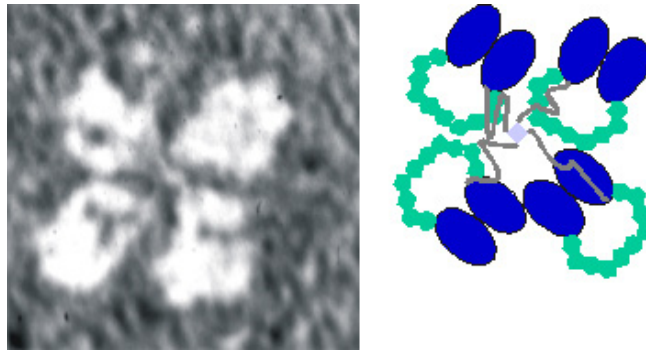


Fig. 1-4 Oligomerization of matrilin-2 visualized by electron microscopy. The figure is modified from (Piecha et al., 1999). In the schematic drawing the VWA domains are in dark blue, the EGF-like domains are in green, the coiled-coil domain is in light blue and the unique sequence is in gray.

The expression pattern of matrilin-2 is much broader than those of matrilin-1 and -3 and, despite being present also in cartilage, matrilin-2 is found mainly in loose connective tissue. The first matrilin-2 expression in the mouse embryo is in heart, just like for matrilin-1, but matrilin-2 is expressed later, at day 10.5 p.c., and the expression continues (Segat et al., 2000). Later in development it is produced by a wide variety of connective tissue cells, but also by smooth muscle cells and some epithelia (Piecha et al., 1999). Matrilin-2 protein is deposited by these cells into their pericellular matrix. In some cases it becomes associated with basement membranes, even though it is uncertain if it is an integral basement membrane protein. In other cases matrilin-2 is found as a component of a filamentous network of unknown overall composition (Piecha et al., 1999). In general, matrilin-2 has a complementary expression pattern to matrilin-1 and -3, even though there is some matrilin-2 present also in cartilage.

Matrilin-2 null mice have been produced and show no gross abnormalities during embryonic or adult development, are fertile, and have a normal lifespan (Mates et al., 2004).

1.2.6. Matrilin-3

The matrilin-3 subunit is the simplest in the matrilin family consisting of only one VWA domain followed by four EGF-like domains and a C-terminal coiled-coil domain (Wagener et al., 1997). By MALDI-TOF mass spectrometry the molecular weight was determined to 49,300 Da. This value closely matches the calculated mass, indicating the lack of glycosylation. Due to the absence of the second VWA domain there is no self-interaction in the subunits and in electron microscopy the tetrameric matrilin-3 appeared to have more extended and flexible arms (Fig. 1-5).

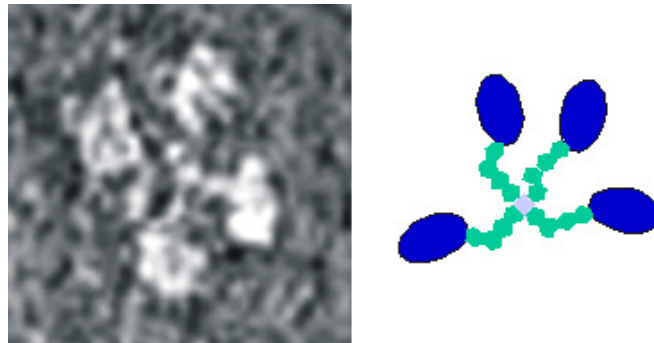


Fig. 1-5 Oligomerization of matrilin-3 visualized by electron microscopy. The figure is modified from (Klatt et al., 2000). In the schematic drawing the VWA domains are in dark blue, the EGF-like domains are in green and the coiled-coil domain is in light blue.

Matrilin-3 can form homotetramers via the coiled-coil domain (Klatt et al., 2000), and, in addition, mixed trimers and tetramers of matrilin-3 and matrilin-1 have been described for man (Kleemann-Fischer et al., 2001) and calf (Klatt et al., 2000; Wu and Eyre, 1998), whereas these heterooligomers could not be identified in mouse (Aszodi et al., 1999).

In mouse, matrilin-3 is expressed in dense connective tissue during growth and remodeling and can be detected earliest at day 12.5 p.c. in the cartilage anlagen of the developing bones. In newborn mice matrilin-3 is abundant in the developing occipital bones and the bones of the nasal cavity, the cartilage primordium of the vertebral

bodies, the ribs and the long bones, as well as in sternum and trachea (Klatt et al., 2000; Klatt et al., 2002), while in 6-week-old mice the expression is restricted to the growth plates of long bones, sternum and vertebrae (Klatt et al., 2002) and the tracheal perichondrium (Klatt et al., 2000). Matrilin-3 is mostly co-localized with matrilin-1, except for the most superficial cell layer in the articular cartilage, where only matrilin-3 can be detected. The matrilin-3 expression gradually ceases after birth while matrilin-1 remains in cartilages throughout life (Klatt et al., 2002).

Mutations in matrilin-3 were found to be linked to autosomal dominant forms of multiple epiphyseal dysplasia (MED), a relatively mild and clinically variable osteochondrodysplasia, primarily characterized by delayed and irregular ossification of the epiphyses and early onset osteoarthritis (Chapman et al., 2001). The mutations mostly affect residues within the conserved β strands of the single VWA domain of matrilin-3 (Jackson et al., 2004; Mabuchi et al., 2004). In bilateral hereditary micro-epiphyseal dysplasia (BHMED), which gives a skeletal phenotype similar to but still distinct from common MED, a site close to the β -strands of matrilin-3 is affected (Mostert et al., 2003). MED is also caused by autosomal dominant mutations in the genes encoding COMP (Briggs et al., 1995) and the $\alpha 1$, $\alpha 2$, and $\alpha 3$ chains of type IX collagen (COL9A1, COL9A2, and COL9A3) (Czarny-Ratajczak et al., 2001; Muragaki et al., 1996; Paasilta et al., 1999) and it is of interest that mutations in the functionally related protein matrilin-3 causes similar phenotypes. In addition, in an autosomal recessive form of another osteochondrodysplasia, spondylo-epi-metaphyseal dysplasia (SEMD), that is associated with vertebral, epiphyseal, and metaphyseal anomalies, again the matrilin-3 gene is affected (Borochowitz et al., 2004). The disease is caused by a change of a cysteine into a serine in the first EGF domain of matrilin-3, which could lead to disturbance in the disulphide bond formation. In a genomic screen of the Icelandic population, a mutation in the first EGF domain of matrilin-3 was linked to the occurrence of hand osteoarthritis. Slightly more than 2% of patients with hand osteoarthritis carry the mutation (Stefansson et al., 2003), but it was also identified in unrelated controls (Jackson et al., 2004; Stefansson et al., 2003). In a recent study, the influence of those MED, SEMD and hand osteoarthritis mutations on the secretion of matrilin-3 was studied (Otten et al., 2005). Whereas matrilin-3 carrying the hand osteoarthritis mutation could be secreted by chondrocytes at a similar rate as wildtype

matrilin-3, the matrilin-3 mutants causing MED and SMED, respectively, were retained in the endoplasmic reticulum. It is likely that this retention causes a chondrocyte dysfunction by which MED and SMED phenotypes could be explained. Similar observations were earlier made for COMP mutations leading to MED (for review see (Briggs and Chapman, 2002; Posey et al., 2004)). In contrast, the mutant matrilin-3 that has been linked to hand osteoarthritis is synthesized, processed, secreted and deposited in a way indistinguishable from the wildtype protein, suggesting, at the most, subtle effects of this mutation on the structure and function of the protein (Otten et al., 2005).

1.2.7. Matrilin-4

Matrilin-4 contains in mouse four EGF domains between the two VWA domains (Wagener et al., 1998). The recombinant protein has a molecular weight of 72,900 Da indicating 7 % posttranslational modifications (Klatt et al., 2001). Although matrilin-4 carries two VWA domains, in electron microscopy these show no obvious interaction (Fig. 1-6). The images show the three C-terminal VWA domains at the center, presumably held together by the coiled-coil domain. The subunits extend from this central structure and end in globular domains representing the N-terminal VWA domain. The structure of matrilin-4 is reminiscent of that of matrilin-3, except for the latter protein forming tetramers.

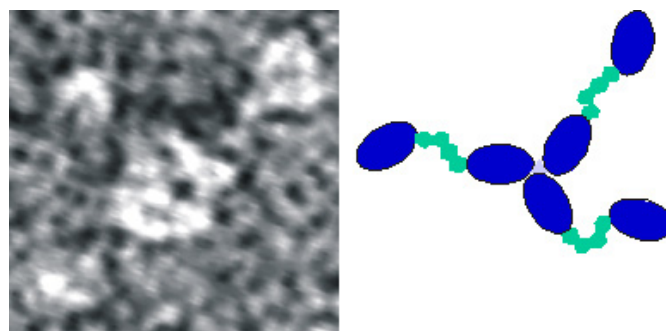


Fig. 1-6 Oligomerization of matrilin-4 visualized by electron microscopy. The figure is modified from (Klatt et al., 2001). In the schematic drawing the VWA domains are in dark blue, the EGF-like domains are in green and the coiled-coil domain is in light blue.

Matrilin-4 is the most ubiquitous of all matrilins and appears to be present wherever another matrilin is found (Klatt et al., 2001). It can be detected by immunohistochemistry in the ectoplacental cone already at day 7.5 p.c. (Klatt et al., 2001). Affinity-purified antibodies detect a broad expression in dense and loose connective tissue, bone, cartilage, central and peripheral nervous system and in association with basement membranes. The expression in nervous tissue is more pronounced than for other matrilins, and indeed the brain appears to be the most abundant tissue source for matrilin-4.

When matrilin-4 expression was studied in the mouse by northern hybridization, mRNA could be detected in lung, sternum, brain, kidney and heart (Wagener et al., 1998). The broad tissue distribution is reminiscent of that of matrilin-2, and phylogenetic analyses show (Deak et al., 1999) that matrilin-4 and matrilin-2 descend from a common ancestor, further indicating a close relationship.

Matrilin-4 is often degraded and is actually seen as a ladder of bands in SDS-PAGE when isolated from tissue or cell culture (Klatt et al., 2001). This processing was studied in some detail. Recombinantly expressed matrilin-4 from human embryonic kidney-derived 293 (HEK-293) cells is found as a mixture of monomers, dimers and trimers (Klatt et al., 2001). Analysis of fragments by MALDI-TOF mass spectrometry and Edman degradation showed that the cleavage occurs at a distinct site in the short linker region which resides between the C-terminal VWA domain and the coiled-coil domain. The processing results in an almost complete subunit being released from the major part of the molecule consisting of the coiled coil together with remaining subunits. Similar linker regions occur also in the other matrilins, but it is noteworthy that in matrilin-1, which is the least sensitive to proteolysis, this linker is the shortest. At least for matrilin-4 it has been shown that fragments corresponding to those characterised for the recombinant protein occur also in tissue extracts (Klatt et al., 2001). It appears that this depolymerization is a physiological process and it may serve the purpose of decreasing the avidity of matrilins for their ligands and thereby cause a disassembly of supramolecular structures held together by matrilins.

1.3. Model organisms

Several model organisms, including mouse, xenopus, zebrafish, chicken, *Drosophila* and *C. elegans*, are widely employed in the search for gene function since each organism has its own advantages and disadvantages. Mouse is the animal model most often used because it is the species closest to human and therefore the gene function in mouse is most likely to mimic that in human. However, the complexity in gene regulation and the occurrence of compensation of one gene product for another often makes it difficult to elucidate the function of a certain protein. This may account for the lack of obvious phenotypes in some knockout mice. Hence, use of different model organisms might be required to unveil protein function.

As matrilins were found only in vertebrates, but not in *Drosophila* or in *C. elegans*, the zebrafish (*Danio rerio*), which is a powerful model organism for the study of vertebrate development, is the lowest animal in which matrilin function can be studied. The embryos develop rapidly, with all organs having been formed by 72 hpf (hours post fertilization). The externally developing embryos are optically clear and are produced in large numbers, therefore large-scale mutagenesis programs can be monitored by simple microscopic observation of the embryos (Haffter et al., 1996). A genome-sequencing project will be completed soon and human diseases that resemble mutations in zebrafish have been extensively analyzed (Shin and Fishman, 2002).

1.4. Zebrafish matrilins

In a screen of the zebrafish databases (NCBI and Ensembl) with sequences of mammalian matrilin VWA domains as query, we identified single orthologue genes for matrilin-1 and -4 and two orthologue genes for matrilin-3. Part of the work performed in my dissertation builds on this identification and both studies were published together (Ko et al., 2005).

In contrast to in mammals, no orthologue of matrilin-2 was found in zebrafish, either by RT (reverse-transcriptase) PCR using degenerated primers or by screening the

databases (Ensembl and NCBI); however, two forms of matrilin-3, matrilin-3a and -3b, are present. Phylogenetic trees show that the VWA domains of zebrafish are located in the same branches as the respective mouse domains, clearly showing that they are orthologues (Fig. 1-8). In apparent contrast to zebrafish, pufferfish (*Fugu rubripes*) contains a matrilin-2 gene.

The identity with the mammalian matrilins is more than 70% for the VWA domains and only 28% for the coiled-coil domains of matrilin-3a and -3b. All zebrafish matrilins show a greater variety of splice forms than in mammals, with splicing mainly affecting the number of EGF-like repeats.

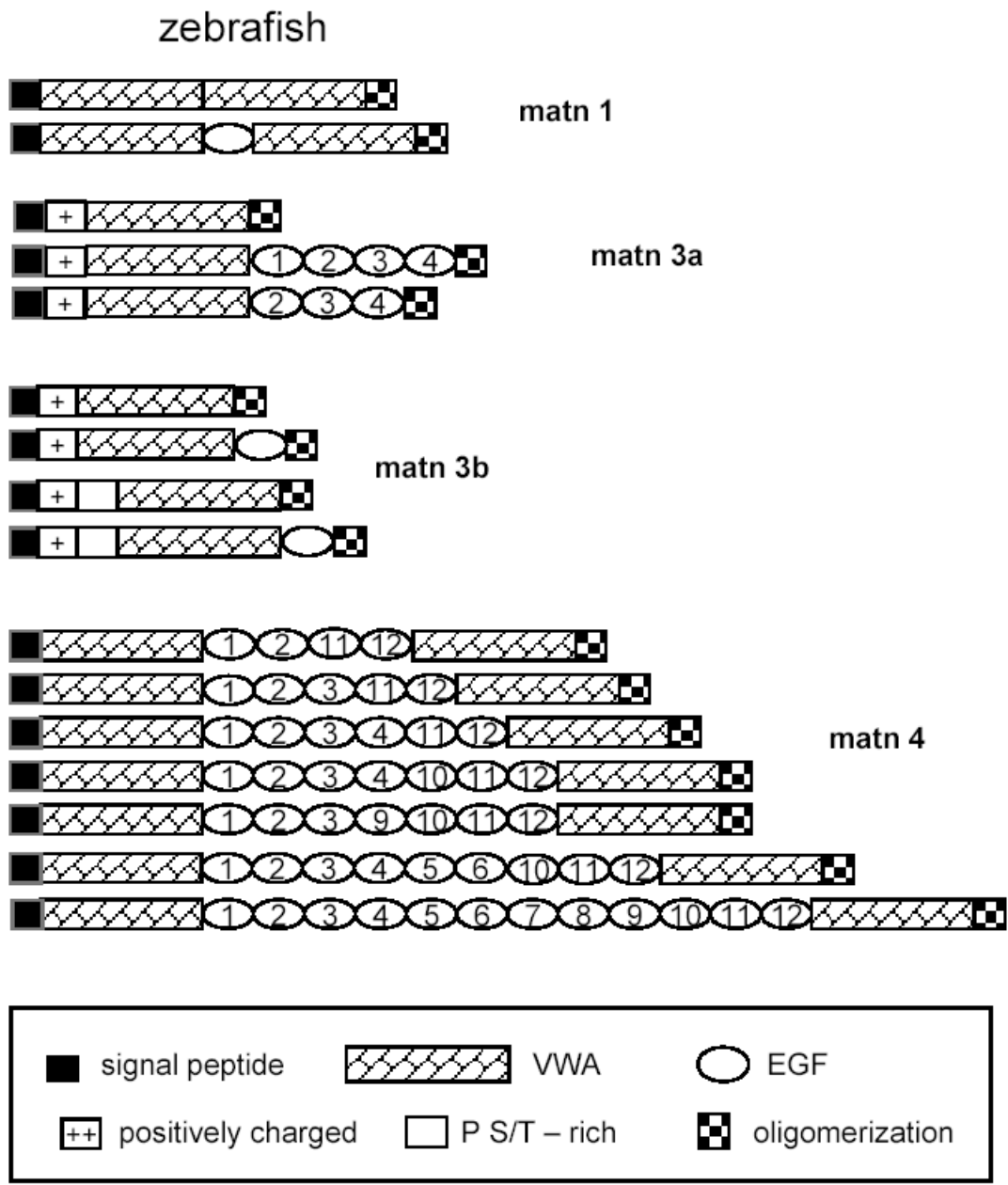


Fig. 1-7 Domain structure of zebrafish matrilins. matn, matrilin; P S/T –rich, proline- and threonine/serine-rich The figure is modified from (Ko et al., 2005).

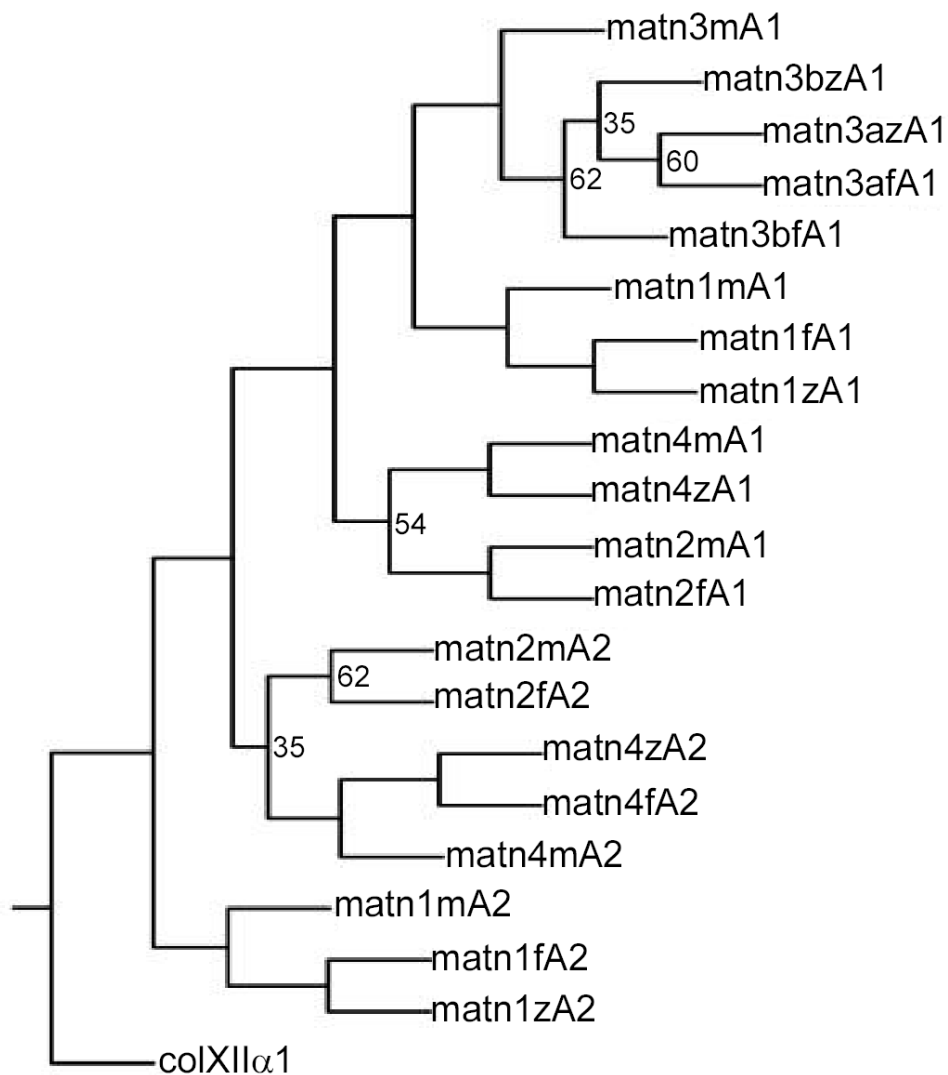


Fig. 1-8 Phylogenetic analyses of matrilin VWA domains. VWA domain amino acid sequences of zebrafish (z), pufferfish (*Fugu rubripes*) (f) and mouse (m) were aligned with the PILEUP program of the GCG package, using the default parameters. The VWA4 domain of human collagen XII α 1 (colXII α 1) was taken as an outgroup. The aligned sequences were used for the construction of a tree by the PROTPARS program of the PHYLIP package, version 3.5. Bootstrap support values were obtained with 100 replicates and are given at the respective nodes when the values are below 70%. The VWA domains of pufferfish (*Fugu rubripes*) were derived from the draft sequence of pufferfish (*Fugu rubripes*) genome, available as pufferfish (*Fugu rubripes*) assembly release 3. The genomic sequence of the VWA1 domain of pufferfish (*Fugu rubripes*) matrilin-4 is not yet available. matn, matrilin. The figure is from (Ko et al., 2005).

1.4.1. Matrilin-1

The mature secreted protein has a calculated M_r of 51,555. It comprises two VWA domains that are connected by a single EGF-like domain followed by an α -helical coiled-coil oligomerization domain, and therefore completely resembles the mammalian matrilin-1 (Fig. 1-7). Furthermore, by RT-PCR an alternatively spliced mRNA that lacks the EGF-like domain was also detected (Fig. 1-7).

1.4.2. Matrilin-3a

For matrilin-3a alternatively spliced cDNAs occur that contain sequences coding for three or four EGF-like domains (Fig. 1-7). In addition, an isoform exists that lacks the four EGF-like domains that in mammals connect the VWA domain and the C-terminal coiled-coil domain (Fig. 1-7). The longest cDNA encodes a protein of 480 amino acid residues with a calculated M_r of 53,006, the shortest protein of 295 amino acid with a calculated M_r of 32,811. The stretch of amino acid residues N-terminal to the VWA domain is conserved between mammalian matrilin-3 and zebrafish matrilin-3a, but with fewer positively charged amino acid residues in zebrafish.

1.4.3. Matrilin-3b

In a later screen of the genomic database, a second matrilin-3 gene was identified. RT-PCR yielded four alternatively spliced matrilin-3b cDNAs. The longest splice variant of matrilin-3b has an open reading frame of 1,437 bp that codes for a protein comprising 478 amino acid residues. After cleavage of a predicted signal peptide of 22 amino acid residues, the mature secreted protein has a calculated M_r of 50,136. The VWA domains of matrilin-3a and -3b are 80% identical at the amino acid level. Uniquely in a matrilin, a proline- and threonine/serine-rich sequence (Fig. 1-9) precedes the N-terminal VWA domain in matrilin-3b, which itself is followed by a single EGF-like domain and the C-terminal coiled-coil domain. The long unique N-terminal stretch of amino acid residues also contains a cluster of positively charged amino acid

residues (Fig. 1-7) similar to that in matrilin-3a. The matrilin-3b variant that lacks the proline- and threonine/serine-rich sequence and the EGF-like domain has the same domain structure as the shortest form of matrilin-3a, containing only the N-terminal positively charged stretch, a single VWA-domain and the coiled-coil domain. In addition, two isoforms exist that lack either the proline- and threonine/serine-rich sequence or the EGF-like domain (Fig. 1-7). The NetOGlyc server (<http://www.cbs.dtu.dk/services/NetOGlyc/>) predicted that the proline- and threonine/serine-rich sequence contains 33 potential mucin-type *N*-acetylgalactosamine O-glycosylation sites.

```

58  .....AHG FNPWFYSYHH PNPHQHHPQR PPWKGPPFIY HRPVPIQPVR
101  PISPVQPARP IVE■SLPRMPV VLPAP■TVPMP VKPIE■TLPPP PPP■STQ■ATTT
151  TTTT■ATT■ATT■ STTTTTTTST TTSQRV■STPR ATTAPAKP■T VPA.....

```

Fig. 1-9 Amino acid sequence of the proline- and serine/threonine-rich domain in zebrafish matrilin-3b. Predicted mucin-type *N*-acetylgalactosamine O-glycosylation sites are shaded black.

1.4.4. Matrilin-4

As in the mammalian matrilin-4, the two VWA domains are connected by EGF-like domains followed by the C-terminal coiled-coil domain (Fig. 1-7). Alternatively spliced mRNAs exist with different numbers of EGF-like domains, ranging from four to twelve (Fig. 1-7). The longest form has a calculated M_r of 102,576 and thereby has nearly the same M_r as mammalian matrilin-2.

1.4.5. Sequence analysis

The identity of zebrafish VWA domains with their mouse counterparts is 71–72% and the lengths of the VWA domains are strongly conserved. The matrilin-3 A1 domains perfectly fit to the MIDAS (metal ion-dependent adhesion site) motif consensus sequence (DXSXSXnTXnD), which is in contrast to human and mouse matrilin-3

where the threonine in the MIDAS motif has been exchanged for a serine residue.

Phylogenetic analysis did not allow construction of a tree of the zebrafish EGF-like domains with reasonable bootstrap values. Nevertheless, the zebrafish matrilin-4 EGF-like domains 7 and 8 are identical on the protein level and the domains 3, 4, 5, 6, 9, 10 and 11 are nearly identical, and are probably the products of recent duplication events. The identity of the orthologue EGF-like domains is lower than for the VWA domains with highest values of 66.7% for the EGF-like domain of zebrafish and mouse matrilin-1, 65% for the EGF-like domain 11 of zebrafish matrilin-4 and EGF-like domain 3 of mouse matrilin-4 and 55.8% for EGF-like domain 4 of zebrafish matrilin-3a and the EGF-like domains 1 and 4 of mouse matrilin-3.

All zebrafish matrilins contain a coiled-coil α -helix at the C-terminus, as predicted by the COILS program (Lupas et al., 1991). As for mouse matrilin-3, the agreement with the consensus is the lowest for zebrafish matrilin-3b, whereas matrilin-3a has a higher match. The coiled-coil domains of zebrafish and mouse matrilin-1 show an identity of 67%, whereas it is 48% for matrilin-4 and only 28% for each of matrilin-3a and -3b.

1.5. Gene silencing methods

Gene silencing by antisense oligonucleotides is increasingly used to achieve loss-of-function or knockdown of genes of interest and forms an attractive alternative to knockouts. Several antisense oligonucleotides with modified backbones have over the past decade been designed to improve specificity and efficacy (Braasch and Corey, 2002). However, their ability to provide unambiguous phenotypes has been debated and, in some instances, they have proven seriously flawed regarding specificity, cell toxicity, efficiency and efficacy (Braasch and Corey, 2002; Summerton and Weller, 1997). The discovery of RNAi was a breakthrough and, indeed, more than 3000 publications have used RNAi since 2002. In addition to RNAi, morpholino antisense oligonucleotides (short: morpholinos) have been in use since 2000 and the two techniques are considered as the most powerful antisense approaches.

1.5.1. RNAi

RNA interference (RNAi) is a gene silencing technique in which exogenous double-stranded RNA (dsRNA) that is complimentary to known targeted mRNA is introduced into a cell and triggers the degradation of that particular mRNA, thereby diminishing or abolishing gene expression (Hannon, 2002).

The specificity component of the RNAi machinery is small-interference RNA (siRNA). dsRNA is cleaved into ~23 bp siRNAs by dicer (Denli and Hannon, 2003), an enzyme that belongs to the RNase III family. Then the siRNA-dicer complex recruits additional components to form an RNA-Induced Silencing Complex (RISC) in which the unwound siRNA base pairs with complementary mRNA, thus guiding the RNAi machinery to the target mRNA resulting in the effective cleavage and subsequent degradation of the mRNA (Denli and Hannon, 2003; Hammond et al., 2000; Zamore et al., 2000) (Fig. 1-10).

The technique has proven effectively in *Drosophila* (Schwarz et al., 2002), *C. elegans* (Fire et al., 1998), plants (Hamilton and Baulcombe, 1999) and, recently, in mammalian cell culture (Chiu and Rana, 2002). The usefulness of RNAi in animal experiments and preclinical drug development remains to be established (Paroo and Corey, 2004).

Even though RNAi is considered as a powerful technique to elucidate the function of a gene in respect of efficiency, efficacy and cost, the real mechanism has been rather mysterious with regard to specificity. It has been observed that two classes of siRNA (21-22nt and 24-26nt) existing in plants differ not only in size but also in their mechanism of gene-silencing (Hamilton et al., 2002). The short siRNA (21-22 nt) is correlated directly with mRNA degradation whereas the long siRNA (24-26 nt) is involved in systemic silencing and DNA methylation (Denli and Hannon, 2003; Hamilton et al., 2002). In addition, micro RNAs (miRNAs) are also found to be processed by dicer from 70 nt pre-miRNA into a 22 nt mature form that can regulate gene expression either through mRNA degradation or translational repression which depends on the degree of the complementation to mRNA sequence (Bartel, 2004; Denli and Hannon, 2003). Nevertheless, siRNA and miRNA induced gene silencing through

mRNA degradation pathways are both mediated by the RNA-induced silencing complex (RISC) (Bartel, 2004). Therefore, it is difficult to distinguish which component accounts for the final gene silencing. The propensity for nonspecific effects is always the main concern in the antisense field. The frequent lack of proper and sufficient controls in papers describing the use of RNAi has been noticed (Anonymous, 2003).

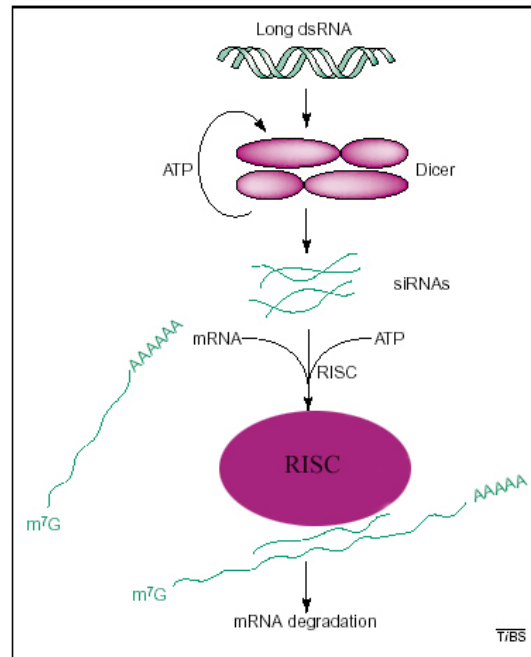


Fig. 1-10 Present model for the RNAi mRNA degradation pathway. Anti-parallel dicer dimers cleave long dsRNAs to form small-interfering RNAs (siRNAs) in an ATP-dependent manner. siRNAs are incorporated in the RNA-Induced Silencing Complex (RISC) and ATP-dependent unwinding of siRNAs activates RISC. Active RISC is thus guided to degrade the specific target mRNAs. The figure is modified from (Denli and Hannon, 2003).

1.5.2. Morpholino antisense oligonucleotides (morpholinos)

Morpholinos are non-ionic DNA analogs comprised of a nucleic acid base, a morpholine ring and a non-ionic phosphorodiamidate intersubunit linkage. (Fig. 1-11)

Morpholinos were first developed for clinical therapeutic applications, where previous antisense approaches had proven seriously flawed (Summerton and Weller, 1997). They were introduced into developmental biology as a tool to inhibit gene function in 2000 (Heasman et al., 2000), and since then they have been used by researchers in various model organisms, including sea urchin (Howard et al., 2001), xenopus (Heasman et al., 2000), zebrafish (Nasevicius and Ekker, 2000), chicken (Kos et al., 2001) and mouse (Coonrod et al., 2001). In addition, a successful and efficient delivery of morpholinos in adherent and nonadherent cultured cells has been reported (Morcos, 2001). Moreover, an entire issue of the journal “Genesis” (volume 30, issue 3, 2001) was dedicated to articles studying gene function in development using the morpholino approach.

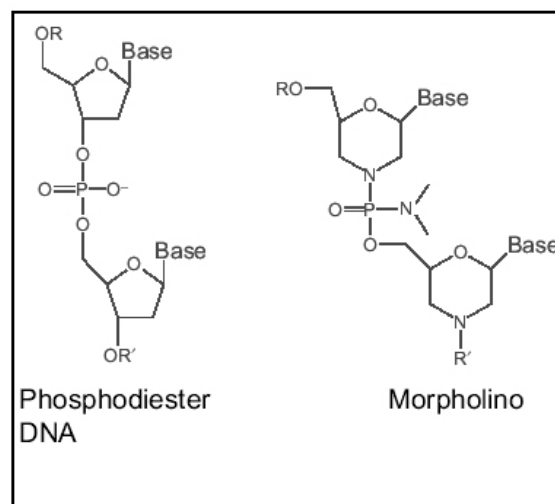


Fig. 1-11 Structure of DNA and morpholino oligonucleotides. The figure is from (Corey and Abrams, 2001).

In contrast to traditional antisense oligonucleotide approaches that utilize RNase H based degradation of mRNA as a mechanism of action, morpholinos do not recruit RNase H and thus the efficacy is achieved through nonclassical antisense approaches (Summerton, 1999; Summerton and Weller, 1997). It has been demonstrated that morpholinos are not subject to a wide range of nucleases (Summerton and Weller, 1997)

and that morpholinos are not degraded in the organism. As a consequence, there is no risk that modified nucleosides or nucleotides resulting from degradation of an antisense oligonucleotide might be toxic or might be incorporated into cellular genetic material and thereby lead to mutations and/or other undesired biological effects.

Moreover, the phosphorodiamidate linkage in morpholinos gives an excellent water solubility and provides a neutrally charged backbone which is less likely to interact with cellular proteins thus reducing the risk for non-specific side effect (Corey and Abrams, 2001; Ekker, 2000).

In summary, morpholinos have greater efficacy, specificity, solubility and stability than other antisense oligonucleotides (Heasman, 2002).

Morpholinos can function either through altering pre-mRNA splicing or inhibiting translation (Ekker and Larson, 2001). Binding of morpholinos to exon/intron junctions will lead to that an entire exon is left out, resulting in the formation of a non-functional mRNA (Fig. 1-12) (Ekker and Larson, 2001). These splice-blocking morpholinos have the advantage that the efficacy of the knockdown can be easily quantified using RT-PCR or standard RNA analysis techniques without the use of antibodies (Draper et al., 2001). It was observed that targeting of the splice donor boundaries gives a better knockdown than blocking at an splice acceptor site but the reason is unknown. Nevertheless, morpholinos targeting splice donor sites have produced pronounced phenotypes in zebrafish embryos (Draper et al., 2001; Yan et al., 2002).

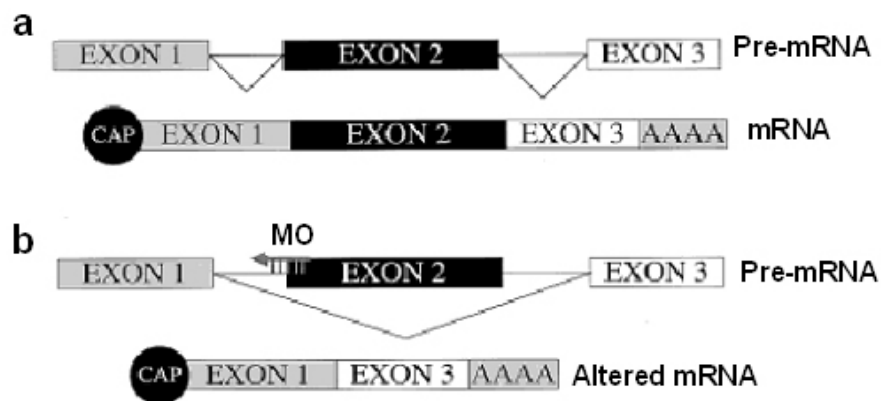


Fig. 1-12 The use of morpholinos in altering RNA processing. (a) Cartoon of RNA splicing events for an arbitrary gene. (b) One example of morpholino induced alterations in RNA splicing, exon skipping. The figure is from (Egger and Larson, 2001).

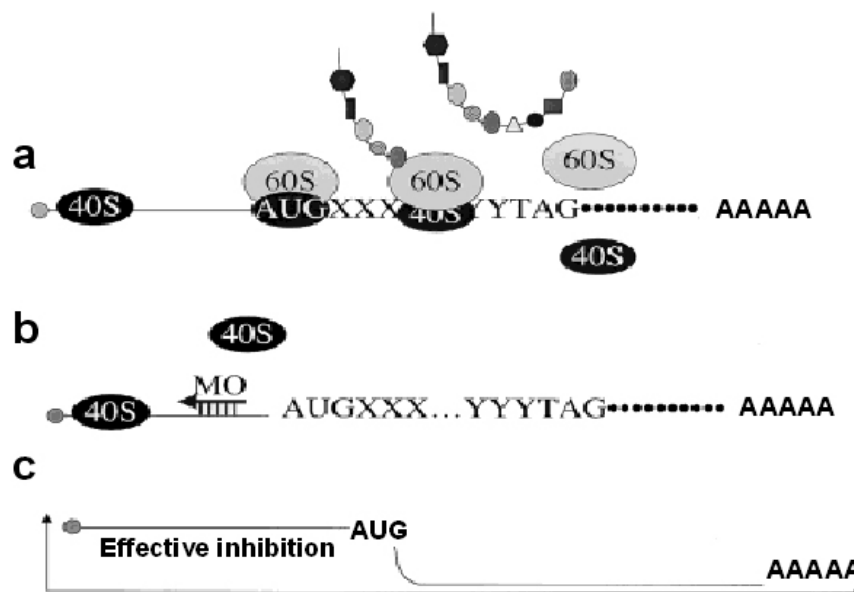


Fig. 1-13 The use of morpholinos (MO) for translational inhibition. (a) Cartoon of the translation of an arbitrary mRNA. The 40S ribosomal subunit scans the leader sequence, identifies the start codon, and then recruits the 60S subunit for polypeptide synthesis initiation. (b) Binding of an MO to the 5' end of the gene inhibits the scanning process and translation. (c) Effective target selection for morpholino. The figure is from (Egger and Larson, 2001).

Translational inhibition is the other morpholino targeting strategy. Morpholinos with a sequence selected to target the leader sequence or nearby bases can sterically inhibit scanning of the mRNA by the 40S ribosomal subunit and subsequently result in translational inhibition (Fig. 1-13). Efficacy appears restricted to target sites within the leader sequence and sequences surrounding the start codon (Fig. 1-13 C) (Egger and Larson, 2001; Summerton, 1999). Once translation has been initiated, morpholinos are not capable of altering the activity of ribosome complex. Binding of morpholinos to mRNA does not appear to facilitate or retard mRNA degradation (Nasevicius and Egger, 2000). Hence, the efficacy of translational-inhibition morpholinos should be evaluated at the protein level instead of the mRNA level.

1.6. The aims of the dissertation

Despite the increased biochemical information on matrilin interactions, the detailed *in vivo* functions are not known. It is clear that matrilins serve as adaptors in the assembly of supramolecular structures in the extracellular matrix, but it is not known if this role is static or dynamic in nature. Matrilins therefore need to be studied in genetic models. Matrilin-3 deficient mice were generated in collaboration with Dr. A. Aszodi, Martinsried, and one aim of this dissertation was to characterize the matrilin-3 gene function in these null mutation mice.

However, the redundancy within the family has caused problems in this regard and the two single gene inactivations performed so far for matrilin-1 and -2 have not yielded any change in phenotype. These studies are at present being continued through the establishment of double knockouts. Matrilin-1/-3 double knockout mice were generated and the biochemical analysis of these mice was the second aim of this dissertation.

Since matrilins are neither found in *Drosophila* nor in *C. elegans* but are present in vertebrates, the zebrafish was chosen as a second model organism and gene silencing by use of morpholinos employed as an alternative way to elucidate matrilin function.

2. Materials and Methods

2.1. Characterization of matrilin-3 deficient mice

2.1.1. Genotyping by PCR

The genotype of offspring from heterozygous mice was screened by PCR. Mouse tails (0.5 cm) were digested with 1 mg/ml proteinase K in 1xPCR buffer at 55°C for 3-5 hours till all tissues were lysed. 0.5 ul of clear supernatant, which contains genomic DNA, was obtained by centrifugation and used for the PCR reaction. DNA polymerase and 10x PCR-buffer were from the Expand High Fidelity PCR kit (Roche).

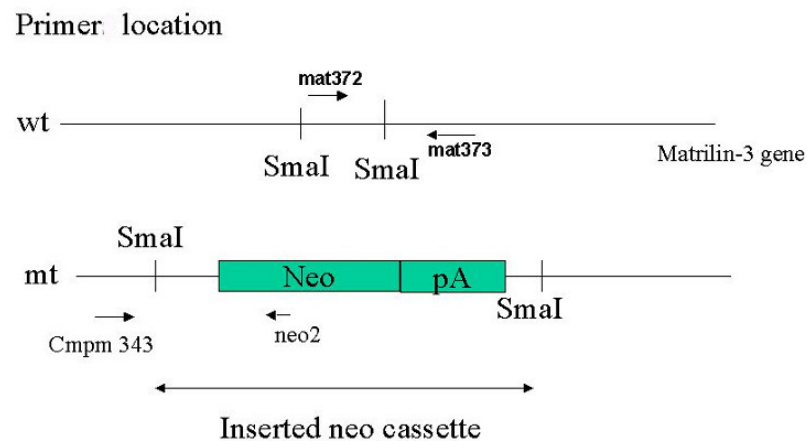


Fig. 2-1 Primer location.

The following specific primers were used.

Designation	Sequence (5'-3')	Direction
mat 372	GCT GAG ACC TCT GAC CCT GTG	forward
mat 373	GGA AGT AGC CAG AGC AGA GAG AT	reverse
cmpm 343	TGC CAC TGG AAT GCA CAG AC	forward
neo2	CCT TCC CGC TTC AGT GAC	reverse

The PCR products were electrophoresed on a 2% agarose gel. The expected sizes were 245 base pairs for the wildtype allele and 836 base pairs for the mutant allele.

Genotyping PCR program:

Step	Time
Initial denaturation	95°C, 5 min
Cycle (5 cycles):	
Denaturation	95°C, 45 sec
Annealing (decrease 1°C per cycle)	64-60°C, 45 sec
Elongation	72°C, 2 min
Cycle (35 cycles):	
Denaturation	95°C, 45 sec
Annealing	59°C, 45 sec
Elongation	72°C, 2 min
Final elongation	72°C, 10 min
Cooling	4°C

2.1.2. Genotyping by Southern blot

2.1.2.1. Dig-labeled probe for Southern blot

The Dig-labeled nucleic acid probes were used for Southern blot analysis. The Dig-labeling was performed by using "PCR Dig probe synthesis kit" from Roche. The 1:3 ratio (Dig-dUTP : dTTP) in the Dig probe synthesis mix worked well for labeling probes up to 1 kb long. 210 ng of matrilin-3 cDNA (clone 16) was used as template and two primers, cmpm 31 and cmpm 37, located in VWA domain were used for PCR. The expected fragment size was 477 bp. The synthesized probe was stored at -20°C .

The PCR products were electrophoresed on a 2% agarose gel and the yield of PCR products was about 20 ng/ul. No further purification was needed. 0.25 ul of Dig-labeled PCR products was tested (con. 0.5ng/ml) and worked in the Southern blot analysis.

<u>Dig-labeling PCR mix</u>		<u>Dig-labeling PCR program</u>	
Template	210 ng	Initial Denaturation	95°C, 2 min
10xPCR-buffer with 15 mM MgCl ₂	2.5 ul	Cycle(30 cycles):	
PCR Dig mix (vial 2)	0.5 ul	Denaturation	95°C, 45 sec
DNA polymerase (vial 1)(3.5 U/ul)	0.6 ul	Annealing	47°C, 1 min
10 uM cmpm31	1 ul	Elongation	72°C, 1 min
10 uM cmpm31	1 ul	Elongation	72°C, 10 min
H ₂ O	36.9 ul	Cooling	4°C

2.1.2.2. Genomic DNA extraction

Murine genomic DNA was prepared from mouse tails (~1 cm) by incubating with 700 ul lysis buffer (10 mM Tris-HCl, pH 7.5; 0.1 M EDTA, pH 8.0; 0.5% SDS) containing 1 mg/ml proteinase K (Sigma) at 55°C for 3-5 hours till all tissues were lysed and became soft. The extracts were cleared by centrifugation and proteins were removed by applying ½ volume of phenol and chloroform. Genomic DNA was precipitated from the aqueous phase with 1 volume of isopropanol and pellets were washed with 70% EtOH and further dissolved in 50 ul double-distilled water.

2.1.2.3. Restriction enzyme digestion

*Bst*XI (purchased from BioLabs) digested murine genomic DNAs were used for Southern blot analysis. The restriction enzyme digestion mixture was prepared and incubated at 55°C overnight. Digested DNAs were electrophoresed on 0.7% agarose gels.

2.1.2.4. Southern blot

DNAs were then depurinated by submerging the gel in 0.25 M HCl, with shaking at room temperature, for up to 10 min until the bromophenol blue marker changed from blue to yellow. Then the DNAs were denatured in denaturation solution twice for 15 min. The gel was submerged twice in neutralization buffer for another 15 min each in order to stop the denaturation reaction. Then the gel was equilibrated in 20x SSC buffer for 10 min. The blot transfer was set up by placing the gel on top of a sheet of Whatman 3 MM paper soaked with 20x SSC solution. A piece of Roti®-Nylon plus membrane (Roth) to the size of the gel was placed on the DNA-containing surface of the gel, avoiding the formation of air bubbles. The blot assembly was completed by adding a dry sheet of Whatman 3MM paper, a stack of paper towels, a glass plate, and a weight of 200 – 500 g. The blot was transferred overnight at room temperature in 20x SSC

buffer. DNAs were subsequently fixed to the membrane by UV cross-linking.

Prehybridization was done with 20 ml hybridization buffer only (without probe) in heat-sealed plastic bags at 42°C for 2 hours. The blot was hybridized with 5 ng/ml of the Dig-labeled DNA probe for final concentration.

The appropriate amount of labeled probe was withdrawn and diluted into 50 ul of double-distilled water in a microcentrifuge tube. The probe was denatured in boiling water for 5 min then quickly chilled in an ice bath. The denatured probe was then immediately added to a tube containing the appropriate amount of hybridization buffer, prewarmed to 42°C and mixed by inversion to form the hybridization solution. The amount of hybridization buffer was according to the size of the blot membrane (3.5 ml per 100 cm²).

In order to remove unbound probe, the blot was first washed with low stringency washing buffer in a plastic tray twice for 5 min each at room temperature and subsequently with high stringency washing buffer twice for 15 min each at 65°C with agitation.

The hybridization solution was stored in a tube at -20°C and could be reused 3-5 times. When reusing the probe, it was denatured at 68°C for 10 min and chilled on ice for another 10 min.

After incubation with an anti-Dig Fab fragment antibody (1:20,000) for another 30 min, the blot was washed twice in washing buffer for 15 min and equilibrated in detection buffer for 2 min. Detection was done with CDP-ready-to-use (Roche) substrate.

2.1.3. Whole mount skeletal staining

Newborn mice were deskinning and eviscerated, fixed in 95% EtOH for 3 days, and then transferred into acetone for 1 day. Staining was performed in a solution of 90% EtOH, 5% acetic acid, and 5% H₂O supplemented with 0.005% alizarin red S (Sigma) and 0.015% alcian blue 8GS (Sigma) for 3 days at 37°C. Samples were rinsed in water

and cleared for 3 days in 1% potassium hydroxide followed by clearing in 0.8% KOH–20% glycerol for 1 week. Samples were then transferred into 50, 80, and finally 100% glycerol for long-term storage.

2.1.4. Immunohistochemistry

For immunohistochemistry, knees dissected from newborn or 4-week-old animals were fixed overnight at 4°C in 95% EtOH / 5% acetic acid, dehydrated in absolute EtOH, and embedded in paraffin. Deparaffinization ensued through incubation twice for 5 min in xylol. After rehydration, endogenous peroxidases were inhibited in 97% methanol/ 0.9% H₂O₂ at room temperature for 25 min and sections then briefly washed with PBS three times for 5 min each. The sections were digested with 0.2% bovine testicular hyaluronidase in PBS, pH 5.0, at 37°C for 20 min. After three washing steps, the sections were blocked for 1 h with 1% (w/v) bovine serum albumin (BSA) in PBS, pH 7.2, together with goat serum from ABC kit (3 drops in 10 ml BSA/PBS), then incubated with primary antibodies against matrilin-1, -2, -3, -4, collagens II, IX, X or aggrecan overnight at 4°C. The primary antibodies were visualized by consecutive treatment of sections with biotinylated secondary antibodies at 37°C for 1 h followed by avidin-biotin-complex (ABC) reagent (Vectastain) treatment at room temperature for 30 min. Color was developed by using fresh 3, 3'- diaminobenzidine (DAB) (Sigma) staining solution for 5-10 min. The reaction was stopped by rinsing sections in water, dehydrating in absolute EtOH, clearing in xylol and mounting in Entellan (Merck) solution. All antibodies were diluted in 1% (w/v) BSA/ PBS.

<u>Antibodies</u>	<u>Dilution</u>	<u>Property</u>
rabbit anti-matrilin-1	1:400	polyclonal, affinity purified
rabbit anti-matrilin-2	1:400	polyclonal, antiserum
rabbit anti-matrilin-3	1:400	polyclonal, affinity purified
rabbit anti-matrilin-4	1:800	polyclonal, affinity purified
rat anti-collagen II	1:600	polyclonal, affinity purified
rabbit anti-collagen IX	1:400	polyclonal, affinity purified
rabbit anti-collagen X	1:800	polyclonal, affinity purified
rabbit anti-aggrecan	1:400	polyclonal, affinity purified

<u>DAB staining solution</u>	<u>Stock I</u>	<u>Stock II</u>
5 ml DAB stock (stock I)	27 mg DAB/ 5 ml dest. water	100 ul 30% H ₂ O ₂ / 0.5 ml dest. water
45 ml dest. water		
50 ml Tris-HCl (pH 7.6)		
120 ul stock II		

2.1.5. Northern blot

Total RNA was isolated from newborn mouse limb cartilage with the Qiagen RNeasy kit according to the instructions of the manufacturer. For northern analysis, 5 ug of total RNA was size fractionated on a 1% agarose–2.2 M formaldehyde gel and blotted to a Hybond XL membrane (Amersham). The membrane was consecutively hybridized with ³²P-labeled cDNA probes specific for mouse *matn-1*, *matn-2*, *matn-3*, *matn-4*, or *GAPHD* (glyceraldehyde phosphodehydrogenase).

2.1.6. In situ hybridization

Nonradioactive in situ hybridization on tissue sections for mouse indian hedgehog (*Ihh*), and parathyroid hormone/ parathyroid hormone-related peptide receptor (*Ppr*) mRNA was performed as described (Brandau et al., 2002). Briefly, newborn limbs were fixed in 4% PFA in Tris-buffered saline (TBS) (pH 9.5) and subsequently dehydrated and embedded in paraffin. Six-um-thick sections were dewaxed, rehydrated, rinsed in TBS (pH 7.4), and postfixed with 4% PFA-TBS (pH 9.5) for 10 min. Sections were rinsed in TBS (pH 7.4), treated with 10 ug of proteinase K/ml for 30 min at 37°C, acetylated with 0.25% acetic anhydride for 10 min, washed three times in TBS (pH 7.4), and dehydrated in an ascending EtOH series. Air-dried sections were hybridized with Dig-UTP-labeled antisense riboprobes overnight at 52°C. After hybridization, sections were washed three times for 30 min each at 55°C in 50% formamide, 2x sodium citrate-chloride buffer (SSC [1xSSC is 0.015 M sodium citrate and 0.15 M NaCl]), and twice in 1xSSC for 15 min at room temperature. The sections were then incubated with an alkaline phosphatase-coupled antibody against Dig (Roche) diluted 1:500 in TBS (pH 7.4) containing 2% sheep serum and 0.1% Triton X-100 for 2 h at room temperature. After rinsing in TBS (pH 7.4), color detection was performed according to the manufacturer recommendation. Radioactive in situ hybridization was performed as described previously (Aszodi et al., 1998) using [³³P]UTP-labeled riboprobes against *Matn-3*.

2.1.7. Hematoxylin-eosin staining

For histological analysis, knees or tails dissected from newborn, 4-week-old, 8-week-old, 12-week-old, 6-month-old and 9-month-old mice were fixed overnight in fresh 4% paraformaldehyde in phosphate-buffered saline (PBS, pH 7.2), washed with PBS, dehydrated in a graded alcohol series, and embedded in paraffin. Samples from mice analyzed after birth were decalcified in 10% EDTA-PBS for one week. After embedding in paraffin, sections were cut at 6 to 8 um and stained with hematoxylin-eosin.

2.1.8. Van Kossa staining

The classic van Kossa silver method is used to stain the mineral component in bone, calcium phosphate, and is a negative stain for osteoid with the calcium component blackened by silver deposition. Nuclei are counterstained red by safranin O. Here a modified van Kossa's method for detecting mineralized bone was used.

Paraffin embedded sections from knees dissected from newborn mice were deplasticized with xylol, and hydrated in distilled water. The sections were placed in silver nitrate solution (5% in H₂O), exposed to strong light for 1 h and the reaction terminated when the mineralized bone turned dark brown to black. Sections were washed in distilled water three times, 1 min each, then treated with sodium thiosulfate (5% in H₂O) for 2 to 3 min and washed intensively in distilled water for 2 min. Counterstaining was performed in 0.5% safranin O solution (0.35 g in 100 ml distilled water) for 20 to 30 sec.

2.1.9. Safranin orange staining

Safranin O staining was used to stain proteoglycans in the cartilage sections. Paraffin embedded cartilage sections which had been decalcified in 10% EDTA were deplasticized with xylol and hydrated in distilled water. Sections were incubated in Weigert's iron hematoxylin solution for 3 min and washed in distilled water a few times until there was no color present in the water. Then the sections were immersed in 1 % HCl-EtOH and washed immediately in distilled water for 10 min. The sections were placed in 0.02 % fast green solution for 12 to 15 min and washed again with distilled water. The muscle in the section started to become green in this step. The sections were then incubated in freshly prepared 1 % acetic acid for 5 min and washed in distilled water. Counter staining was performed by use of 0.5 % safranin O solution for 2-3 min until the growth plates turned red. The muscle presented a blue color after counter staining.

The safranin O solution could be stored for 2-3 days. Solutions were prepared freshly when the red color in cartilage became too weak.

<u>Weigert's solution</u>	<u>Stock A</u>	<u>Stock B</u>	
mix stock A and stock B	1 g hematoxylin	FeCl ₂ · 6H ₂ O	2 g
in 1:1 ratio.	100 ml EtOH	25 % HCl	1 ml
		distilled water	95 ml

2.1.10. TRAP staining

Osteoclasts activity was detected through staining for tartrate-resistant alkaline phosphatase (TRAP) by using a leukocyte acid phosphatase kit (Sigma). Paraffin embedded sections of knees dissected from newborn mice were deplasticized with xylol and hydrated in PBS. The slides were incubated in a cuvette which contained solution A (see below) at 37°C for 1 h, protected from light. After 1 hour, the slides were rinsed thoroughly in deionized water and mounted in Aquamount solution.

<u>Solution A</u>	<u>Diazotized fast garnet GBC</u>
45 ml 37°C deionized water	Mix 0.5 ml fast garnet GBC base solution with 0.5 ml sodium nitrite solution by gentle inversion for 30 sec and let stand for 2 min
1 ml diazotized fast garnet GBC	
0.5 ml naphthol AS-BI phosphate solution	
2 ml acetate solution	
1 ml tartrate solution	

2.1.11. Glycosaminoglycan assay

The stable dimethylmethylene blue (DMB) solution was prepared by dissolving 21 mg of DMB in 5 ml of absolute EtOH containing 2 g of sodium formate. The volume was set to 1 liter with distilled water and the pH was adjusted to 1.5 using concentrated formic acid.

The standard curve was made with serial 1:2 dilutions of chondroitin 6-sulfate (c-6-5, Fluka, cat no 27043) in water with 10 mg/ml as starting concentration. Samples from cartilage extractions were precipitated with 96% EtOH and dissolved in 100 μ l of 4 M GuHCl.

The glycosaminoglycan-dimethylmethylene blue complex was not stable and started to aggregate as soon as glycosaminoglycan and dye were mixed. This was seen as a slow, progressive decrease of absorbance at 525 nm during the first 10 min. Vigorous mixing accelerated the precipitation process. Therefore, 100 μ l of each chondroitin 6-sulfate dilution or sample were first placed in disposable plastic cuvette, 625 μ l of DMB solution gently added to the cuvette and the sample then mixed by gently pipetting up and down once. The absorbances were determined at 525 nm and measured 15 sec after mixing.

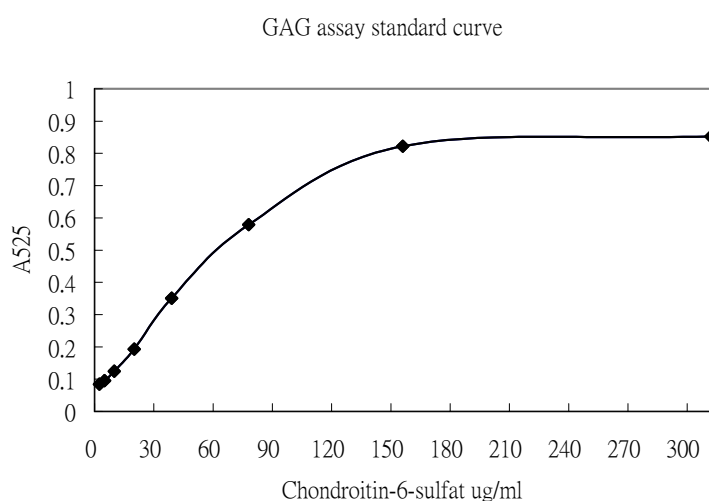


Fig. 2-2 Standard curve of glycosaminoglycan assay.

2.1.12. Cartilage extraction

Knee joints and sterna were dissected and frozen at -80°C . On the day of extraction, the specimens were cut into 1 mm^3 pieces. 10 ml volumes of chilled buffer 1 (0.15 M NaCl, 50 mM Tris, pH 7.4) were added per gram of wet tissue and the tissue was extracted for 7 to 10 h at 4°C with continuous mixing. The extracts were clarified by centrifugation, and the supernatants stored at -20°C . The pellets were reextracted in an identical manner with buffer 2 (1 M NaCl, 10 mM EDTA, 50 mM Tris, pH 7.4), and the remaining insoluble material extracted with buffer 3 (4 M GuHCl, 10 mM EDTA, 50 mM Tris, pH 7.4). All extraction buffers contained 2 mM phenylmethylsulfonyl fluoride and 2 mM *N*-ethylmaleimide. 100 μl aliquots of the extracts obtained with buffers 1, 2, and 3 were precipitated with 1 ml of 96% EtOH overnight at 4°C . The precipitates were washed with a mixture of 9 volumes of 96% EtOH and 1 volume of TBS for 2 h at 4°C with gentle agitation. After centrifugation, the pellets were air dried and suspended in 150 μl of water and the same volume of 2x nonreducing SDS-PAGE sample buffer was added. Aliquots were applied to 4-15% SDS-polyacrylamide gels. SDS-PAGE was performed as described by Laemmli (Laemmli, 1970).

2.1.13. Western blot

Western blots were conducted according to standard protocols with some minor modifications. After being separated in SDS-PAGE, proteins were electrically transferred to nitrocellulose membrane in 10% methanol/ 50mM boric acid, pH 8.5, at 400 mA for 1 hour or 100 mA over night in the cold room. After confirming transfer efficiency and protein load by Ponceau S staining, the membrane was blocked with 5% low-fat milk powder in TBS for 20 min. Subsequently, appropriate affinity-purified rabbit antibodies diluted in TBS were applied. Bound antibodies were detected by luminescence using peroxidase-conjugated immunoglobulin G (Dako), 3-aminophthalhydrazide (1.25 mM), p-coumaric acid (225 μM), and 0.01% H_2O_2 . The "Super RX" film from Fuji was used for exposure.

<u>Antibodies</u>	<u>Dilution</u>	<u>Property</u>
rabbit anti-matrilin-1	1:500	polyclonal, affinity purified
rabbit anti-matrilin-2	1:500	polyclonal, antiserum
rabbit anti-matrilin-3	1:400	polyclonal, affinity purified
rabbit anti-matrilin-4	1:500	polyclonal, affinity purified
rabbit anti-rat COMP	1:1600	polyclonal, antiserum
mouse anti-chick collagen II	1:1000	monoclonal antibody; II-II6B3
rabbit anti-mouse biglycan	1:3000	LF-106, from NIH, Dr. L. Fisher, antiserum
rabbit anti-mouse decorin	1:1000	LF-113, from NIH, Dr. L. Fisher, antiserum

2.2. Characterization of matrilin-1/-3 double null mice

2.2.1. Double fluorescence analysis for matrilin-4 and -1 in western blots of cartilage extracts

Knee and sternal protein extracts derived from newborn and 4-week-old mice were dissected as described for matrilin-3 single null mice. Proteins were separated by non-reducing SDS polyacrylamide gel electrophoresis and subsequently blotted onto a nitrocellulose membrane. Specific antibodies against matrilin-4 and matrilin-1 raised in different species were applied. Bound antibodies were detected by infrared fluorescence using Alexa Fluor® 680-labeled anti-rabbit (Molecular Probes) and IRDye™ 800 conjugated affinity purified anti-chicken immunoglobulin G (Rockland). The fluorographs were developed with the ODYSSEY infrared imaging system (LI-COR Biosciences)

Antibodies	Dilution	Property
chicken anti-bovine matrilin-1	1:50	polyclonal, affinity purified
rabbit anti-mouse matrilin-4	1:500	polyclonal, antiserum
IRDye-800 anti-chicken IgG	1:10,000	green fluorescence; Rockland
Alex-680 anti-rabbit IgG	1:10,000	red fluorescence; gift from Prof. T. Langer

2.3. Characterization of zebrafish matrilins

2.3.1. Expression and purification of recombinant matrilin-1, -3a, -3b and -4 VWA1 domains

cDNAs coding for zebrafish matrilin-1, -3a, -3b and -4 VWA1 domains were generated by PCR on the full-length cDNA. Suitable primers (see Table) introduced 5'-terminal *NheI* and 3-terminal *NotI* restriction sites. The cDNA was inserted into the expression vector pCEP-Pu downstream of the sequences encoding the BM-40 signal peptide (Kohfeldt et al., 1997) and an N-terminal His₆-tag (Smyth et al., 2000). The recombinant plasmids were introduced into HEK-293/ EBNA (Epstein–Barr nuclear antigen) cells (Invitrogen) by transfection with FuGENE™ 6 (Roche). Following selection with puromycin (1 ug/ml) the cells were transferred to serum-free medium for harvesting of the recombinant protein. After filtration and centrifugation (1 h, 10,000g), cell culture supernatants containing the N-terminally His₆-tagged matrilin-1, -3a and -4 VWA1 domains were applied to TALON metal affinity columns (1 ml; BD Biosciences). After washing with 5 mM imidazole in buffer A (0.1 M NaCl, 20 mM Tris, 50 mM NaH₂PO₄, pH 8.0), the bound protein was eluted with 0.25 M imidazole in buffer A containing 0.2% sodium azide. The purity of proteins was further confirmed by electrophoresis on

a 12% SDS-polyacrylamide gel.

In the case of purification of matrilin-4 VWA1 domain, fast protein liquid chromatography (FPLC) was applied since an albumin contamination was observed in the fraction eluted from the TALON metal affinity column. A column of Superdex 200 HR 10/30 (Amersham Pharmacia) was employed and saturated in buffer A (0.1 M NaCl, 20 mM Tris, 50 mM NaH₂PO₄, pH 8.0) with a flow rate of 0.5 ml/ min. Protein purity was further confirmed by electrophoresis on a 12% SDS-polyacrylamide gel before immunization.

Primers for expression VWA1 domains of zebrafish matrilins

Designation	Sequence (5'-3')	Direction
zmat1F	CAATGCTAGCAGGTCTGTGTAACACCAAGCCCAC	forward
zmat1R	CAATGCGGCCGCTTAACCGCACAATGTCTCCCGG	reverse
zmat3aF	CAATGCTAGCTACAGATTCACAGTGTAGG	forward
zmat3aR	CAATGCGGCCGCTTAACCGCACAATGTCTCCCGG	reverse
zmatn3bF	CAATGCTAGCAGAGCCCTGCAAGAG	forward
zmatn3bR	CAATGCGGCCGCTTAACCACAGAGCGTTTCCC	reverse
zmat4F	CAATGCTAGCGTGTAATCTGGCCCGGTTG	forward
zmat4R	CAATGCGGCCGCTTACCGCAGAGCTTGTCTTGG	reverse

2.3.2. Preparation of antibodies against matrilin-1, -3a and -4

The purified matrilin-1, -3a and -4 VWA1 domains were used to immunize rabbits. The antisera obtained were purified by affinity chromatography on columns with the original antigens coupled to CNBr-activated Sepharose (Amersham Biosciences). The specific antibodies were eluted with 0.1 M glycine, pH 2.5, and the eluate was immediately neutralized through addition of 1 M Tris-HCl, pH 8.8.

Since cross-reactivity of antisera with other members of the matrilin family was observed, affinity purified antibody against for example matrilin-4, was first depleted by applying it to affinity chromatography columns containing bound matrilin-1 and matrilin-3a with a slow flow rate of 100 ul/ min in the cool room in a closed system for about 30 hours. Then the flow through, which should contain antibodies against matrilin-4, was collected. The cross-reactivity was checked by ELISA analysis.

2.3.3. Determination of cross-reactivity of antibodies against each matrilin with the other matrilins

ELISA analysis was performed to test for cross-reactivities. Affinity purified recombinant VWA1 domain matrilin proteins were coated with 0.5 ug/ well on immunoplates (Nunc F96 Max sorp, cat. 442402) at 37°C for 4 hours. After blocking with 5% low-fat milk powder dissolved in PBS, 100 ul/ well of a serial dilution of affinity purified antibodies were added and further incubated at 37°C for another hour. Subsequently alkaline phosphatase-conjugated swine anti-rabbit IgG (Dako) was applied for one hour. After a 30-min incubation with the substrate, 4-nitrophenylphosphate disodium salt hexahydrate (pNPP) (Fluka 71768), bound antibodies were determined in an ELISA reader at 405 nm. The substrate was dissolved in 10% diethanolamin/ 0.5 mM MgCl₂, pH 9.8.

A strong cross-reactivity of antibodies against matrilin-1 with the matrilin-3b VWA1 domain was observed and it was not possible to deplete this cross-reactivity on a matrilin-3b affinity column. Therefore a preincubation of the antibody with recombinant matrilin-3b VWA proteins was performed in order to eliminate the matrilin-3b titer. Serially diluted antibodies against matrilin-1 were incubated with 0.1 ug/well of recombinant matrilin-3b VWA1 protein at 37°C for 3 to 4 hours prior to application to the ELISA plate. Other procedures were as in the ELISA protocol above.

2.3.4. Determination of cross-reactivity of the antibody against matrilin-3a with matrilin-3b

Cell culture supernatant of HEK-293/EBNA cells transfected with cDNA coding for the zebrafish matrilin-3b VWA1 domain was subjected to SDS/PAGE together with a dilution series of purified zebrafish matrilin-3a VWA1 domain. After transfer onto nitrocellulose the immunoblot was incubated with the affinity-purified zebrafish matrilin-3a specific antibody diluted in TBS containing 5% low fat milk powder. The bound antibodies were detected by luminescence using peroxidase-conjugated swine anti-rabbit IgG (Dako), 3-aminophthalhydrazide (1.25 mM), p-coumaric acid (225 uM) and H₂O₂ (0.01%).

2.3.5. Whole mount immunostaining

Zebrafish larvae [5 dpf (days post fertilization)] were fixed overnight at 4°C in 4% PFA in PBS, pH 7.4, washed in PBT (PBS containing 0.1% Tween) and finally washed and stored in methanol at -20°C. To bleach pigment and block endogenous peroxidases, larvae were incubated overnight in 3 ml of 10% H₂O₂ in methanol, then 10 ml of PBT was added and the incubation continued for further 16 to 24 h. Larvae were washed in PBT, digested with 2 ug/ml proteinase K for 8 min and fixed again in 4% PFA for 15 min. After washing, larvae were treated with hyaluronidase (Sigma; 500 units/ml in 0.1 M NaH₂PO₄, 0.1 M sodium acetate, pH 5.0) at 37°C for 2 h and blocked in 3% normal goat serum for 2 h. Affinity purified antibodies were applied at appropriate dilutions

(matrilin-1 and -3a, 1:1000; matrilin-4, 1:500) and the specimens were incubated for 2 h.

The primary antibodies were visualized by consecutive treatment of larvae for 2 h each with the biotinylated secondary antibody and a streptavidin–peroxidase conjugate (ABC kit, Vectastain). All antibodies were diluted in 3% (w/v) normal goat serum in PBT. For color development, larvae were pre-soaked in diaminobenzidine (0.2 mg/ml PBT) for 30 min and 1 ul of 0.3% H₂O₂ solution was added while the larvae were observed under a dissection microscope. For detailed analysis, larvae were post-fixed in 4% PFA for 15 min, washed in PBT and gradually transferred into 90% glycerol. Except for when indicated, all procedures were carried out at room temperature (20°C). Occasionally, specimens were kept overnight at 4°C between steps in the staining procedure.

2.3.6. Immunostaining on sections

Adult fish were euthanized by an over dose of ethyl-m-aminobenzoate methanesulfonate (tricaine) and fixed in 4% PFA/PBS over night at 4°C. After washing with PBS twice, 45 min each, fish were dehydrated in 70%, 80%, 90% and 96% EtOH for 10 min each and finally in 100% EtOH for 20 min twice. Subsequently, fish were incubated in 50% xylol/50% EtOH for 20 min and then in 100% xylol twice for 20 min each. Next, paraffin type 3 (Richard-Allan Scientific) was allowed to penetrate fish for at least 1h at 68°C followed by paraffin type 6 (Richard-Allan Scientific) for a few hours. Finally, fish were embedded in paraffin type 6 and stored at 4°C.

Immunostaining was performed on paraffin-embedded sections of 5 dpf and 4-month-old zebrafish. Sections were deparaffinized by two 5-min incubations in xylol. After rehydration in PBS, the sections were digested with hyaluronidase (500 units/ml in 0.1 M NaH₂PO₄, 0.1 M sodium acetate, pH 5.0) at 37°C for 30 min. After washing, the sections were blocked with 5%(w/v) BSA in TBS for 1 h and incubated with the affinity-purified antibody overnight at 4°C. The primary antibodies were visualized by consecutive treatment with biotin–streptavidin–peroxidase-conjugated goat anti-rabbit IgG (Dianova) and alkaline phosphatase conjugated streptavidin (Dianova) for 1 h each.

Antibodies and enzyme conjugates were diluted in 1% (w/v) BSA in TBS and the slides developed with FAST™ Fast Red TR/naphthol AS-MX (Sigma). Immunofluorescence microscopy was performed as described previously (Klatt et al., 2000) using the affinity-purified rabbit antibodies against the zebrafish matrillin VWA1 domains and a Cy3-conjugated affinity-purified anti-rabbit IgG as secondary antibody.

Antibody dilutions

Designation	Whole mount staining	IHC on section
1za1	1:1000	1:1000
3aza1	1:1000	1:1000
4za1	1:500	1:250
Goat anti rabbit- HRP (ABC kit)	1:200	
Cy3-Goat anti rabbit		1:400
Biotin-SP-Goat anti rabbit		1:1000
AP-streptavidin		1:500

2.3.7. Temporal expression analysis by RT-PCR

Primers were designed according to EST and genomic sequences deposited in the databases (see Table).

Designation	Sequences (5'-3')	Direction
m1z3	CAGTCTGTCTCTGGTTTTGG	forward
m1z4	GAACTCCTGCTTCACAGTG	reverse
m3az3	AGCAAGCAATCACCCGTATC	forward
m3az4	TTGCTCACACAAACGTGCTGAC	reverse
m3bz2	AGGCACGACGAAGATCAAAC	reverse
m3bz4	GGTCAAAACTCTCACCGTG	forward
m4z1	GCATGAGTGTGTGAGTGTCC	forward
m4z4	TTGATCTCGTCTTTGCTGTG	reverse

2.3.8. Whole mount skeletal staining

5-day-old larvae were killed by an overdose of 0.2% tricaine and subsequently fixed in 4% paraformaldehyde in PBS at room temperature for several hours. Specimens were stained for cartilage as described (Piotrowski et al., 1996). The larvae were transferred into a 0.1% alcian blue solution dissolved in 80% EtOH/20% glacial acetic acid over night. After staining, the larvae were rinsed in EtOH and gradually rehydrated into PBS. They were then transferred into a solution of 1% KOH/3% H₂O₂ for about 1 hour to bleach all pigmentation. Subsequently, the tissue was softened in a 0.05% trypsin solution (Sigma), dissolved in saturated sodium tetraborate for another 4 hours and cleared in 18% glycerol/ 0.8% KOH/ 0.2% Triton x-100/PBS. The specimens were stored in 70% glycerol/30% phosphate-buffered saline at 4°C. The specimens were then photographed with a Leica MZFL111 microscope.

2.3.9. Morpholino microinjection

Zebrafish (*Danio rerio*) of the Cologne wildtype strain (obtained from the Institute for Developmental Biology, University of Cologne, Germany) were used throughout these studies. They were maintained at 28°C and embryos were staged according to Kimmel et al. (Kimmel et al., 1995). Morpholino antisense oligonucleotides were designed by and obtained from Gene-Tools Inc.. Morpholinos covered the ATG translational start codon resulting in translational inhibition. All the morpholino oligonucleotides were dissolved in 1x Danieau buffer (58 mM NaCl, 0.7 mM KCl, 0.4 mM MgSO₄, 0.6 mM Ca(NO₃)₂, 5.0 mM HEPES; pH 7.6) at a concentration of 1 mM and stored at -20°C. Morpholinos were generally diluted to 0.5 mM in 1x Danieau buffer and 0.2% phenol red was added as color indicator prior to injection. Morpholino oligonucleotides were injected in a volume of 2 to 10 nl into the yolk sac of one-cell embryos just beneath the animal cell. Embryos were kept in embryo buffer (5 mM NaCl, 0.17 mM KCl, 0.33 mM CaCl₂, 0.33 mM MgSO₄, 1.68 mM HEPES, pH 7.0) at 28°C for further analysis.

Morpholino oligonucleotides sequences:

Designation	Sequences (5'-3')
Matn1	CGGCAATGTCATACTGTAGCGCGGC
Matn1-5mis	CGGg*AATcTCATAgTGTAGaGCcGC
Matn3z (3a)	GAAGGACTTCATTGTCTCGCTGTTC
Matn3z-5mis	GAAcGAgTTCATTcTCTCcCTcTTC
Matn4	CCCAATCTCACCACAAAAACCCAG
Matn4-5mis	CCgAATgTCACCAgAAAAAgCCgAG
Std. Negative control	CCTCTTACCTCAGTTACAATTTATA
Chordin	ATCCACAGCAGCCCCTCCATCATCC

Small letters indicate the mismatch positions.

3. Results

3.1. Matrilin-3 deficient mice

3.1.1. Generation of matrilin-3 deficient mice

(done by Dr. A. Aszodi and Dr. R. Wagener prior to the start of my dissertation)

The genomic DNA of mouse matrilin-3 gene contains 8 exons. The mouse matrilin-3 gene (*matn3*) was inactivated by homologous recombination in ES cells with a targeting vector in which a part of exon 1 was replaced by a neomycin resistance cassette (Fig. 3-1 A). The targeting strategies were as following: The exon 1 fragment, which encodes the signal peptide and the positively charged region, was cut out with *XbaI* and subcloned into the vector pKS (named pKS-*Xba* vector). Then, in the pKS-*Xba* vector, the 5' part end of exon 1 was cut by *SmaI*, which in turn resulted in a blunt-end linear fragment. The insert, a neomycin resistance cassette, was prepared from the pGK vector by cutting at *XbaI* and *Sal I* sites, and Klenow polymerase was used to fill in 5' overhangs. Next, the neomycin resistance cassette gene was ligated into pKS-*Xba* vector. Finally, the recombinant exon 1 was conjugated with upstream and downstream genomic sequences.

The targeting vector was transfected into ES cells and selected with G418. Out of 360 ES cell clones surviving the G418 selections, eight correctly targeted clones were identified by Southern blot analysis of *BstXI*-digested genomic DNA using an external probe (Fig. 3-1). ES cells from two targeted clones were used to generate germ line chimeric males, which were subsequently mated with C57/B6 females to generate heterozygous offspring. Heterozygous breeding produced wildtype, heterozygous, and mutant offspring (Fig. 3-1). Thereafter, two inbred strains were generated by backcrossing homozygous males with either 129/sv or C57/B6 females.

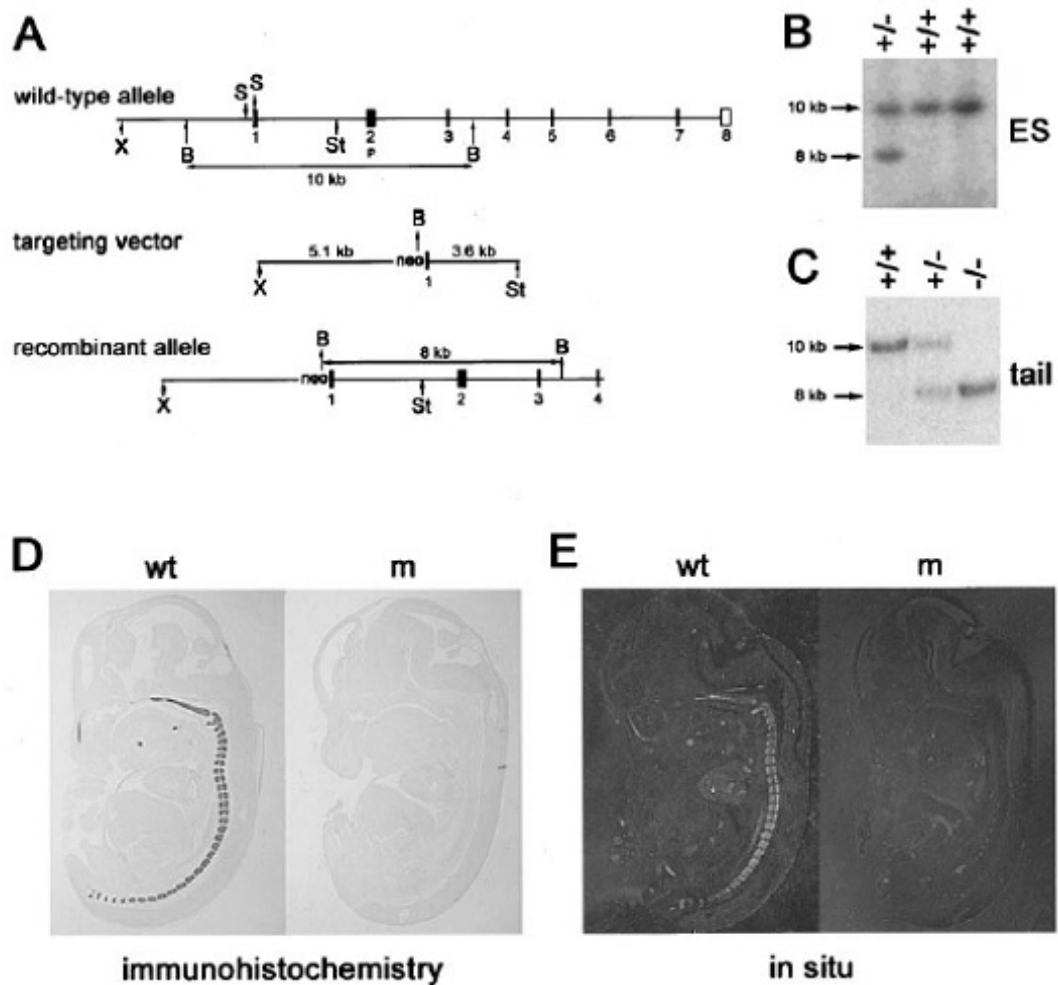


Fig. 3-1 Targeted disruption of mouse *Matn-3*. (A) Structure of the mouse *Matn-3* gene, targeting construct, and targeted allele after homologous recombination. Black and open boxes indicate the translated and untranslated regions of exons (1 to 8), respectively. The expected fragment sizes for wildtype and targeted alleles are 10 and 8 kb, respectively, following digestion with *Bst*XI and hybridization with the indicated external probe (p). neo, neomycin cassette. (B) Southern blot analysis of genomic DNA from ES cell clones shows the wildtype (10 kb) and the targeted (8 kb) alleles. (C) Southern blot analysis of tail DNA isolated from a mouse homozygous for the wildtype allele (-/-), a heterozygous mouse (-/-), and a homozygous mutant mouse (-/-). (D) Immunohistochemistry using a matrilin-3-specific antibody on tissue sections from embryonic day 13.5 embryo confirms the lack of matrilin-3 in the mutant. m, mutant; wt, wild type. (E) In situ hybridization shows the absence of matrilin-3 mRNA in a homozygous mutant embryo.

3.1.1.1. Genotyping of offspring

Matrilin-3 mutant mice were obtained by mating heterozygous parents. Mutant newborn offsprings were identified by genomic PCR while at other ages the mice were genotyped by Southern blot analysis.

The primers used in PCR genotyping were located as indicated in Fig. 2-1. Mouse tail genomic DNA was prepared by incubation in 1x PCR buffer with 0.4 mg/ml proteinase K at 55°C for 3 to 5 hours. Supernatants were cleared by centrifugation and diluted 1:10 in H₂O. 0.5 ul of diluted supernatant was used as template in the PCR reaction. The expected fragment size was 245 base pairs for the wildtype allele and 836 base pairs for the mutant allele.

For Southern blot analysis, genomic DNA was isolated from mouse tails by incubation in lysis buffer and further purified by phenol-chloroform extraction and isopropanol precipitation (see Materials and Methods for detail). Purified genomic DNA was digested with *Bst*XI and hybridized with the Dig-labeled probe, binding to a sequence in exon 2, as shown in Fig. 3-1 A. The expected fragment size after *Bst*XI enzyme digestion was 10 kb for the wildtype allele and 8 kb for the recombinant allele.

The null mutation was confirmed on tissue sections at embryonic day 13.5. Immunohistochemistry using an affinity-purified rabbit polyclonal antibody against matrilin-3 and in situ hybridization using an antisense RNA probe demonstrated the complete absence of the matrilin-3 protein and mRNA in homozygous mutant mice, respectively (Fig. 3-1 D and E).

3.1.2. Gross morphology of the skeleton is normal in matrilin-3 deficient mice

Matrilin-3 deficient mice showed no obvious abnormalities in size, gross morphology and motor behavior up to 15 months of age (not shown). They were fertile and had normal life spans. Since matrilin-3 is expressed by chondrocytes and osteoblasts during endochondral bone formation, first the gross skeletal morphology of newborn and adult mutant mice was analyzed.

Whole mount staining with alcian blue (for cartilage) and alizarin red (for bone) of newborn mice revealed that all bones of the appendicular, axial, and craniofacial skeleton formed normally in *Matn-3* null mice (Fig. 3-2 A). A closer view of the limbs (Fig. 3-2 B, C), rib cage (Fig. 3-2 D), trunk region (Fig. 3-2 E), and the base of the skull (Fig. 3-2 F) showed no evidence of size reduction or any malformation in mutants compared to controls. Furthermore, careful measurement of the length of skeletal elements of the hind limbs and forelimbs demonstrated no significant difference between homozygous mutant mice and wildtype mice (Fig. 3-2 G). Taken together, these data indicate that the lack of matrilin-3 has no impact on normal skeletal growth.

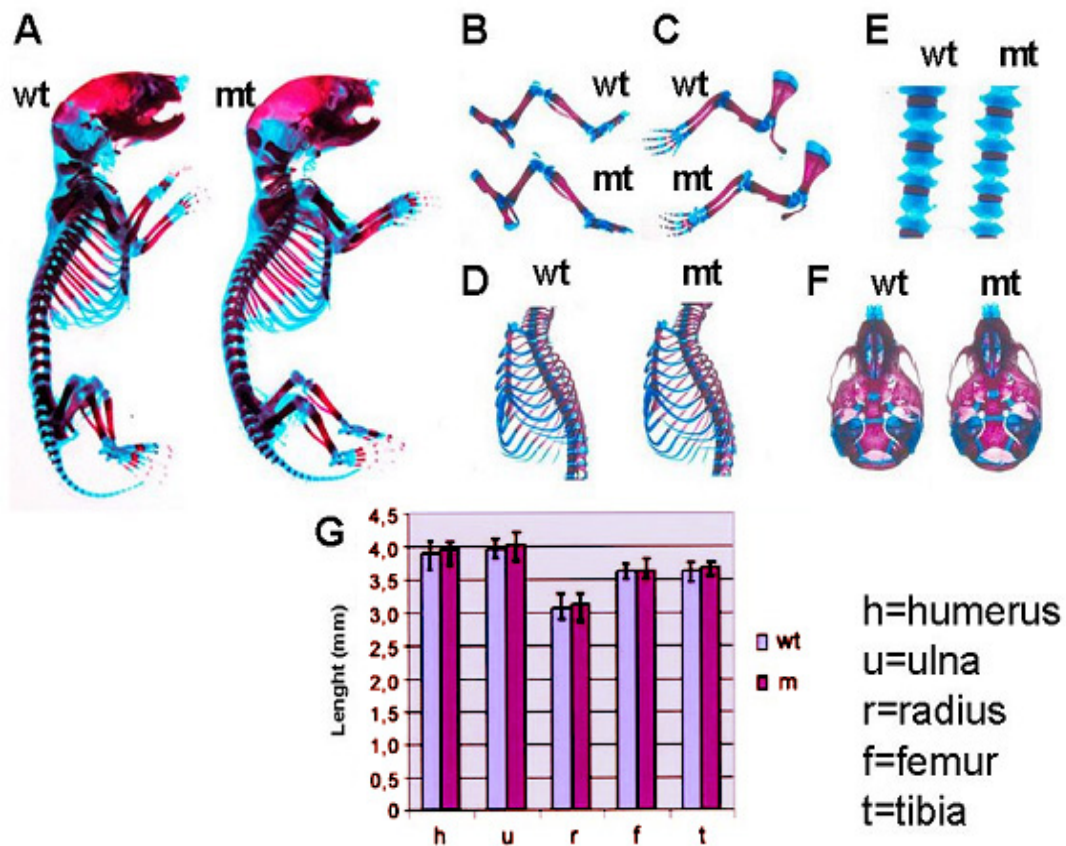


Fig. 3-2 Analysis of the skeletal anatomy in wildtype and matrilin-3-deficient mice. (A) Whole mount staining shows that newborn mutant (m) mice have a skeletal structure that does not differ from that of wildtype (wt) mice. The size and the appearance of the long bones of the limbs (B), rib cage (D), trunk (E), and the base of the skull (F) are indistinguishable between wildtype and mutant littermates. (G) There is no statistically significant difference in the length of the long bones of newborn limbs between wildtype and mutant mice ($n = 5$). Error bars represent \pm standard errors of the mean. Abbreviations: h, humerus; u, ulna; r, radius; f, femur; t, tibia.

3.1.3. Matrilin-3-deficient mice show normal endochondral bone formation and intervertebral disk development

To investigate the skeletal development of the *Matn-3* null mice in greater detail, histological, immunohistological and in situ hybridization analyses were performed. Haematoxylin-eosin staining of tibias derived from newborn mice, 4-week-old and 8-week-old mice and tails from 4-week-old, 12-week-old and 9-month-old mice were examined. The results showed a normal columnar chondrocyte arrangement and growth

plate architecture in the proliferating zone of newborns (Fig. 3-3A, B) and in the growth plate of older mice (Fig. 3-3 C-F). The appearance of the primary and secondary ossification centers were identical in control and null mice (Fig. 3-3). Similar to that of long bones, the development of intervertebral disks was normal in *Matn-3* null mice (Fig. 3-4). Safranin orange staining for proteoglycans showed no sign of degenerative changes of the articular cartilage in mutants up to 9 months of age (Fig. 3-5).

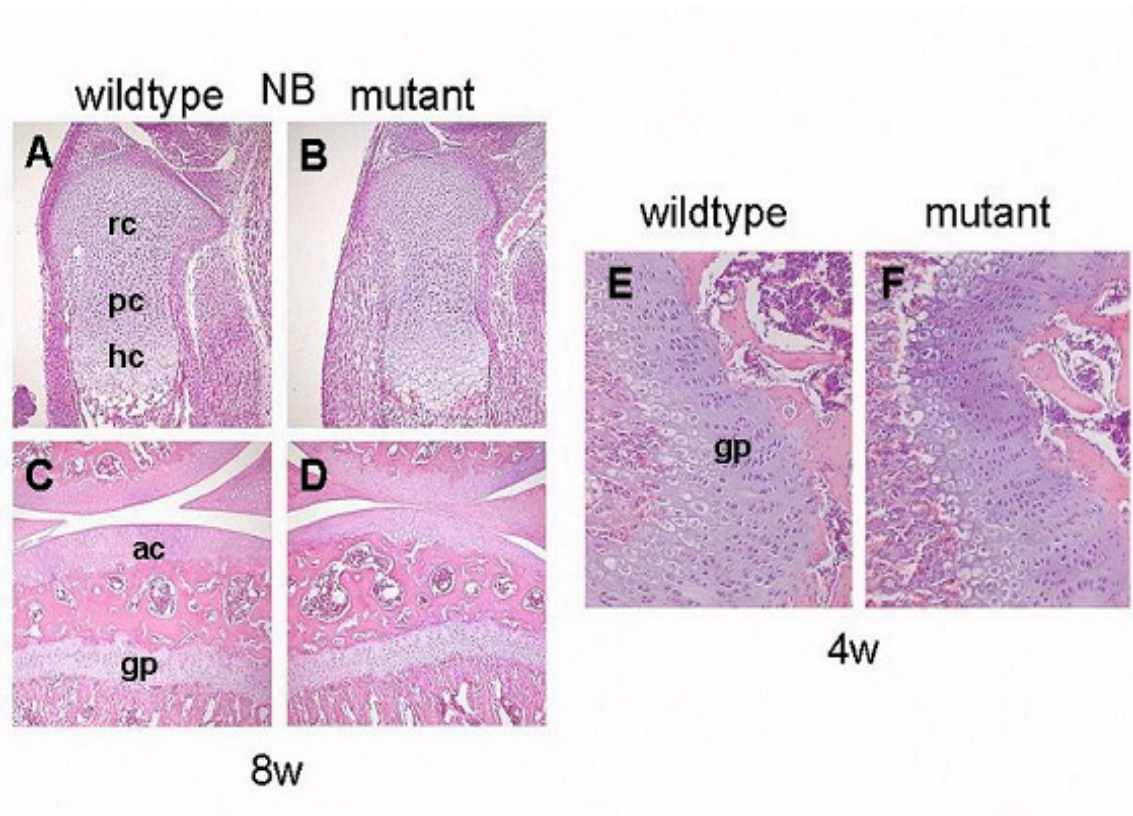


Fig. 3-3 Histological analysis of skeletal development. HE staining of the proximal part of the tibia from newborn wildtype (wt) and mutant (m) mice (A,B) and the knee region from 8-week-old mice (C,D) shows comparable size and ultrastructure between control and mutant. (E,F) The columnar organization in the growth plate of 4-week-old control and mutant mice is identical. rc, resting cartilage; pc, proliferating cartilage; hc, hypertrophic cartilage; ac, articular cartilage; gp, growth plate.

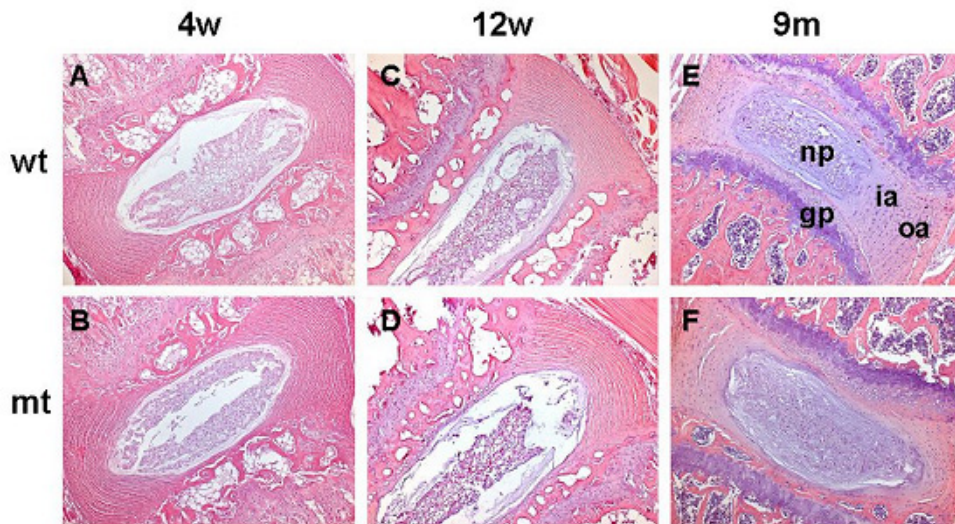


Fig. 3-4 HE staining shows normal intervertebral disk formation of 4-week-old (4w), 12-week-old (12w) and 9-month-old (9m) mutants (mt) and wildtype (wt) mice. No difference in morphology between wt and mt was seen. np, nucleus pulposus; ia, inner annulus; oa, outer annulus; gp, growth plate.

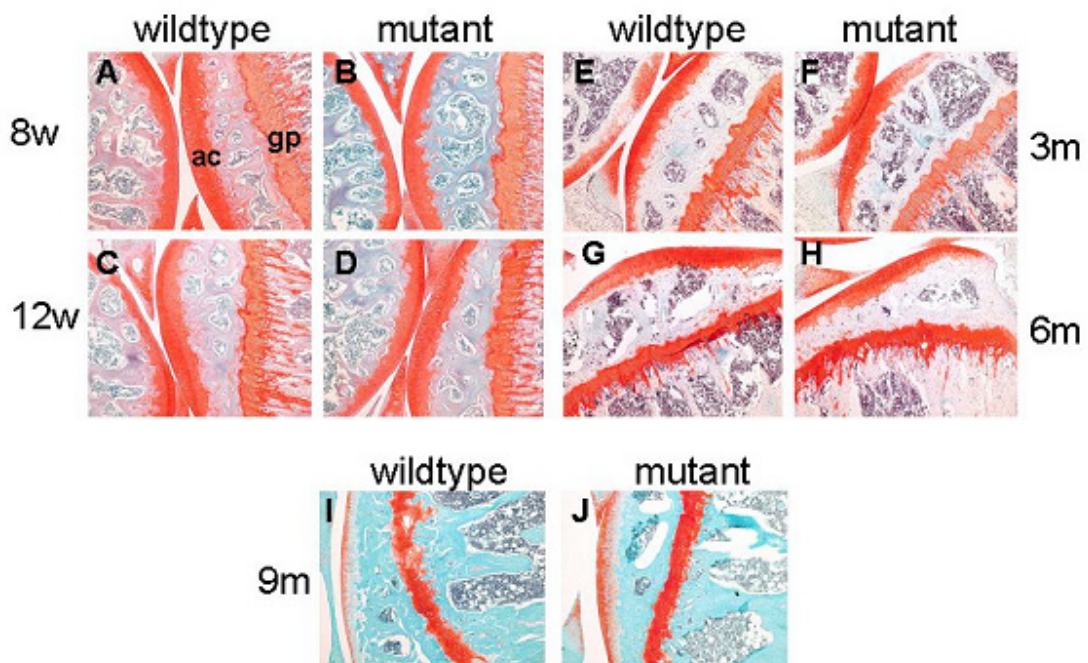


Fig. 3-5 Safranin orange staining of the tibial head at 8 weeks (8w), 3 months (3m), 6 months (6m) and 9 months of age gives no indication of degenerative changes in the articular cartilage in mutants.

Further, we investigated markers for chondrocyte differentiation in the mutant long bones. Immunostaining of the humerus from newborn mice showed the normal deposition of the typical cartilage proteins, including collagen II, collagen X, and aggrecan (Fig. 3-6 A). In situ hybridization of tibial sections with riboprobes for indian hedgehog (*Ihh*), and parathyroid hormone/parathyroid hormone-related peptide receptor (*Ppr*) revealed a normal differentiation of mutant growth plate chondrocytes (Fig. 3-6 B).

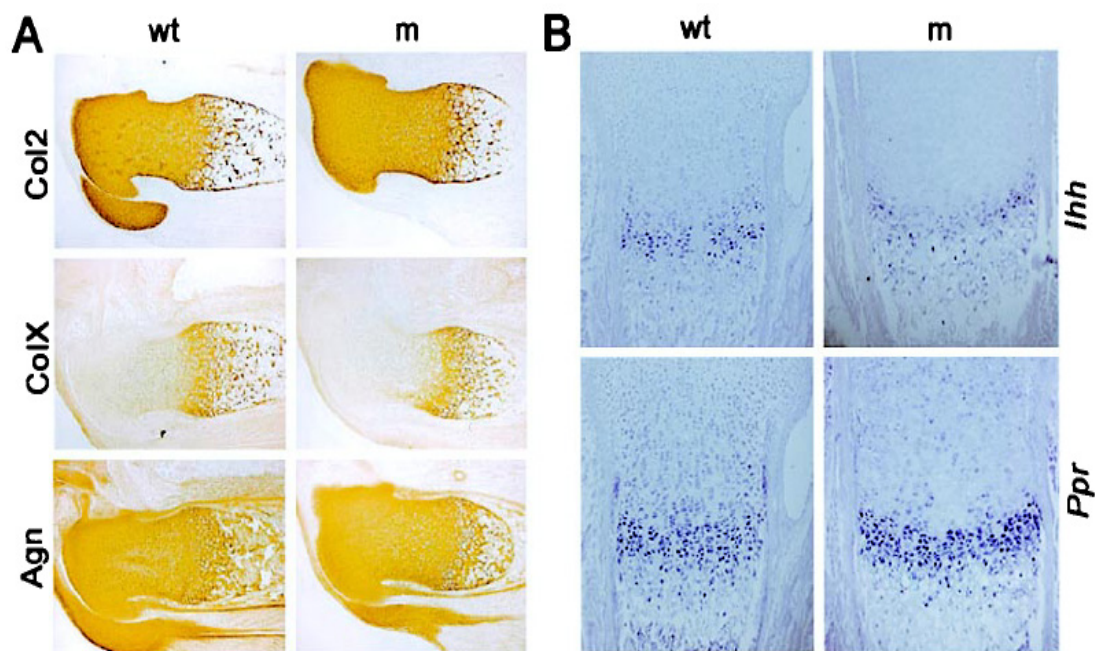


Fig. 3-6 Cartilage differentiation and bone development are normal in *Matn-3* null mice. (A) Immunohistochemistry shows normal deposition of cartilage-specific proteins. Consecutive sections of the humerus from wildtype (wt) and mutant (m) mice were stained with antibodies against type II collagen (Col2), aggrecan (Agn), and type X collagen (ColX). (B) In situ hybridization with probes specific for indian hedgehog (*Ihh*), and parathyroid hormone/parathyroid hormone-related peptide receptor (*Ppr*) mRNA shows similar expression of these growth plate differentiation markers in wildtype and mutant newborn tibial sections.

During development, the cartilage tissue is gradually replaced by bone tissue in a process called endochondral ossification. It begins with the transformation of the perichondrium into a bone-producing periosteum. Calcification occurs by the deposition of calcium salts. This is the first indication of bone formation and the site where it occurs is called the primary center of ossification. The perichondrium in this area now contains an inner layer of osteogenic cells which differentiate into osteoblasts. These cells synthesize and secrete the materials which form the intercellular matrix and soon a bony collar becomes visible around the cartilage of the center of ossification. Vessels enter from the periosteum and carry other osteogenic cells, or osteoblasts, with them. As a result, the diaphysis becomes encased in compact bone.

To check whether the speed of bone development was changed in matrilin-3 null mice, van Kossa staining was applied to newborn tibia sections to stain for calcium phosphate deposition. The results showed no distinguishable difference between wildtype (Fig. 3-7 A) and null mice (Fig. 3-7 B), indicating that both the ossification of the bony collar and the trabecular bones occurs normally in mutants. Osteoblast and osteoclast activities were also examined by alkaline phosphatase and tartrate-resistant alkaline phosphatase (TRAP) staining and results showed normal numbers of osteoblasts and osteoclasts, respectively (Fig. 3-7 C-F). The vascular invasion front of the growth plate cartilage was investigated by immunostaining for endomucin as a marker for endothelial cells (Brachtendorf et al., 2001). No difference was observed in vascularization between wildtype and mutant growth plates (Fig. 3-7 G, H).

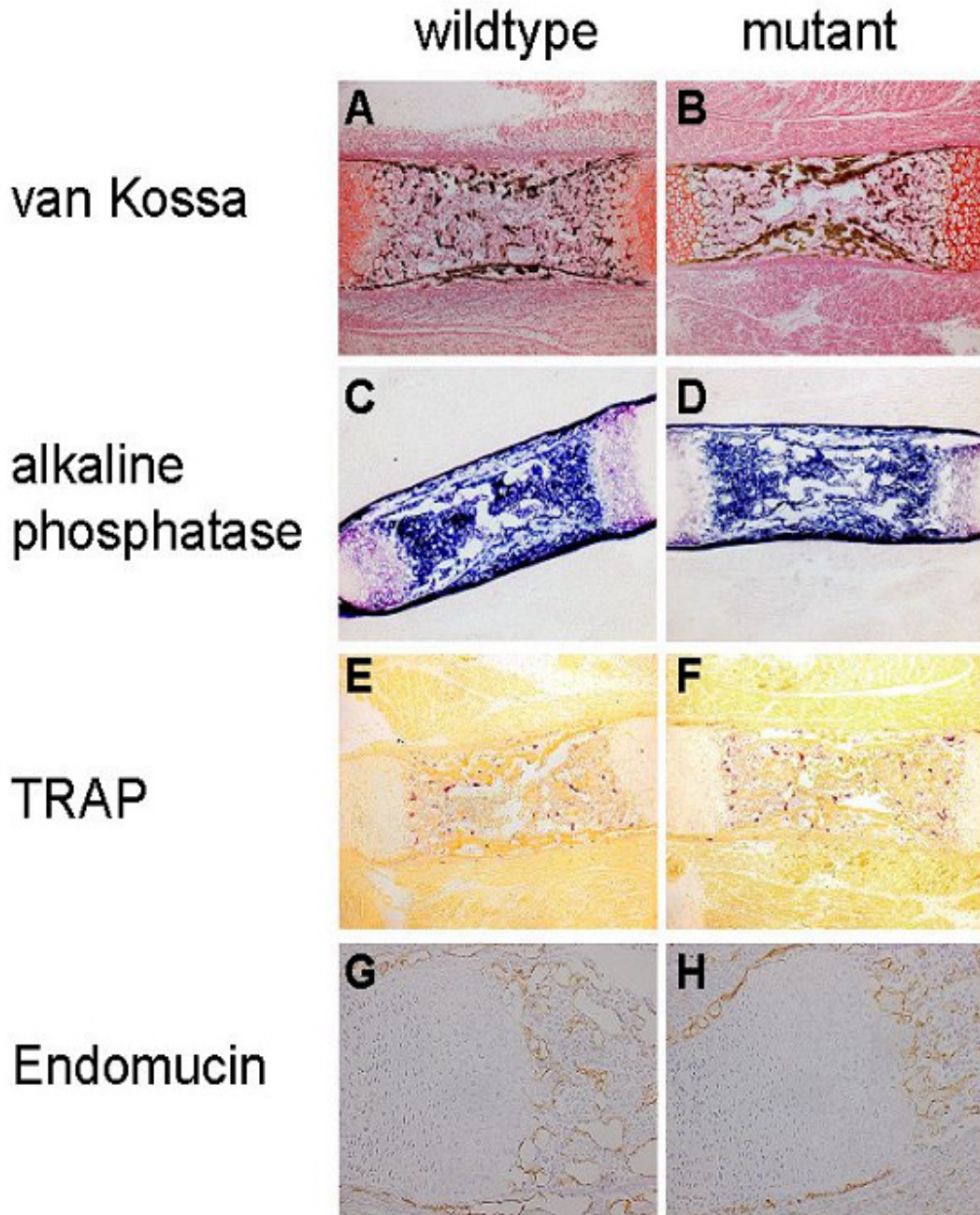


Fig. 3-7 Van Kossa staining (A, B) indicates normal mineral deposition in the tibia of newborn mutant mice. The sections were counterstained with safranin orange. (C, D) Alkaline phosphatase histochemistry (blue staining) shows that differentiation and activity of osteoblasts are normal in mutant mice. (E, F) Staining for tartrate-resistant acid phosphatase (TRAP) activity (red staining) indicates comparable numbers of osteoclasts in wildtype and mutant long bones. (G, H) Immunostaining for endomucin, a marker for vascular endothelial cells, shows a normal vascular invasion front in the mutant growth plate.

3.1.4. Normal expression of other members of the matrilin family in matrilin-3-deficient skeletal tissues

To address the question of whether the lack of an apparent skeletal phenotype in the *Matn-3* null mice is due to compensation by structurally and functionally related proteins, we analyzed the expression of other members of the matrilin family using various methods.

Northern hybridization of total RNA isolated from newborn limb cartilage demonstrated that the steady-state levels of *Matn-1*, *Matn-2*, and *Matn-4* mRNAs were not significantly altered in mutant mice compared to those in wildtype mice (Fig. 3-8).

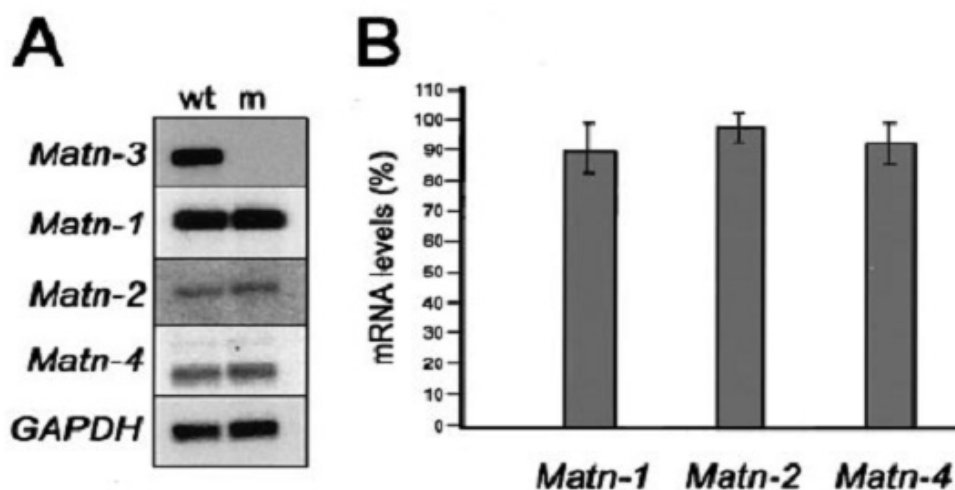


Fig. 3-8 Northern blot analysis. (A) A representative northern blot analysis of total RNA isolated from wildtype (wt) and mutant (m) newborn limb cartilage. The filter was consecutively hybridized with probes specific for *Matn1-4* and *GAPDH*. (B) Diagram showing the percentage of *Matn1*, *Matn2*, and *Matn4* mRNA levels in the mutant compared to that of the wild type ($n = 3$). The hybridization intensities were normalized to the amount of *GAPDH* mRNA. Error bars represent standard errors of the mean.

The tissue distribution patterns of all matrilins were also examined on newborn tibia sections using specific polyclonal antibodies. Immunostaining of newborn tibias revealed that matrilin-3 was distributed in the epiphyseal and growth plate cartilage but was absent at the superficial zone of the epiphyses in normal animals (Fig. 3-9 A). No matrilin-3 was detected in mutant mice (Fig. 3-9 B). Matrilin-2 was expressed in the perichondrium-periosteum, in the superficial zone, and very weakly in the hypertrophic zone of growth plate (Fig. 3-9 E), while matrilin-1 showed the same staining pattern as matrilin-3 (Fig. 3-9 C). Matrilin-4 was expressed in whole growth plate and epiphyseal cartilage including superficial zone of the epiphyses in normal animals (Fig. 3-9 G). Immunostaining for matrilin-1, -2 and -4 in mutant tissue revealed no alterations in either distribution or staining intensity compared to those of the wildtype (Fig. 3-9 D, F and H).

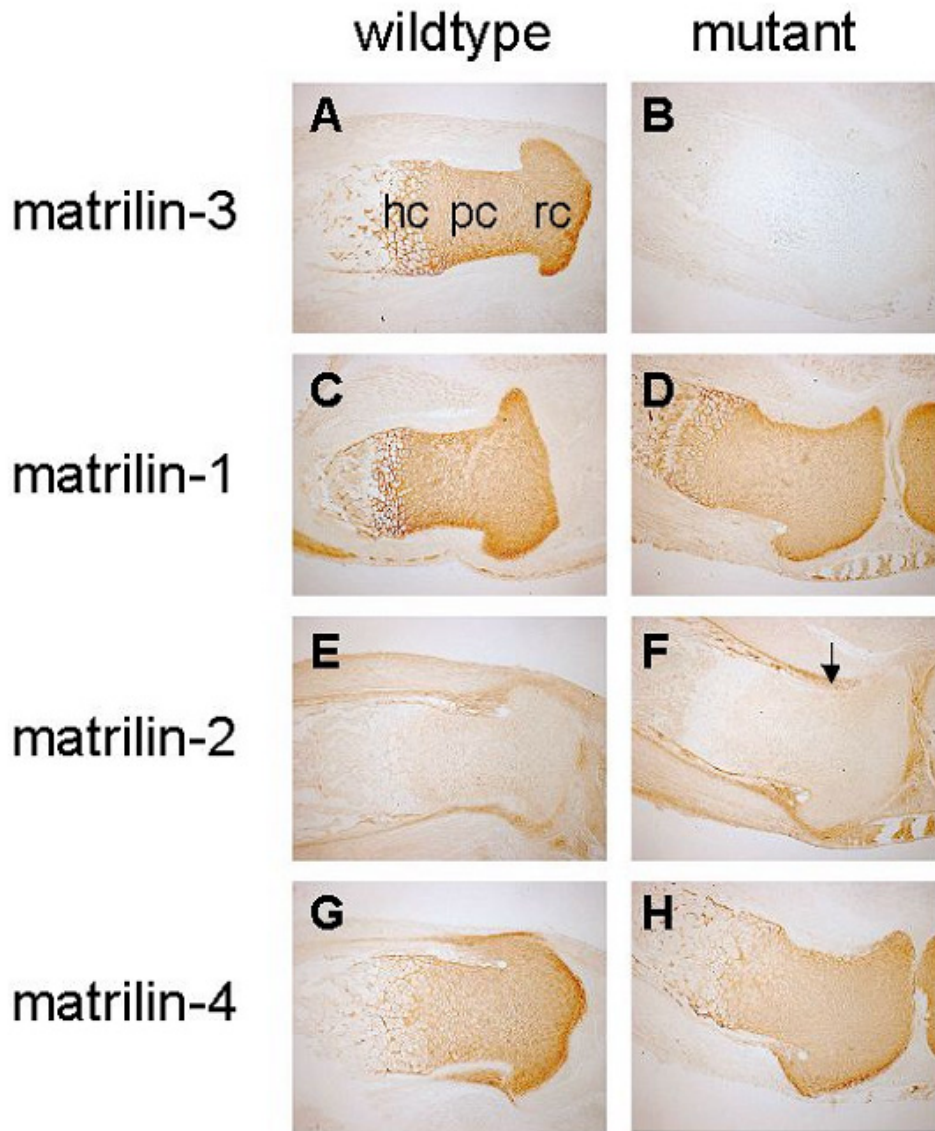


Fig. 3-9 Immunohistochemical staining of developing bones for matrilins on consecutive sections of the tibia from wildtype (A, C, E, and G) and matrilin 3-deficient (B, D, F, and H) mice. Newborn littermates were stained with specific antibodies against matrilin-1, matrilin-2, matrilin-3, and matrilin-4. hc, hypertrophic cartilage; pc, proliferating cartilage; rc, rest cartilage. The arrow indicates a ligament.

Tail sections were also examined at 4-weeks of age. Matrilin-3 was strongly expressed in the cartilage of inner annulus, articular surface and growth plate, but absent in the outer annulus and the nucleus pulposus (Fig. 3-10 A). Matrilin-3 deficient cartilage did not stain for matrilin-3. (Fig. 3-10 B), whereas matrilin-1 was expressed weakly in the

growth plate (Fig. 3-10 C, D). Matrilin-2 expression could be detected neither in wildtype nor in mutant mice (Fig. 3-10 E, F). Matrilin-4 was expressed identically in growth plate in wildtype mice and in mutant mice (Fig. 3-10 G, H).

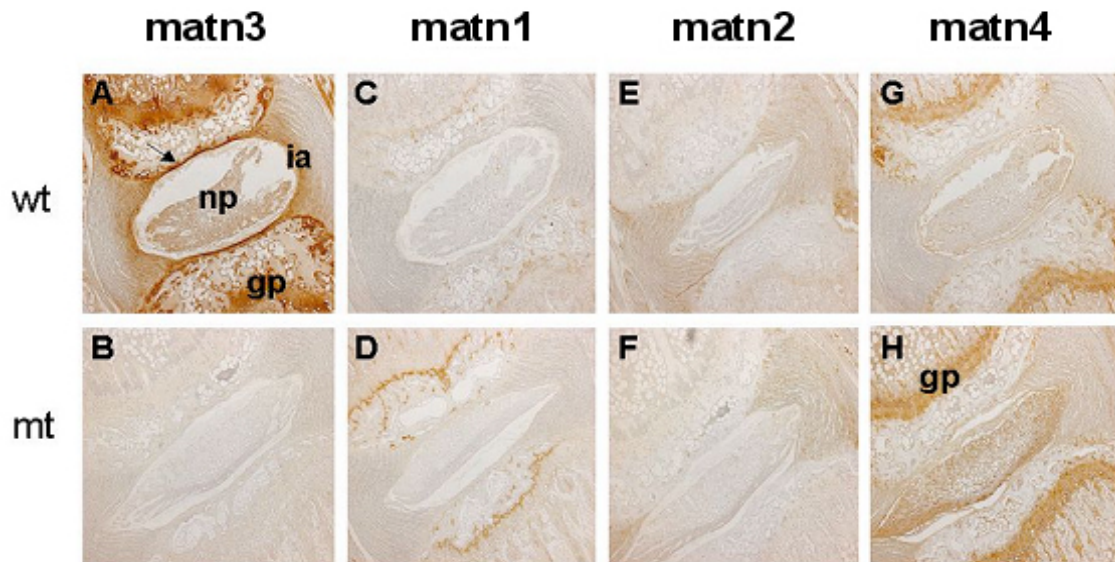


Fig. 3-10 Immunohistochemical localization of matrilins in wildtype (wt) and matrilin-3 deficient (mt) vertebral columns. Sagittal sections of the vertebrae from 4-week-old wildtype (+/+; A, C, E, and G) and matrilin-3 deficient (mt) (-/-; B, D, F, and H) mice were stained with specific antibodies against matrilin-3 (matn3), matrilin-1 (matn1), matrilin-2 (matn2), and matrilin-4 (matn4). In the wildtype (A), matrilin-3 was present in the cartilage of inner annulus (ia), articular surface and growth plate, but absent in the outer annulus (oa) and the nucleus pulposus (np). Matrilin-3 deficient cartilage lacked matrilin-3. (B), while matrilin-1 (C and D) weakly expressed in growth plate. Almost no matrilin-2 (E and F) expression can be seen neither in wildtype nor in mutant mice. Matrilin-4 (G and H) was expressed in growth plate in wildtype as well as in mutant mice. np, nucleus pulposus; ia, inner annulus; oa, outer annulus; gp, growth plate. The arrow indicates the articular cartilage.

3.1.5. Biochemical analyses reveal no difference in matrix protein content in matrilin-3 null mice

From the skeletal analysis, based on histological and immunohistological staining, there was no obvious phenotype in matrilin-3 null mice. Since matrilins have been proposed to function as adaptor proteins in the extracellular fibrous network, the lack of matrilin-3 protein could, potentially, result in weaker interactions between matrix proteins.

In order to test this hypothesis, cartilages from sternum and knee were isolated and extracted sequentially with buffers of different strength. Buffer 1 contained only TBS in order to wash out blood and very loosely bound proteins. Buffer 2 contained high salt and EDTA and therefore proteins which are immobilized by divalent cation dependent interactions were solubilized in this step. In the last step 4 M GuHCl was used in order to solubilize most of the residual proteins.

Neither additional bands nor changes in band intensity could be detected in Coomassie stained gels when extracts from wildtype and mutant mice were compared (Fig. 3-11). The extracts were also blotted onto nitrocellulose membranes and analysed with specific antibodies against all matrilins. Matrilin-3 was solubilized in high salt/EDTA containing buffer in wildtype mice while matrilin-3 proteins were absent in null mice (Fig. 3-12). Matrilin-1 and matrilin-4 were also mainly extracted with high salt/EDTA containing buffers, both in wildtype and matrilin-3 deficient mice. In contrast, matrilin-2 was obtained already in TBS, indicating that matrilin-2 is more weakly bound than other matrilins. Nevertheless, no differences could be detected between wildtype and mutant mice (Fig. 3-12).

It has been demonstrated that COMP (cartilage oligomeric matrix protein) (Mann et al., 2004) and collagen type II (Winterbottom et al., 1992) bind to matrilins. To address the question of whether lack of matrilin-3 influences the stability and solubility of those binding partners, immunostaining of knee and sternal extracts were performed using specific antibodies against COMP and collagen type II. A small portion of COMP was solubilized in TBS, however, most protein was extracted by high salt/EDTA

containing buffers. In contrast, most collagen type II was extracted in GuHCl. The same was observed in matrilin-3 null mice (Fig. 3-12).

Taken together, neither expression nor solubility of matrilin-1, -2, -4, COMP or collagen type II were altered in mice lacking matrilin-3.

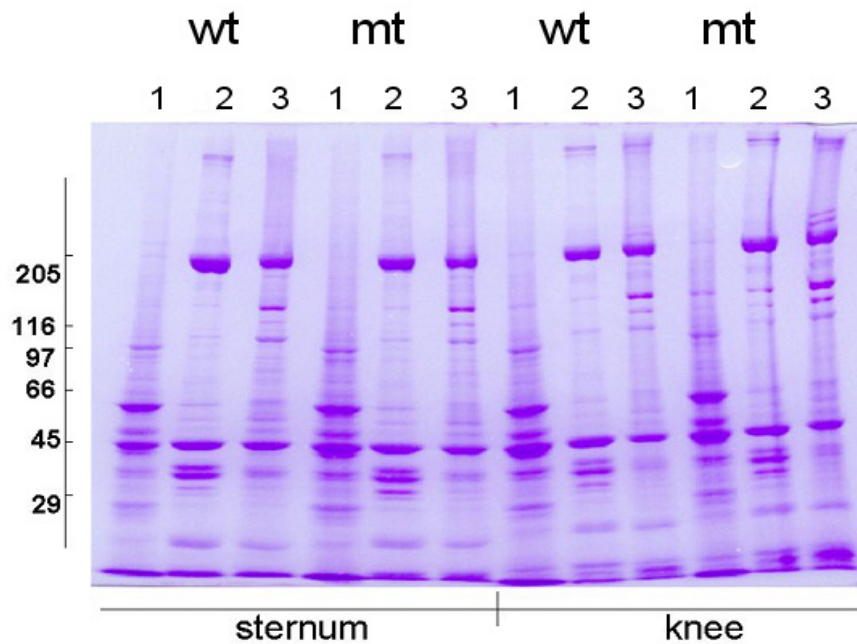


Fig. 3-11 Biochemical analysis of wildtype (wt) and mutant (mt) knee joint and sternal cartilages. Coomassie-stained SDS-polyacrylamide gel (4-15%) of proteins sequentially extracted with buffer1 (TBS), buffer 2 (high salt/EDTA), and buffer 3 (GuHCl) (see Materials and Methods) from newborn knee joint and sternal cartilage.

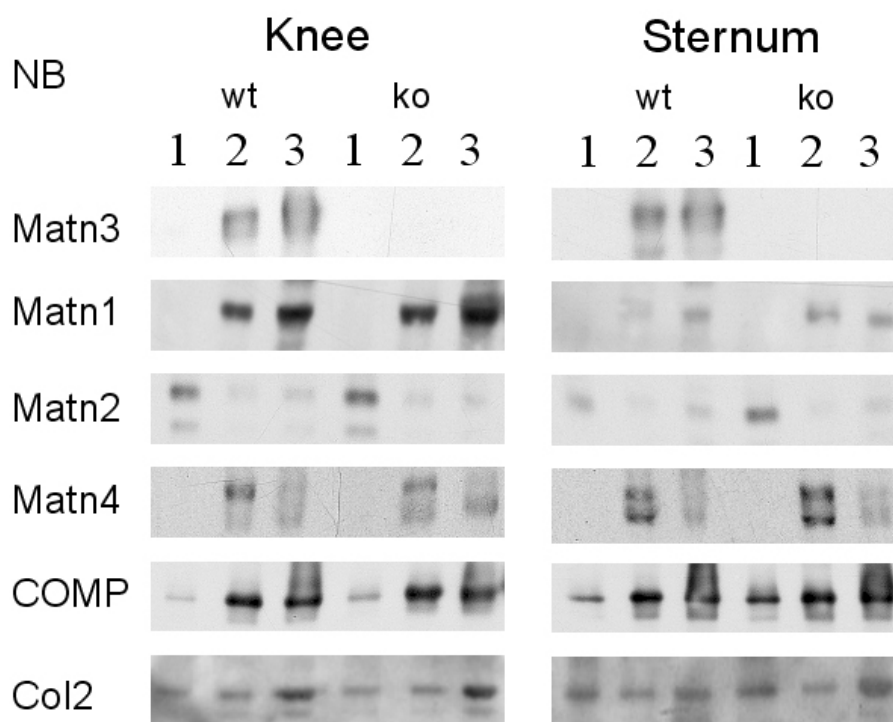


Fig. 3-12 Western blot analysis of proteins sequentially extracted with buffer 1 (TBS), buffer 2 (high salt/EDTA), and buffer 3 (GuHCl) from wildtype (wt) and mutant (ko) knee joint and sternal of newborn mice. Proteins were immunostained with specific antibodies against matrilin-1 (matn1), matrilin-2 (matn2), matrilin-3 (matn3), and matrilin-4 (matn4) and for COMP and collagen II (col2).

Proteoglycans are one of the major constituents of the extracellular matrix and it has been shown that matrilin-1 binds to aggrecan, the most abundant proteoglycan in cartilage (Hauser et al., 1996). In addition, matrilins were shown to bind to the small leucine-rich repeat proteoglycans decorin and biglycan (Wiberg et al., 2003). Since matrilin-1 and matrilin-3 have the same tissue distribution pattern, the proteoglycan content was determined in cartilage from the matrilin-3 deficient mice.

Proteoglycans are complex macromolecules consisting of a protein core with one or more covalently attached glycosaminoglycan (GAG) chains. The dimethylmethylene blue assay for sulphated glycosaminoglycans has found wide acceptance as a quick and simple method of measuring the sulphated glycosaminoglycan content of tissue and fluids. (Enobakhare et al., 1996).

The glycosaminoglycan contents were analysed in single knee and sternal extracts (Fig. 3-13). Three independent experiments were done under slightly different conditions. There was no significant difference in the contents of sulphated glycosaminoglycans between wildtype and matrilin-3 mutant mice.

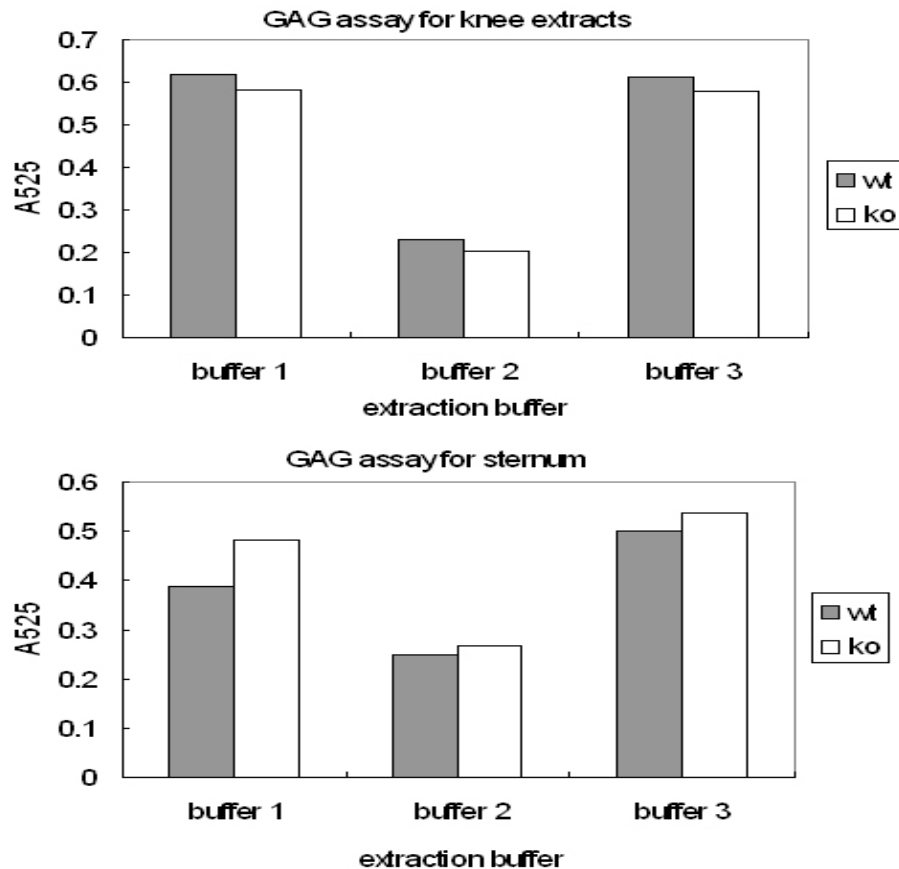


Fig. 3-13 GAG assay of knee and sternum cartilage extracts derived from 4-weeks-old wildtype (wt) and matrilin-3 knockout (ko) mice with buffer 1 (TBS), buffer 2 (high salt/EDTA) and buffer 3 (GuHCl).

3.1.6. Summary

In summary, our results show that the absence of matrilin-3 in mice does not have an impact on endochondral bone formation. Therefore it is unlikely that loss-of-function mutations in the matrilin-3 gene account for MED and MED-like disorders seen in humans. Generation of multiple-knockout mice or mice carrying dominant-negative mutations might be necessary to clarify the function of matrilins in skeletal development and the etiology of chondrodysplasias, respectively.

Matrilin-1 null mice have been generated earlier (Aszodi et al., 1999) and breeding to create matrilin-1 and matrilin-3 double deficient mice was therefore the next logical step to elucidate matrilin function in skeletal development.

3.2. Matrilin-1/matrilin-3 double deficient mice

Matrilin-1/ matrilin-3 double deficient mice were obtained by crossing the single deficient mice. Detailed histological assessments were performed as for matrilin-3 single null mice (collaboration with Dr. A. Aszodi, Munich). However, the double null mice did not show any obvious abnormalities, were fertile and had normal life spans.

To determine whether the apparent lack of an skeletal phenotype in the *Matn-1/-3* null mice is due to compensation by structurally or functionally related proteins, the tissue contents of other members of the matrilin family as well as of known matrilin binding partners were analyzed.

As performed earlier for the matrilin-3 single knockout mice, proteins were extracted from sternum and knee cartilage with buffer 1 (TBS), buffer 2 (high salt/EDTA), and buffer 3 (GuHCl). The reproducibility of the extraction was checked on Coomassie stained SDS-polyacrylamide gels (not shown). The amounts of matrilin-1, -2, -3 and -4, COMP, collagen type II, biglycan and decorin were examined by immunoblotting after nonreducing SDS-polyacrylamide gel electrophoresis. In initial analyses it was shown that there were no obvious differences between homozygous and double heterozygous

wildtype mice or single homozygous and heterozygous single mutants (not shown). To detect potential quantitative effects of allele-loss, the double heterozygous wildtype animals were compared with the double mutant mice and single matrilin-1 or -3 mutant mice that lacked also one additional allele of matrilin-1 or -3. Cartilage from newborn double knockout mice contained matrilin-2 and matrilin-4 (Fig. 3-14). The amounts of matrilin-2 in mutant cartilages were similar to those of the control (Fig. 3-14) whereas matrilin-4 gave significantly stronger signals in high salt/EDTA and GuHCl extracts of cartilages from knees of newborn mice. This result was confirmed in three independent extraction experiments (Fig. 3-15). Sternal cartilages showed a less pronounced increase in matrilin-4 both in newborn (Fig. 3-14) and in 4.5-week old mice (not shown). Interestingly, the upregulation of matrilin-4 was seen also in the mice lacking only matrilin-1, whereas it was not detected in the matrilin-3 knockout mice (Fig. 3-14). In addition, the matrilin-4 band pattern was altered in the matrilin-1 and the matrilin-1/-3 deficient newborn mice. By double fluorescence staining of immunoblots with antibodies specific for matrilin-1 and -4 we could show that a major band (Fig. 3-16 arrow b) that disappears in the matrilin-1 and the matrilin-1/-3 deficient mice does not represent heterooligomers of matrilin-1 and -4, whereas a second much weaker band (Fig. 3-16 arrow c) could. This latter band is, however, so close to the strong matrilin-1 homotrimer band that an overlap cannot be excluded. *In vitro* experiments with recombinant coiled-coil domains have shown the propensity of matrilin-1 and -4 for heterooligomer formation (Frank et al., 2002). In addition to the changes in matrilin-4 expression, also other slight changes could be detected in the single knockouts for matrilin-1 and -3. In wildtype mice a minor band (Fig. 3-14, asterisk) was found above the main matrilin-1 containing band and the corresponding band was missing in the matrilin-3 null mice (Fig. 3-14). As it has the same electrophoretic mobility as a matrilin-3 positive band it is likely to represent heterooligomers formed of matrilin-1 and -3 (Fig. 3-14). Further, in the mice lacking only matrilin-1, the pattern of matrilin-3 oligomers is clearly altered (Fig. 3-14). In contrast, immunoblot analysis of the matrilin interaction partners COMP, collagen type II, biglycan and decorin revealed no apparent differences between control and mutant cartilage (Fig. 3-14).

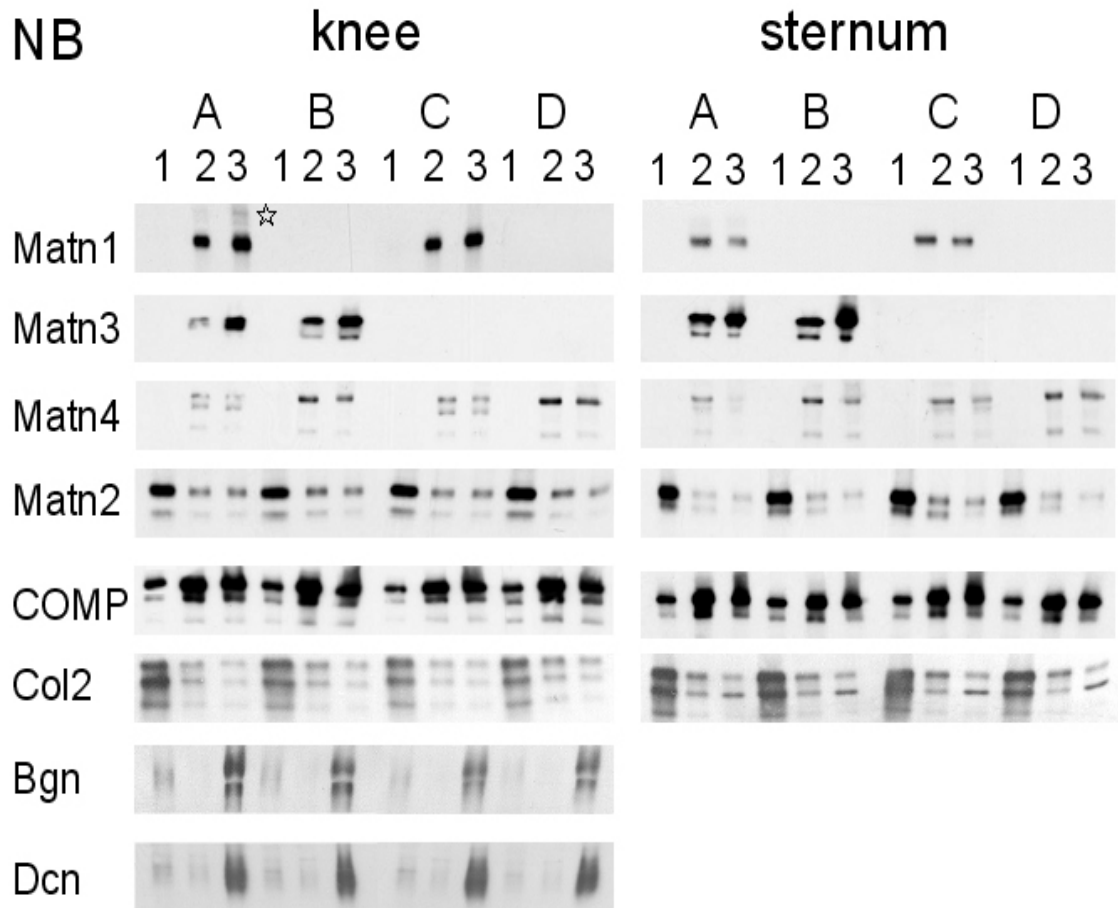


Fig. 3-14 Biochemical analysis of wildtype and mutant knee joint cartilages. Proteins were sequentially extracted with buffer 1(TBS), buffer 2 (high salt/EDTA), and buffer 3 (GuHCl) from newborn knee joint and sternum cartilage. Western blot analysis was performed for matrilin-1 (Matn1), matrilin-2 (Matn2), matrilin-3 (Matn3), matrilin-4 (Matn4), COMP, collagen II (Col2), biglycan (Bgn) and decorin (Dcn). A: matn1 +/-, matn3 +/-, B: matn1 -/-, matn3 +/-, C: matn1 +/-, matn3 -/-, D: matn1 -/-, matn3 -/-. Asterisk, additional band which is missed in matrilin-3 single knockout mice (C).

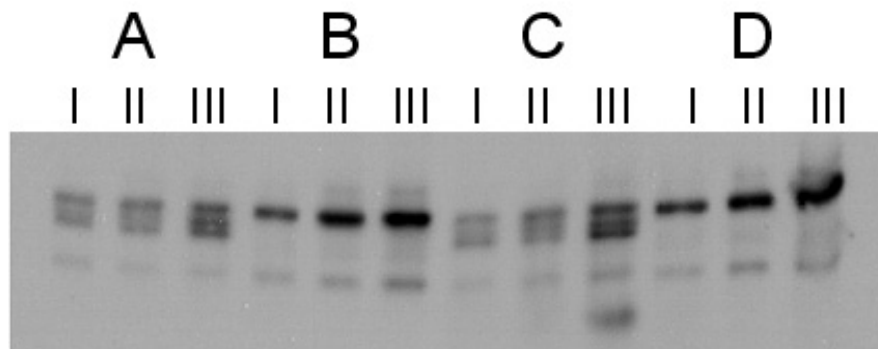


Fig. 3-15 Changes of matrilin-4 expression in matrilin-1 and matrilin-1/-3 deficient mice. Protein extracts obtained with buffer 2 (high salt/EDTA) from knee cartilage of three different mice (I, II and III) from each group of newborn mice (A, B, C and D as in Fig. 3-14) were submitted to immunoblot analysis using matrilin-4 specific antibodies.

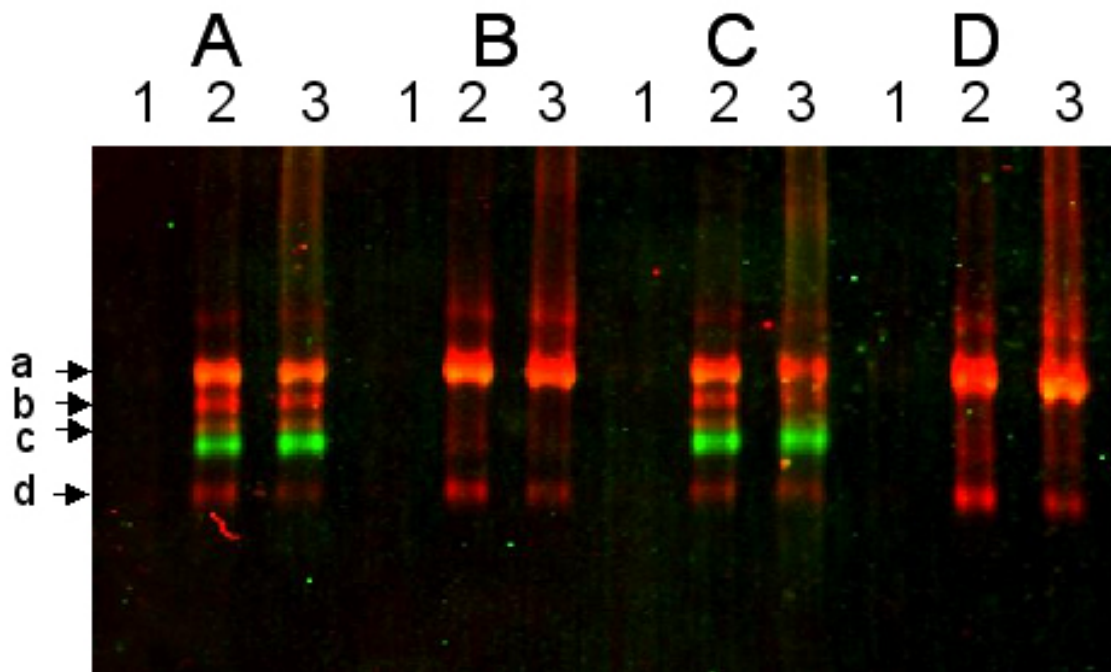


Fig. 3-16 Changes of matrilin-4 expression in matrilin-1 and matrilin-1/-3 deficient mice. Infrared fluorograph of an immunoblot of knee cartilage extracted with buffers 1 (TBS), buffer 2 (high salt/EDTA) and buffer 3 (GuHCl). A, B, C and D as in Fig. 3-14. Green, matrilin-1 homotrimer; Red, matrilin-4. a, matrilin-4 trimer; b, major band; c, minor band; d, matrilin-4 dimer.

3.2.1. Summary

Although mice lacking either matrilin-1 (Aszodi et al., 1999) or matrilin-3 did not show apparent abnormalities by histological and immunostaining analyses, biochemical analyses revealed a molecular phenotype in matrilin-1/-3 double null mice in which the amount of matrilin-4 protein is increased and the band pattern of matrilin-3 and -4 is altered. The upregulation of matrilin-4 is likely to represent a compensatory mechanism. Inactivation of the matrilin-4 gene, in addition to matrilin-1 and -3, may yield further information on matrilin function.

In the process of evolution, genes become more diverse and protein expression is regulated in a more complex manner. Therefore, elucidation of the function of a certain gene or protein is particularly difficult in higher organisms. A simple vertebrate model organism may give a better insight into the function of matrilins. The zebrafish (*Danio rerio*) is a powerful model organism for the study vertebrate development and was chosen as an alternative system in which to investigate matrilin function.

3.3. Matrilins in zebrafish

The zebrafish (*Danio rerio*) is a well established model organism. The embryos develop rapidly, with all organs having been formed by 72 hpf (hours post fertilization). The externally developing embryos are optically clear and are produced in large numbers, therefore large-scale mutagenesis programs can be monitored by simple microscopic observation of the embryos (Haffter et al., 1996). The genome sequencing project has been completed to 60% and is expected to be finished by the end of 2005. For this part of the dissertation, a fish facility was set up with the long-term goal of using the zebrafish to study matrilin function. The structure and genetic organization of matrilins in zebrafish has been characterized (Ko et al., 2005). My experiments focused on the investigation of matrilin expression in zebrafish and on functional analyses by a morpholino knockdown approach.

3.3.1. Generation of zebrafish-matrilin-specific antisera

Specific antibodies against each zebrafish matrilin family member were generated in order to study their temporal and spatial expression.

cDNAs encoding the sequences of zebrafish matrilin VWA1 domains of matrilin-1, -3a, -3b and -4 were cloned into the pCEP-Pu vector utilizing the BM-40 secretion signal sequence and an N-terminal His₆-tag (Smyth et al., 2000). The recombinant plasmids were introduced into HEK-293/EBNA cells and maintained in an episomal form. The recombinant proteins secreted into the cell culture medium were, except for matrilin-3b, subsequently purified by affinity chromatography on a cobalt column. The purified proteins appeared in non-reducing SDS-PAGE mainly as monomeric molecules, but small amounts of higher oligomers could also be detected (Fig. 3-17). After reduction single bands with apparent molecular masses in the range expected for monomeric VWA domains were seen (results not shown). The purified proteins (Fig. 3-17) were used to immunize rabbits.

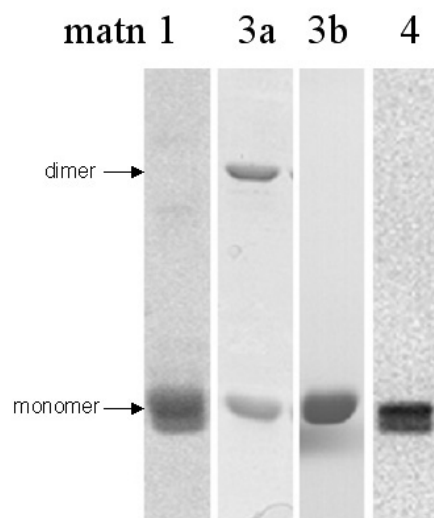


Fig. 3-17 Purity of recombinant VWA1 domains. Affinity purified VWA1 domains proteins of matrilin-1 (matn1), matrilin-3a (matn3a), matrilin-3b (matn3b) and matrilin-4 (matn4) were checked on 12% non-reducing SDS-polyacrylamide gel. Matrilin-1, -3b and -4 VWA1 domains were mainly present as monomers, whereas matrilin-3a occurred both as monomers and dimers.

The antisera obtained were first tested for specificity by ELISA analysis. The results showed that the antisera against matrilin-1 had negligible cross reactivity to matrilin-3a and -4 recombinant proteins (Fig. 3-18). However, antibodies against matrilin-3a and -4 had strong cross reactivities to matrilin-1/-4 and matrilin-1/-3a proteins, respectively (Fig. 3-18). After further purification by affinity chromatography on columns carrying the original antigens, the antibodies were shown by ELISA to be highly specific for the matrilin form used for immunization (Fig. 3-19).

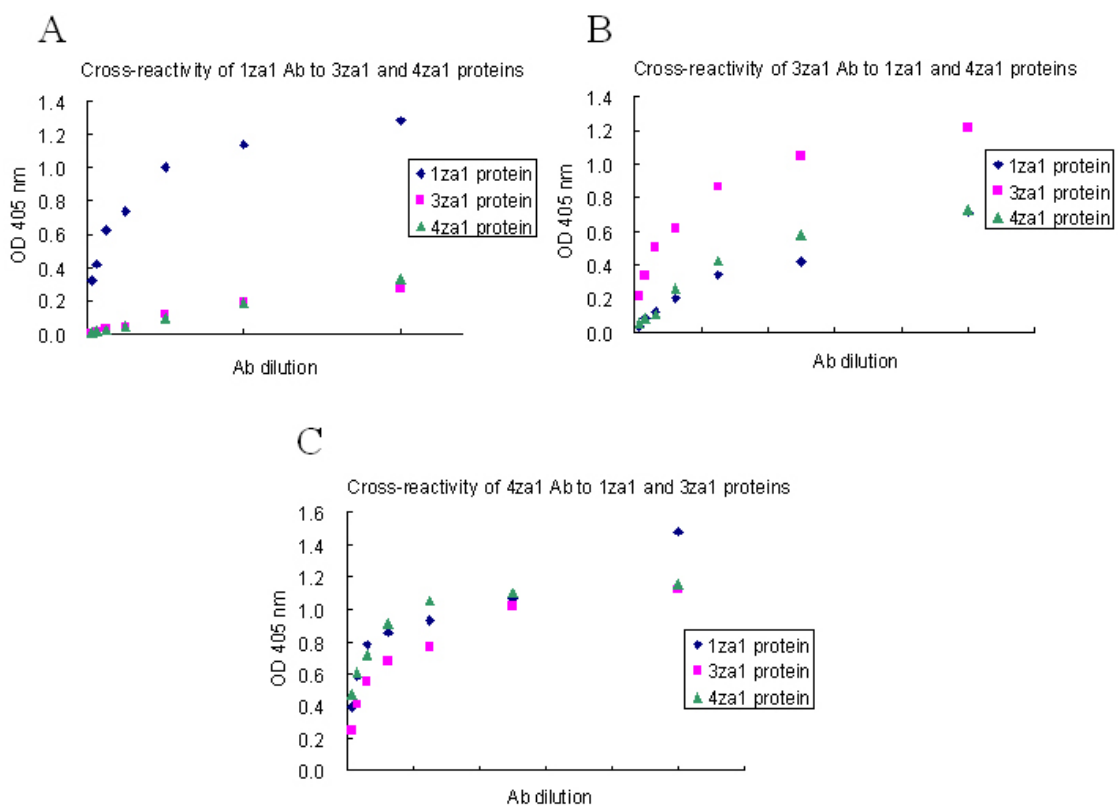


Fig. 3-18 Cross-reactivity of crude sera against matrilin-1 (A), matrilin-3a (B) and matrilin-4 (C) with VWA1 proteins. (A) Crude serum against matrilin-1 showed high affinity to matrilin-1 with minor cross-reactivities to matrilin-3a (3za1) and matrilin-4 (4za1) VWA1 proteins. Crude sera against matrilin-3a (B) and matrilin-4 (C) have strong cross-reactivities to matrilin-1 (1za1), 3za1 and 1za1/ 3za1, respectively.

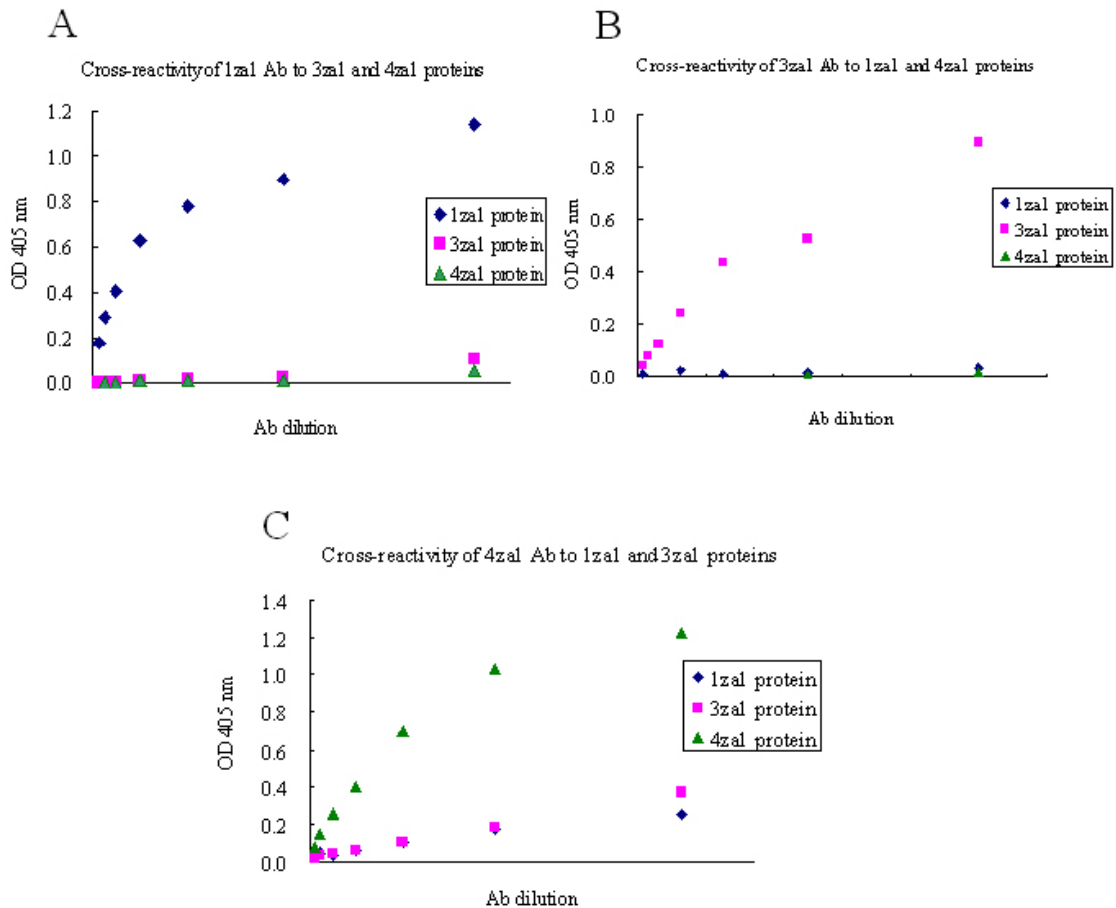


Fig. 3-19 Cross reactivity of affinity purified antibodies. After purification by affinity chromatography on a column carrying the original antigen, the antibody against matrilin-1 (A) and matrilin-3a VWA domains (B) showed no remaining cross-reactivity to recombinant VWA1 domains of matrilin-3a (3za1), matrilin-4 (4za1) and matrilin-1 (1za1) and 4za1, respectively. (C) The affinity purified antibody against matrilin-4 showed a minor cross-reactivities with matrilin-3 (3za1) and -1 (1za1).

As the discovery of matrilin-3b was only recent, an antiserum to this protein is still underway. Hence, the cross-reactivity of each of the matrilin-1, -3a and -4 antibodies to the matrilin-3b protein was first examined. The antibody to matrilin-3a showed only a marginal cross-reactivity with the matrilin-3b VWA1 domain (Fig. 3-20 and Fig. 3-21), despite their high sequence identity. Surprisingly, matrilin-1 had strong cross-reactivity to matrilin-3b and the cross-reaction was still present after depletion on a chromatography column carrying recombinant matrilin-3b protein (Fig. 3-21). After reiterating the depletion procedure, the anti-matrilin-1 titer was lost (data not shown).

Cross-reactivity via His₆ epitope could be ruled out (not shown) and the results indicate that matrilin-1 and matrilin-3b share a common epitope. Fortunately, preincubation of matrilin-1 antibody with matrilin-3b recombinant protein before applying it in the ELISA assay could inhibit this cross-reactivity (Fig. 3-22 B) without loss of affinity to matrilin-1 protein (Fig. 3-22 A).

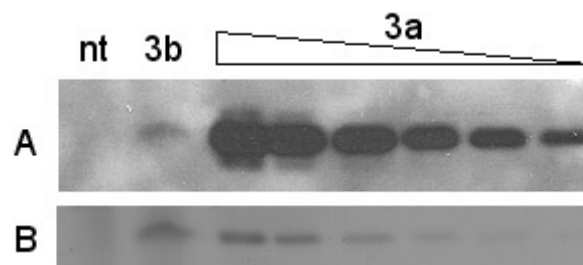


Fig. 3-20 Cross-reactivity of the antibody to matrilin-3a with matrilin-3b. (A) Immunoblot analysis of cell culture supernatant of non-transfected (nt) and matrilin-3b VWA domain-expressing (3b) HEK-293/EBNA cells and purified matrilin-3a VWA domain at different concentrations (3a) using the antibody specific for matrilin-3a. (B) Ponceau staining of (A) to show protein loading.

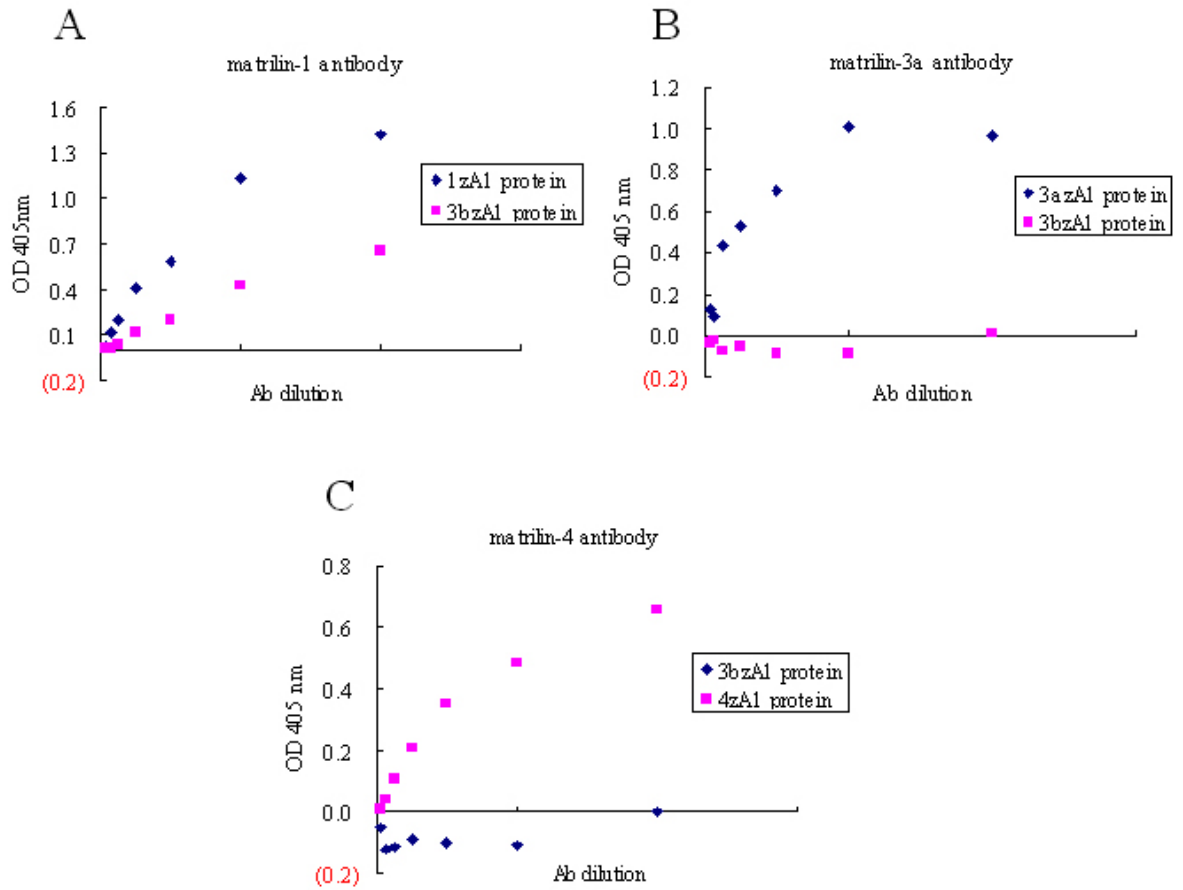


Fig. 3-21 Cross-reactivities of affinity purified antibodies against matrilin-1 (A), matrilin-3a (B) and matrilin-4 (C) VWA domains with matrilin-3b recombinant VWA domain (3bza1). The antibody against matrilin-1 has a strong cross-reactivity to 3bza1 protein (A), whereas the antibodies against matrilin-3a (B) and matrilin-4 (C) do not.

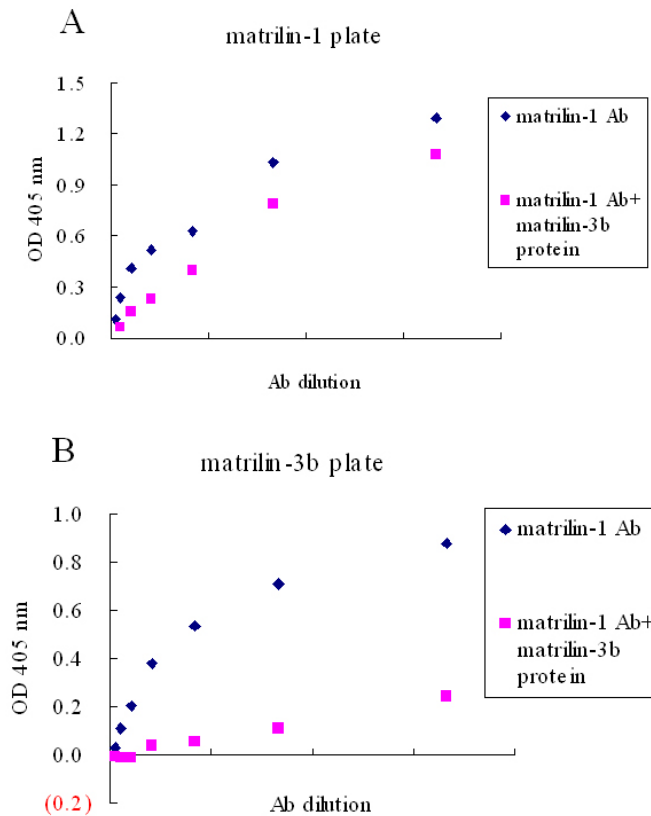


Fig. 3-22 ELISA after blocking the matrilin-1 antibody with matrilin-3b protein. The antibody against matrilin-1 retains high titer to the matrilin-1 VWA1 domain after preincubation with matrilin-3b VWA domain (A), while the titer to matrilin-3b was markedly decreased (B).

3.3.2. Matrilin expression during development

The differential expression of the four zebrafish matrilin genes was studied by RT-PCR at 24, 48, and 72 hpf as well as in adult fish (Fig. 3-23). At 24 hpf, matrilin-4 is already clearly expressed, whereas PCR products corresponding to matrilin-3a and -3b were weak and matrilin-1 could be detected only after overexposure (not shown). At 48 hpf matrilin-4 is strongly expressed and matrilin-3a and -3b are clearly present, again matrilin-1 could hardly be detected. All matrilins show the highest expression at 72 hpf. In adult fish, mRNAs for matrilin-1, -3a and -4 are clearly present, whereas for matrilin-3b only the shortest splice variant containing the VWA domain and the coiled-coil domain could be detected as a weak band. The splice variants carrying the proline- and threonine/serine-rich stretch of amino acid residues were not found in adult fish.

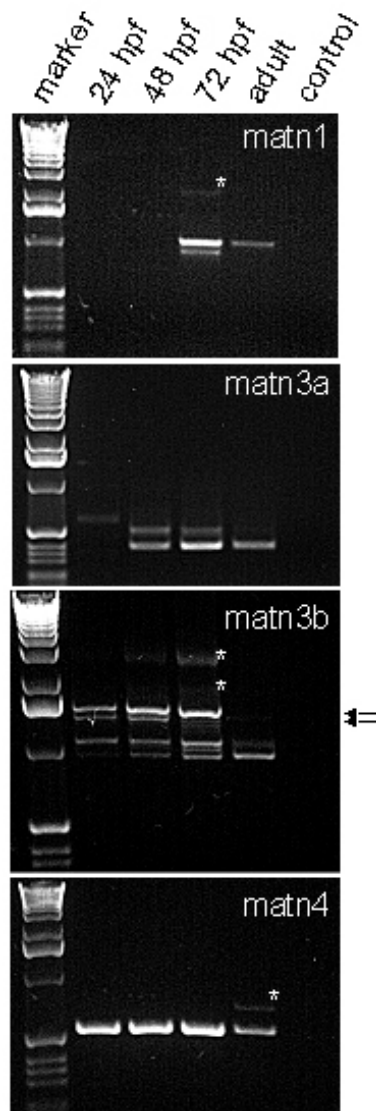


Fig. 3-23 RT-PCR analysis of matrilin mRNA species expressed during zebrafish development. RT-PCR analysis was performed at 24, 48 and 72 hpf, as well as in adult fish using primer pair m1z3 and m1z4 for matrilin-1, m3az3 and m3az4 for matrilin-3a, m3bz2 and m3bz4 for matrilin-3b, and m4z1 and m4z4 for matrilin-4 (see Materials and Methods). The 1-kb ladder from Gibco-BRL was used as a marker. Bands marked with asterisks have been shown by sequencing to be artefactual. In the control sample water was included instead of an cDNA solution. matn, matrilin. Arrows mark the bands coding for matrilin-3b splice variants carrying the proline and threonine/serine-rich domain.

3.3.3. Matrilins are differentially expressed

Whole mount immunostaining was performed on 4-day-old fish using the affinity-purified matrilin antibodies (Fig. 3-24 F–L). All matrilins are present in the developing skeleton. The matrilin-3a antibody strongly stained Meckel's cartilage, the palatoquadrate, the ceratohyal, the ethmoid plate, the anterior basicranial commissure, the parachordal, the hyosymplectic and the auditory capsule, as well as the basis of the pectoral fin (Fig. 3-24 G and K). In addition, matrilin-1 was found in the posterior part of the notochord (Fig. 3-24 I). In contrast to matrilin-1 and -3a, matrilin-4 showed similar staining intensity in Meckel's cartilage, the ceratohyal and the five ceratobranchials (Fig. 3-24 H and L). Further, the matrilin-4 antibody stained the eye (Fig. 3-24 H and L), the skin (Fig. 3-24 H and L) and the myosepta (Fig. 3-24 L). In all fins matrilin-4 staining could be detected in the fin rays (Fig. 3-24 L).

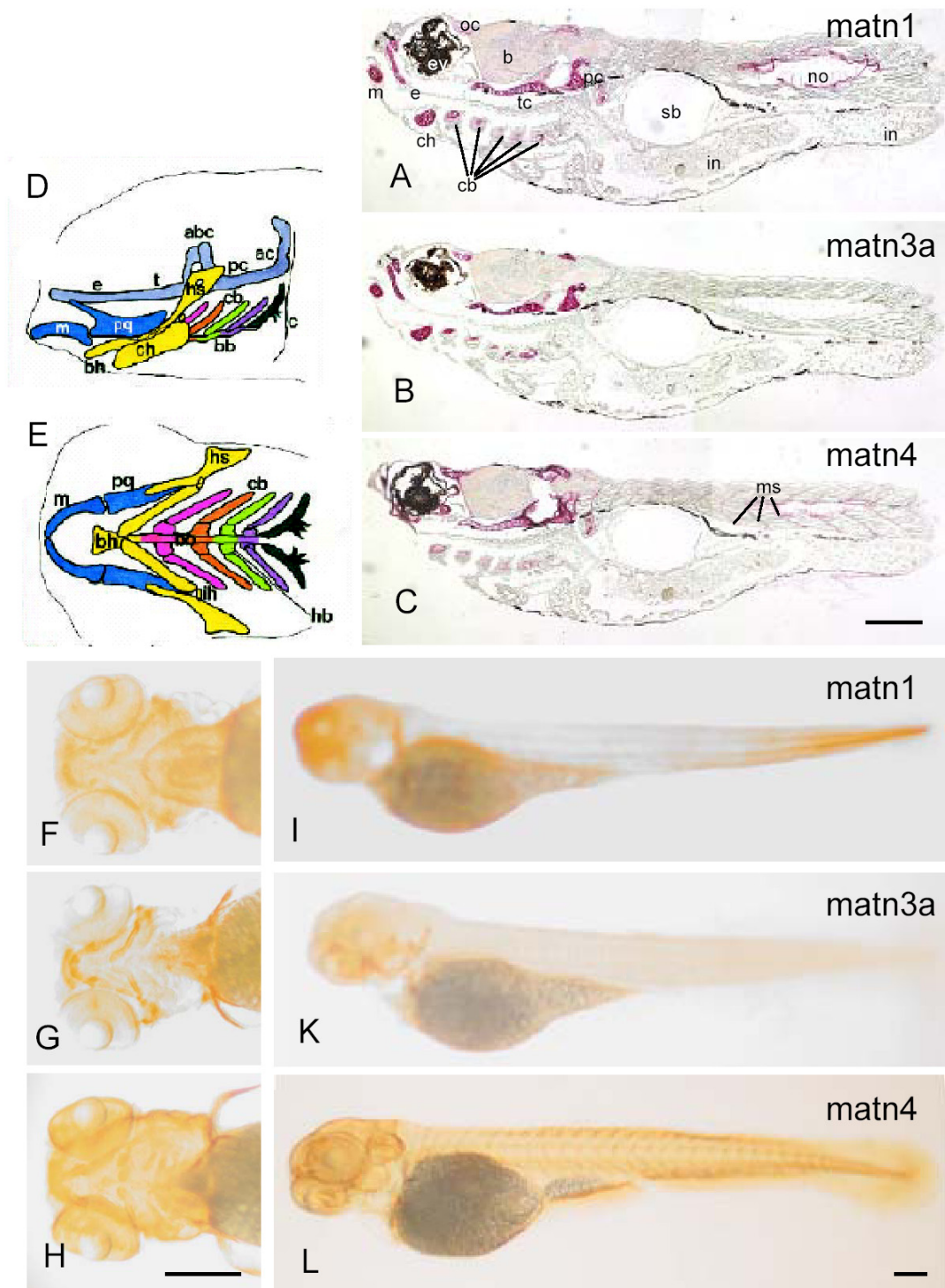


Fig. 3-24 Matrilin tissue distribution in zebrafish larvae. (A-C) Immunostaining of sectioned 5 dpf zebrafish larvae heads and trunks. Paraffin-embedded sections were incubated with affinity-purified antibodies against matrilin-1 (A), -3a (B) or -4 (C), followed by biotin–streptavidin–peroxidase-conjugated goat anti-mouse IgG and alkaline phosphatase-conjugated streptavidin. Matrilin-1 (A), -3a (B) and -4 (C) were expressed throughout the skeletal tissues, including orbital cartilage (oc), Meckel’s cartilage (m), ethmoid plate (e), trabecular cartilage (tc), parachordal cartilage (pc), ceratohyal (ch) and

ceratobranchials (cb) one to five. Matrilin-1 was also found in the notochord (no) and matrilin-4 in myoseptum (ms), surrounding the eyes (ey), and in the brain cortex (b). (F–L) Whole mount immunostaining of 4 dpf zebrafish larvae. Specimens were incubated with affinity-purified antibodies against matrilin-1 (F, I), -3a (G, K) or -4 (H, L), followed by biotin–streptavidin–peroxidase-conjugated goat anti-mouse IgG and alkaline phosphatase-conjugated streptavidin. Ventral views of the head (F–H) and lateral views of whole fish (I–L) are shown. The pharyngeal skeleton is shown schematically (Schilling et al., 1996) in lateral (D), and ventral (E) views. Cartilages of the same segment share the same color: P1 (mandibular, blue), P2 (hyoid, yellow), P3 (first branchial, pink), P4 (orange), P5 (green), P6 (purple) and P7 (black). The neurocranium is shaded uniformly grey. abc, anterior basicranial commissure; ac, auditory capsule; bb, basibranchial; bh, basihyal; c, cleithrum; hb, hypobranchial; hs, hyosymplectic; ih, interhyal; ot, otic capsule; pq, palatoquadrate; t, trabeculae cranii. Scale bars, 200 μ m. matn, matrilin.

In addition, the tissue distribution of zebrafish matrilins was investigated on paraffin sections of 5 dpf and 4-month-old zebrafish. Sectioning of 5 dpf fish (Fig. 3-24 A–C) clearly confirmed the restricted skeletal staining of matrilin-3a seen in whole mount stainings (Fig. 3-24 K). In contrast, matrilin-1 could be detected in the notochord and in intestine, albeit after long exposure (Fig. 3-24 A). Matrilin-4 is more widespread and could be detected in the eye and in the myoseptum (Fig. 3-24 C), as well as in skeletal tissues. The overall expression pattern was not altered in sections of 4-month-old fish, but as the fish were larger a more detailed analysis could be performed (Fig. 3-25). In consecutive sections through the trabecular bone of the skull matrilin-1 (Fig. 3-25 G) and matrilin-3a (Fig. 3-25 H) showed a similar expression in proliferating, and more strongly in hypertrophic cartilage, but only matrilin-3a was found in perichondrium (Fig. 3-25 H). In contrast, matrilin-4 revealed a strong zonal expression in the proliferating cartilage (Fig. 3-25 I). In vertebrae the staining for matrilin-3a was broad and strong (Fig. 3-25 L), whereas matrilin-1 and -4 are expressed only around proliferating chondrocytes (Fig. 3-25 K, M). Uniquely, matrilin-1 shows a staining in the notochord and in the surrounding secondary chordal sheath (Fig. 3-25 A, B, K), whereas matrilin -3a is not present in these tissues (Fig. 3-25 D). Matrilin-1 can still be detected in intestine (Fig. 3-25 C) and, as in 5 dpf fish, matrilin-4 was found in myoseptum (Fig. 3-25 F). Interestingly, matrilin-4 is strongly expressed in the adenohypophysis (Fig. 3-25 E).

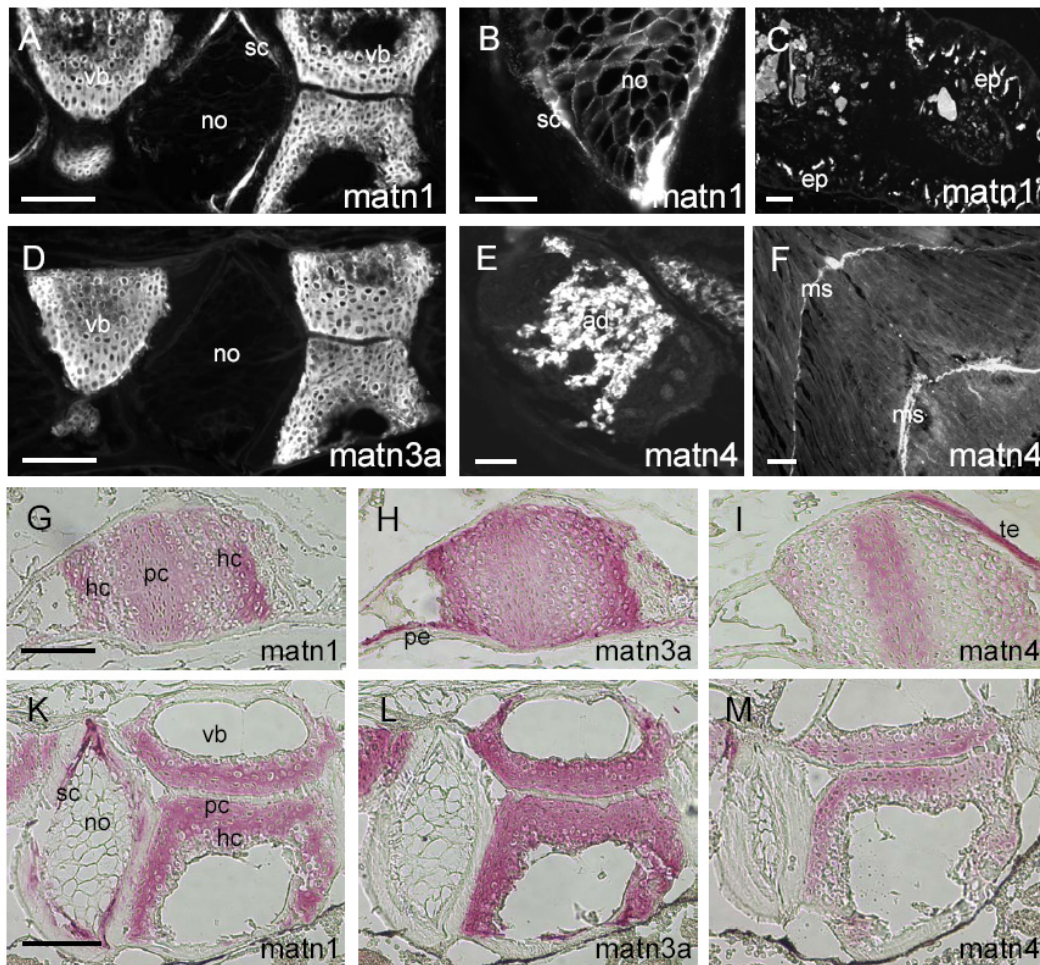


Fig. 3-25 Matrilin tissue distribution in 4-month-old zebrafish. (A–F) Immunofluorescence microscopy was carried out on paraffin-embedded tissue sections which were incubated with affinity-purified antibodies against matrilin-1 (A–C), -3a (D) or -4 (E, F), followed by Cy3-conjugated goat anti-rabbit IgG. In the vertebrae (vb), matrilin-1 was detected in the cartilage, in the secondary chordal sheath (sc) (A), the notochord (no) network (B) and in the intestinal epithelium (ep) (C), whereas matrilin-3a was found in the cartilage of the vertebrae (vb) (D). Strong signals for matrilin-4 were found in the adenohypophysis (ad) (E) and in myosepta (ms) (F) throughout the fish. (G–M) Immunohistochemistry was performed on paraffin-embedded tissue sections by staining with affinity-purified antibodies against matrilin-1 (G, K), -3a (H, L) or -4 (I, M) followed by biotin–streptavidin–peroxidase-conjugated goat anti-mouse IgG and alkaline phosphatase-conjugated streptavidin. In the trabecular bone (G–I) and vertebrae (K–M), matrilin-1 is deposited in proliferating (pc) and hypertrophic cartilage (hc) and in the secondary chordal sheath (sc) (G, K); matrilin-3a is expressed throughout the cartilage including proliferating (pc) and hypertrophic cartilage (hc) (H, L) and perichondrium (pe) (H); whereas matrilin-4 is weakly expressed only in the proliferating cartilage (pc) (I, M). te, tendon. Scale bars represent 100 μ m, except for those in (B, E) which represent 50 μ m. matn, matrilin.

3.3.4. Morpholino knockdowns of matrilins

3.3.4.1. Specificity of morpholinos

In this project, morpholino antisense oligonucleotides were employed to investigate matrilin function in zebrafish. Since the morpholinos we used function by covering the AUG translational starting site, which in turn inhibits translation, the downregulation of protein would be important evidence to prove whether the morpholinos really function. 0.5 nl morpholino solution (0.5 mM) directed against matrilin-4 was microinjected into one-cell embryo yolk sacs and whole mount immunostaining of 24 hpf embryos with a specific antibody against matrilin-4 revealed a decreased matrilin-4 protein content in myosepta (Fig. 3-26). At a higher dose (2 nl), signals in myosepta disappear and in addition, a curled body shape and poorly developed eyes were observed. A morpholino which does not bind to any gene was used as negative control and showed the same matrilin-4 protein amount as in non-injected wildtype embryos (Fig. 3-26). These results demonstrate that the morpholino is functional and the knockdown effect is specific.

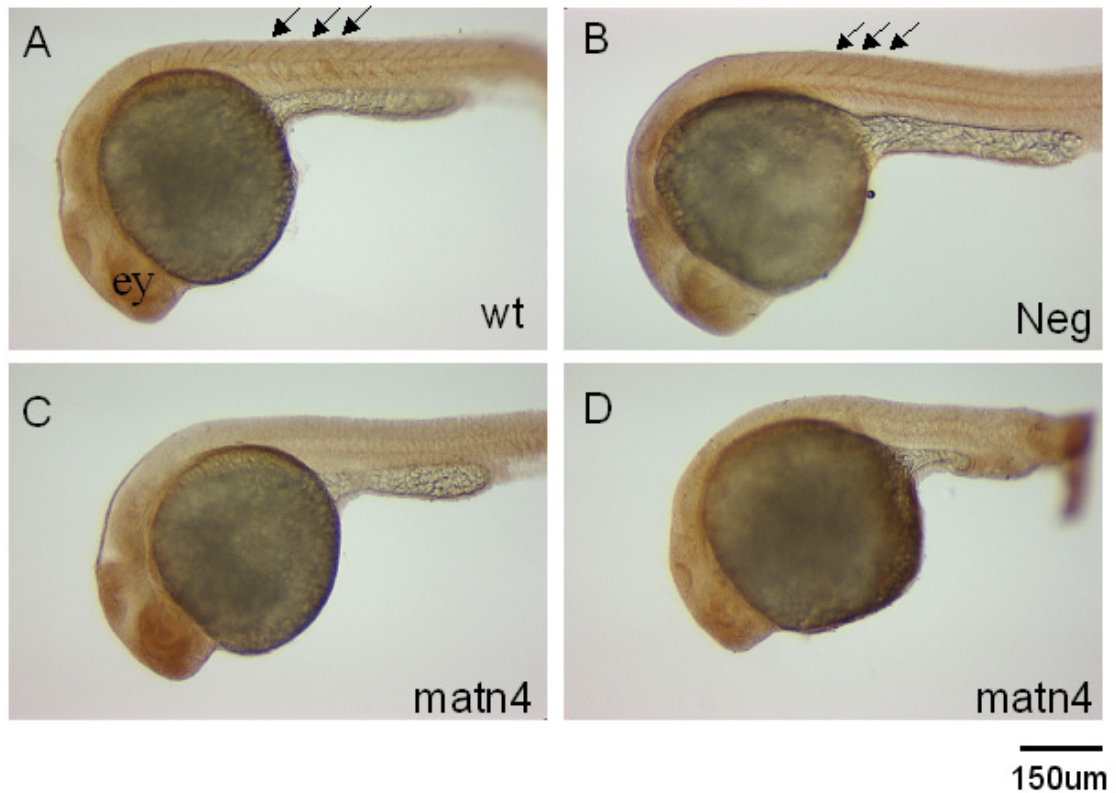


Fig. 3-26 Protein loss in matrilin-4 morpholino knockdown embryos at 24 hpf. (A) Whole mount immunostainings were performed in embryos of non-injected wildtype (wt), (B) embryo injected with 2 nl of 0.5 mM negative control morpholino (Neg) and 0.5 nl (C) and 2 nl (D) of 0.5 mM morpholino against matrilin-4 (matn4) at 24hpf. In wildtype embryos and embryos injected with negative control morpholino (Neg), matrilin-4 was stained in myosepta and eyes (ey) (A , B), whereas in embryos injected with 0.5 nl morpholino against matrilin-4 (C), expression of matrilin-4 in myoseptum disappeared even though the embryos did not show any apparent abnormality in body shape and immunostaining could still be seen in the eyes (C). In matrilin-4 knockdown embryos injected with a higher morpholino dose (2 nl), abnormalities in body shape occurred together with a poor eye development (D). Immunostaining with specific antibody against matrilin-4 revealed a decreased signal in eyes, while myosepta were truncated and the notochord bent.

3.3.4.2. Matrilin knockdown phenotypes

In the morpholino knockdown experiments, chordin, an antagonist of bone morphogenetic protein, is often used as a positive control. The knockdown phenotypes of chordin have been well characterized showing abnormal u-shaped somites, abnormal tail fin, smaller head and expanded blood island (Nasevicius and Ekker, 2000).

Observation of the same phenotypes (Fig. 3-27) indicates a specific knockdown effect of morpholino and thereby technically successful microinjection.

The phenotypes seen in *matrilin-1*, *-3a* and *-4* knockdown embryos are shown in Fig. 3-27. Upon injecting anti-*matrilin-1* morpholinos, we observed an u-shaped body with an abnormal caudal fin (Fig. 3-27). Zebrafish injected with *matrilin-3a* morpholinos also present small body size and a malformed caudal fin (Fig. 3-27), while injection of *matrilin-4* morpholinos yields a truncated caudal region (Fig. 3-27) and a lower survival rate (not shown). This may indicate that loss of the *matrilin-4* gene has a stronger effect on early development due to earlier or broader expression. *Matrilin-3b* had not yet been identified at the time of these experiments and its knockdown phenotype remains to be studied.

Skeletal malformations occur in all *matrilin* knockdown embryos, indicating that *matrilins* play important roles during zebrafish skeletal development. However, within the scope of this work, it was only possible to investigate one member of the *matrilin* family in detail.

Since *matrilin-1* is the most abundant *matrilin* and had been most extensively characterized in mammals and birds, *matrilin-1* was chosen for in depth study.

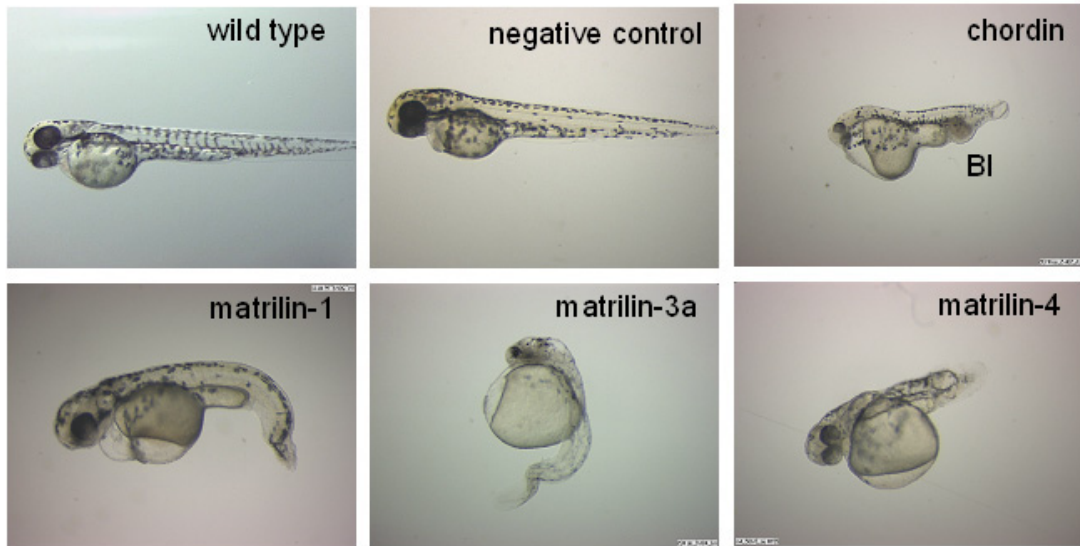


Fig. 3-27 Phenotypes of matrilin knockdown embryos. Chordin knockdown embryos showed a smaller head, an enlarged blood island (BI) and an abnormal caudal fin. Upon injection of matrilin-1 morpholinos embryos took on a curled body shape and displayed an abnormal caudal fin. In knockdowns of matrilin-3a, the embryos had a smaller head and a bent body axis. The matrilin-4 knockdown embryos showed a truncated caudal region and the caudal fin did not develop.

3.3.4.3. Matrilin-1 knockdown phenotype

Upon injecting anti-matrilin-1 morpholinos, at 48 hpf we observed a small head and an abnormal spinal cord (Fig. 3-28 D and E). When the doses were increased, the body was truncated, the heads smaller and the eyes poorly developed (Fig. 3-28 E, arrow). Zebrafish injected with nonsense (MO-Neg) or 5-mismatch matrilin-1 morpholino (5m-m1) did not present any obvious abnormalities (Fig. 3-28 B and C). A closer view of matrilin-1 knockdown embryos at 48 hpf showed that some have not developed the notochord and the pectoral fin (Fig. 3-29 A-C), but also that some embryos appear more normal (Fig. 3-29 D-F), even though these fish still have a curled body shape.

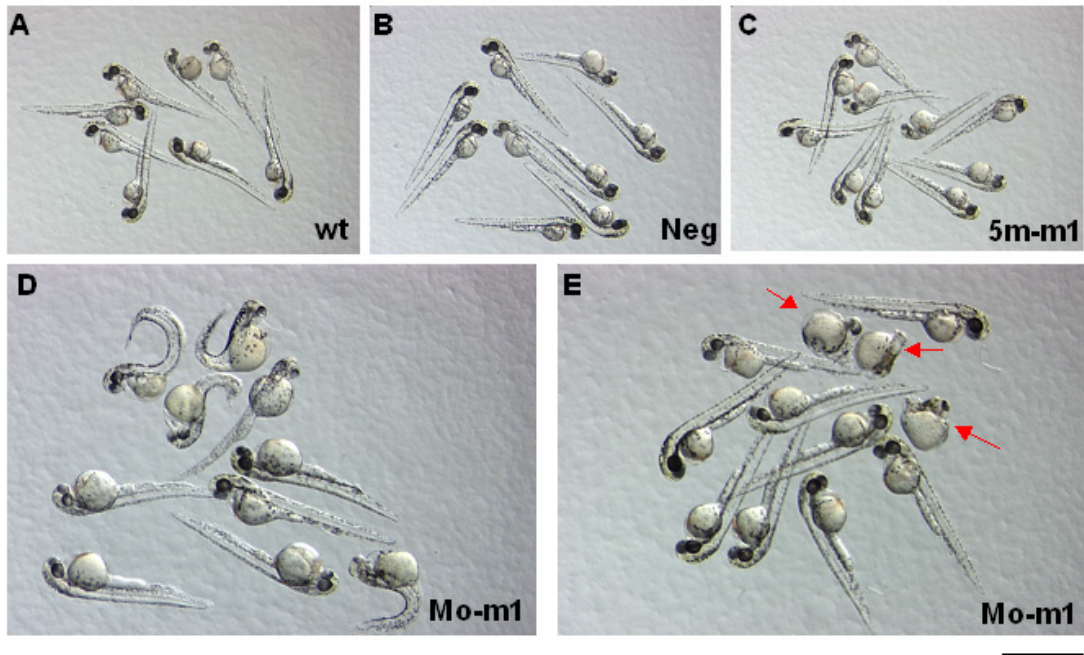


Fig. 3-28 Phenotypes of matrilin-1 knockdown embryos at 48 hpf. Overview of embryos without any injection (wt, A), injected with negative control morpholinos (Neg, B), 5-mismatch of matrilin-1 morpholino (5m-m1, C) and matrilin-1 morpholino (Mo-m1, D and E). Neither injection of 5-mismatch matrilin-1 (C) nor standard control morpholino cause abnormalities (B). However, matrilin-1 knockdown embryos had a curled body shape and a slightly smaller head (D, 2 nl). In higher doses (2.87 nl), the body axis did not longer develop (E, red arrow). Scale bar: A, Band C, 1180 μ m ; D and E, 800 μ m.

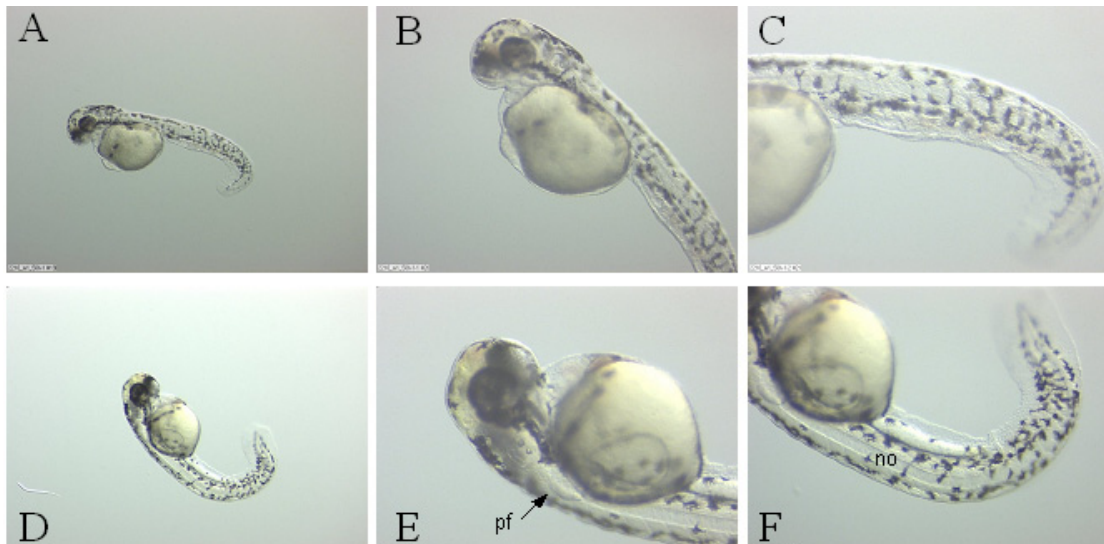


Fig. 3-29 Matrilin-1 knockdown phenotype. Matrilin-1 knockdown embryos at 48 hpf showed a curled body shape (A, D). Some of them had normal notochord (no) and pectoral fin (pf) development (D, E, F) but some did not (A, B, C). B and C are higher magnifications of A, and E and F of D.

To examine whether skeletal architecture was altered, whole mount alcian blue staining for cartilage of wildtype and matrilin-1 knockdown embryos was performed at 48 hpf (Fig. 3-30). The overall size of the head was smaller and shorter in matrilin-1 knockdown embryos (Fig. 3-30 D), but the reduction was not so pronounced that it could be seen in anesthetized live embryos (Fig. 3-30 B). Alcian blue staining also showed a shorter ethmoid plate and the lack of the fifth ceratobranchial (Fig. 3-30 D). Meckel's cartilage did not protrude as it does in wildtype (Fig. 3-30 D). In addition, the optic capsules were not stained in matrilin-1 knockdown embryos (not shown). In live embryos, it was seen that injection of matrilin-1 morpholino caused a retarded eye development as compared to that of wildtype (Fig. 3-30 B and D).

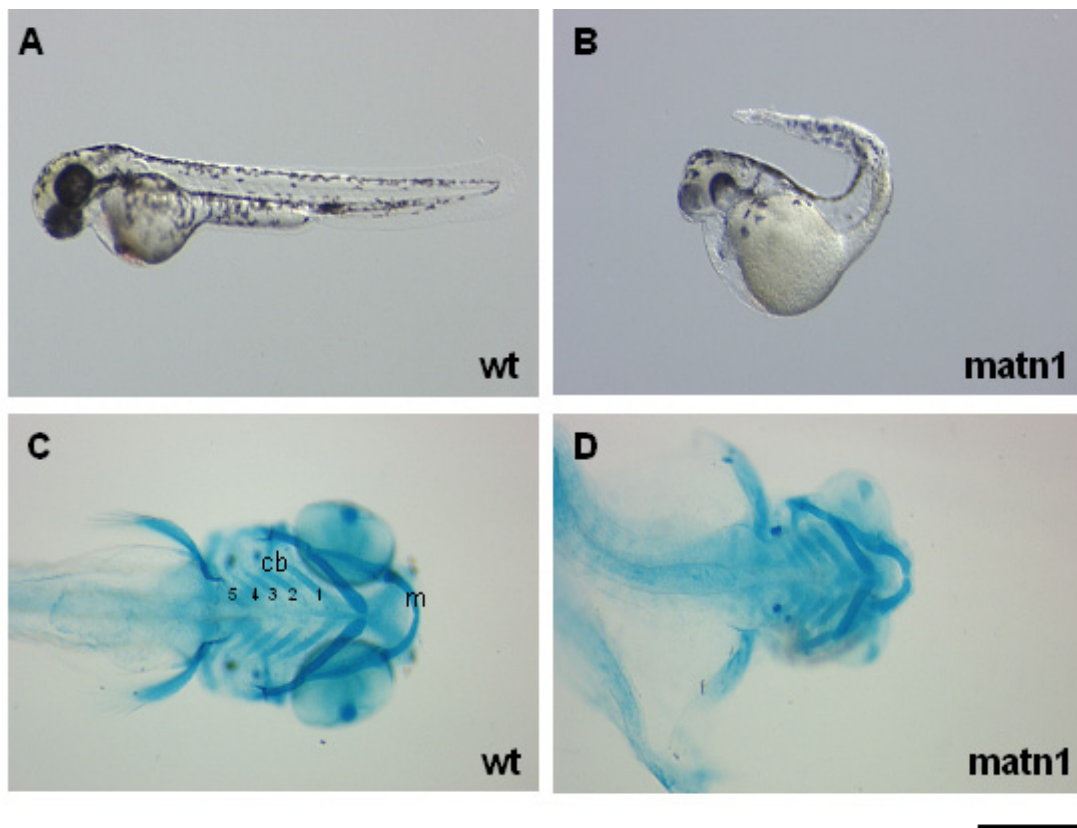


Fig. 3-30 Skeletal phenotype of matrilin-1 knockdown embryo. Matrilin-1 knockdown (*matn1*, B) embryos were observed at 48 hpf and showed a curled body shape and smaller eyes compared to that of wildtype (*wt*, A). A ventral view of alcian blue stained cartilages showed that matrilin-1 knockdown embryos (D) have smaller heads, shorter ethmoid plates and lack the fifth ceratobranchial (*cb*). Meckel's cartilage (*m*) also does not protrude as it does in wildtype embryos (C). Scale bar, A and B, 400 μ m; C and D, 200 μ m.

3.3.4.4. First characterization of matrilin-3a and matrilin-4 knockdown embryos

Matrilin-3a and -4 knockdown embryo phenotypes are shown in Fig. 3-31. Upon injection of matrilin-3a morpholinos, embryos showed a curled body axis (Fig. 3-31 A-C). Injection of matrilin-4 morpholino caused abnormal caudal fins and a shorter body axis (Fig. 3-31 D and E) sometimes smaller eyes (Fig. 3-31 F).

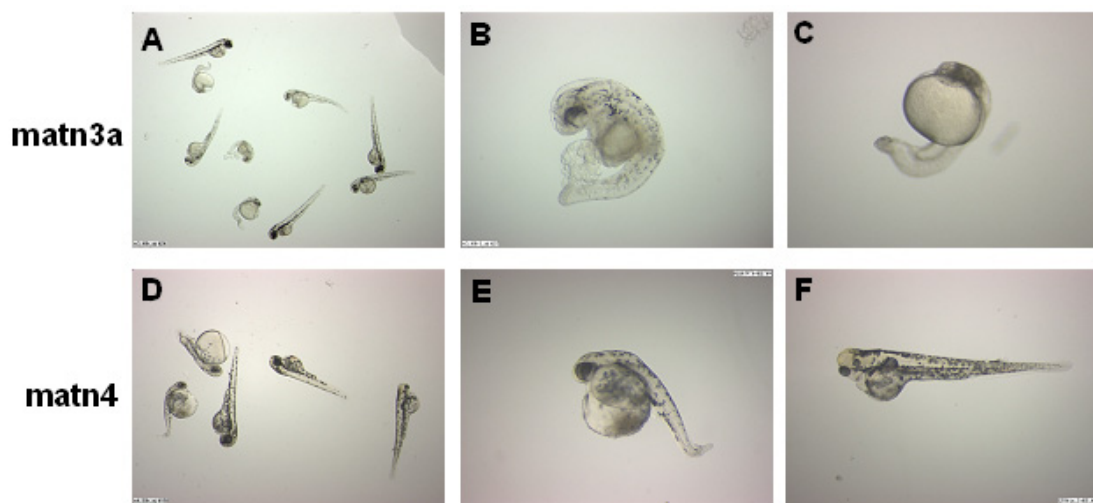


Fig. 3-31 Phenotypes of matrilin-3a (A-C) and matrilin-4 (D-F) knockdown embryos at 48 hpf.

3.3.4.5. Phenotype frequency and survival rate

It is obvious that not all morpholino injected embryos present abnormalities. This variation may be due to the efficiency of delivery of the morpholino from the yolk sac to the animal pole depending on the position of injection. Therefore it is important to calculate the phenotype frequency in order to judge the statistic significance.

The survival rate was first calculated. A nonsense morpholino and a morpholino directed against chordin were used as a negative and a positive control, respectively. The survival rate of embryos injected with the anti-matrilin-1 morpholino was the same

as that of controls. 40% of matrilin-1 knockdown embryos survive at 24 hpf and only half of them can survive for further 24 h. Therefore the phenotype frequency was calculated at 48 hpf.

About 10% of embryos injected with negative control morpholino showed an abnormal phenotype, whereas 60% of embryos injected with the anti-chordin morpholino showed a phenotype. Embryos injected with the anti-matrilin-1 morpholino revealed a 55% phenotype frequency.

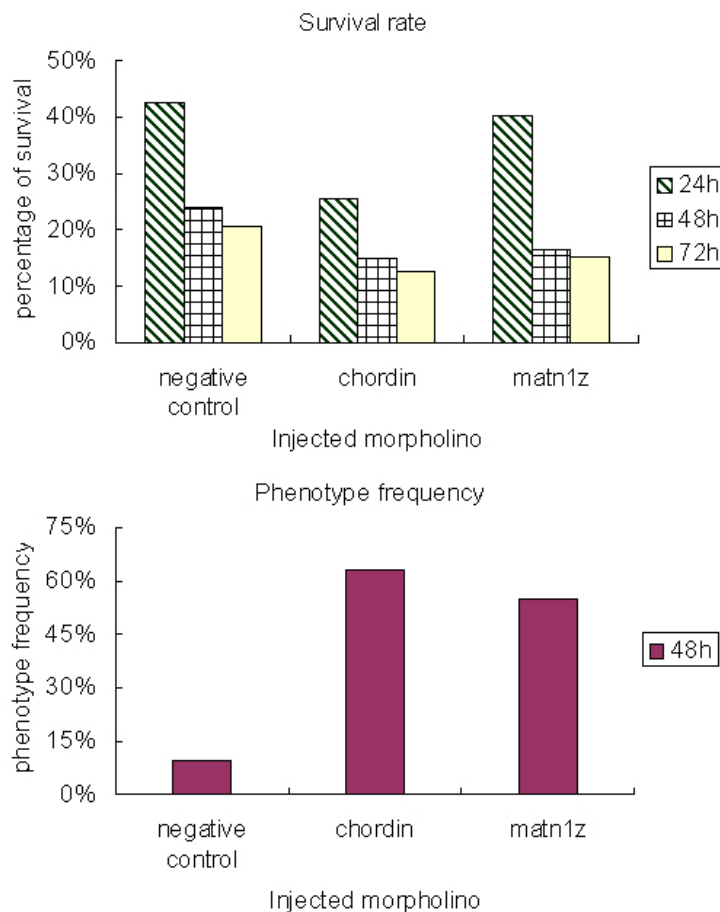


Fig. 3-32 Survival rate and phenotype frequency of morpholino knockdown embryos. Survival rates were measured at 24, 48 and 72 hpf for embryos injected with negative control, chordin and matrilin-1 (matn1z) morpholino. The phenotype frequency was calculated at 48 hpf.

4. Discussion

4.1. Mouse matrilins

It has been proposed that matrilins play an important structural role in extracellular matrices by being part of filamentous networks. In cartilage, all four members of the matrilin family are expressed, suggesting important biological role(s) for matrilins in this tissue. Studies with chondrosarcoma cell lines or with primary chondrocytes revealed that matrilin-3/matrilin-1 networks connect neighboring cells in a collagen-dependent manner, whereas in the pericellular matrix, these matrilins also form collagen-independent filaments (Chen et al., 1995; Chen et al., 1999; Klatt et al., 2000). Matrilin-1, the best-characterized matrilin, binds with a certain periodicity to type II collagen fibrils (Winterbottom et al., 1992) and becomes covalently attached to aggrecan (Hauser et al., 1996), presumably forming a bridge between the two major supramolecular components of the cartilage. Based on structural similarities, this bridging, or adaptor function was suggested as a common feature of all matrilins (Deak et al., 1999). A study in the Swarm rat chondrosarcoma indicates that the actual interactions between matrilins and other cartilage matrix proteins might be even more complex. It was shown that matrilin-1, matrilin-3, and matrilin-4 form complexes with the small leucine-rich repeat (LRR) proteoglycans decorin and biglycan, which in turn bind to the N terminal VWA domains of collagen type VI. In this manner matrilins and LRR proteoglycans may together link collagen VI microfibrils to aggrecan or collagen II (Wiberg et al., 2003).

The biological relevance of such matrilin-mediated interactions is not clear. Matrilin-1-deficient mice have no obvious skeletal defects (Aszodi et al., 1999; Huang et al., 1999), and in this dissertation it is shown that mice lacking matrilin-3 are indistinguishable from wildtype mice and display normal cartilage and bone development. There are also no alternations in the deposition of cartilage matrix proteins, such as collagen II and aggrecan, in chondrocyte differentiation, growth plate structure, and replacement of cartilage by bone. In contrast to *Matn-1* null mice,

where one of the two strains produced show a mild defect in collagen fibril organization in the maturation and hypertrophic zone of the growth plate (Aszodi et al., 1999; Huang et al., 1999), no ultrastructural abnormalities were observed in *Matn-3*-deficient mice. These results suggest that the absence of matrilin-3 alone has no influence on skeletal development and the proper assembly of the extracellular matrix.

4.1.1. Matrilin-3 is dispensable for mouse skeletal development

The lack of an apparent phenotype in matrilin-3 null cartilage could be explained by a functional compensation by other members of the matrilin family expressed in skeletal tissues. Matrilin-3 is coexpressed with matrilin-1 and matrilin-4 in the resting, proliferative, and hypertrophic zones of the developing knee joint, and all four matrilins are present in the proliferative and upper hypertrophic zones (Klatt et al., 2002) (Fig. 3-9). Similarly, matrilin-3 is coexpressed with at least one other matrilin in the articular, sternal, costal, and vertebral cartilage and the inner part of the annulus fibrosus of the intervertebral disk (Klatt et al., 2002). Northern blot, immunohistochemical, and biochemical analyses of newborn knee joint or sternal cartilage did not reveal a compensatory upregulation of *Matn-1*, *Matn-2* or *Matn-4* in *Matn-3* null mice, but redundancy between matrilin-3 and, especially, matrilin-1 and/or matrilin-4 cannot be excluded. Such a redundancy among matrilins was already suggested to explain the lack of an overt phenotype in the matrilin-1-deficient mice (Aszodi et al., 1999; Huang et al., 1999).

4.1.2. A biochemical phenotype in matrilin-1/matrilin-3 double deficient mice

Despite the lack of perceptible changes from biochemical analysis of single matrilin knockout mice (Aszodi et al. 1999; Huang et al, 1999; Ko et al., 2004, Mates et al., 2004), in this dissertation an increased amount of matrilin-4 was found in cartilage

extracts of newborn matrilin-1/matrilin-3 double knockout mice as compared to wildtype mice. Reexamination of the matrilin-1 single knockout mice showed an upregulation of matrilin-4 also in these animals, a feature missed in the original examination of the matrilin-1 knockout (Aszodi et al., 1999) as matrilin-4 antibodies were not yet available at that time. As the northern blot shows no upregulation of matrilin-4 at the transcriptional level, either translation is increased, the turnover decreased or the extractability of matrilin-4 increased. As the matrilins act as adaptor proteins, it could be that the loss of another member of the family leads to a less stable supramolecular assembly. Further evidence for a close association of matrilin-1 and -4 comes from the loss of a particular matrilin-4 containing oligomer in both matrilin-1 and matrilin-1/-3 deficient animals (Fig. 3-16). It was excluded that this band represents heterooligomers of matrilin-1 and -4. Based on the electrophoretic mobility the molecular mass lies between that of a full-length matrilin-4 trimer and that of a proteolytically cleaved dimer (Klatt et al., 2001), which could be due to the occurrence of shorter splice variants or N- terminally processed forms of matrilin-4. However, it remains unclear why these forms of matrilin-4 are lost in the mice lacking matrilin-1. In contrast, the extractability of COMP, collagen type II, biglycan and decorin, which have been described as binding partners of matrilins, was not affected.

4.1.3. Matrilins in disease

Mutations in extracellular matrix proteins expressed in cartilage frequently lead to human osteochondrodysplasias of varying severity. To date, matrilin-3 is the only known member of the matrilin family found to be associated with such disorders (Chapman et al., 2001). In addition, in a genomic screen of the Icelandic population a mutation in the first EGF domain of matrilin-3 was linked to the occurrence of hand osteoarthritis (Stefansson et al., 2003). A mild form of the autosomal dominant multiple epiphyseal dysplasia (MED) is caused by missense mutations in the second exon of the *MATN3* gene encoding the VWA domain (Chapman et al., 2001; Mabuchi et al., 2004). Another missense mutation in the same region of *MATN3* (A128P) was discovered in a family with bilateral hereditary microepiphyseal dysplasia (BHMED), which gives a skeletal phenotype similar to but still distinct from common MED (Mostert et al., 2003).

In addition, an autosomal recessive form of another osteochondrodysplasia, spondylo-epi-metaphyseal dysplasia (SEMD), is caused by a change of a cysteine into a serine residue in the first EGF domain of matrilin-3 (Borochowitz et al., 2004), which could lead to a disturbance in the disulphide bond formation. These mutations were suggested to alter the folding and/or function of the protein, indicating that the disorder is most probably due to a dominant-negative effect rather than being caused by haploinsufficiency (Briggs and Chapman, 2002; Chapman et al., 2001). This hypothesis is further strengthened by the observation that a single nucleotide deletion in *MATN3*, which creates a premature stop codon at amino acid residue 164, has no pathophysiological consequence (Briggs and Chapman, 2002). Indeed, the influence of the matrilin-3 mutations causing MED, SEMD and hand osteoarthritis on the secretion of matrilin-3 was recently studied. The results revealed that matrilin-3 with the mutations causing MED and SEMD is retained in the endoplasmic reticulum whereas matrilin-3 carrying the hand osteoarthritis mutation could be secreted by chondrocytes at a similar rate as wildtype matrilin-3 (Otten et al., 2005). It is likely that this retention causes a chondrocyte dysfunction by which MED and SMED phenotypes could be explained.

A similar contrast between the null mutation in mice and the human disorder was recently described for COMP. COMP-deficient mice are normal and display no detectable skeletal defects (Svensson et al., 2002). Mutations in the human *COMP* gene, however, lead to MED and the clinically more severe pseudoachondroplasia (PSACH) (Briggs and Chapman, 2002). Most of these mutations cause conformational changes of COMP, resulting in its reduced secretion and accumulation in the rough endoplasmic reticulum. The misfolded COMP molecules, in turn, coretain their physiological matrilin partners, including collagen type IX, decorin, and aggrecan, in the rough endoplasmic reticulum, leading to an accumulation of intracellular protein and, as a consequence, reduced cell viability (Dinser et al., 2002).

The lack of a chondrodysplasia phenotype in the matrilin-3-deficient mice is in line with these results and strongly points to dominant-negative effects as the pathomechanism of MED.

In summary, the results show that the absence of matrilin-3 in mice has no impact on endochondral bone formation and indicates that loss-of-function mutation(s) in the matrilin-3 gene cannot account for MED and MED-like disorders seen in humans. The lack of obvious phenotypes even in matrilin double knockout mice will make the analysis of matrilin function by the knockout technology complicated and laborious as probably only triple or even quadruple knockouts will show an effect. Therefore an alternative animal model, which possibly displays a lesser redundancy would be desirable.

4.2. Zebrafish matrilins

The zebrafish is a powerful model organism for the study of vertebrate development. The rapid embryonal development, the transparency of embryos and the high fertility leading to large numbers of embryos allows large-scale mutagenesis in a fast and easy way. As matrilins are not found in invertebrates as *Drosophila* or *C. elegans*, zebrafish is among the simplest organisms, which express matrilins. The presence of highly conserved zebrafish orthologues points to an important biological function of this gene family.

Therefore zebrafish was chosen as a second model organism in which to study matrilin function. In contrast to mouse, only three members of the matrilin family can be found in zebrafish, matrilin-1, -3 and -4, even though the matrilin-3 gene has been duplicated (Ko et al., 2004). A matrilin-2 gene could not be identified in zebrafish by screening the draft sequence of the zebrafish genome project, which is finished to 60%, or by performing RT-PCR using degenerate primers (Ko et al., 2004). The temporal and spatial expression patterns of zebrafish matrilins are characterized in this dissertation and show similarities to those of their mouse orthologues (Klatt et al., 2002).

Matrilin-1 can be clearly detected in zebrafish embryos at 72 hpf by RT-PCR and the protein is expressed not only in cartilage but also in notochord, secondary chordal sheath and intestine. Similar to in mammals (Mundlos and Zabel, 1994), matrilin-1 can also be detected in the eyes of adult fish (data not shown). In addition, in situ

hybridization with probes specific for matrilin-1 gives a strong signal in pectoral fins in 56 hpf embryo (B. Kobbe, pers. communication). The notochord is a source of bone matrix and in addition plays a key role in the segmental patterning of vertebrae (Fleming et al., 2004), and the expression of matrilin-1 in notochord indicates a role in skeletal development.

Zebrafish matrilin-3a is clearly expressed at 48 hpf. In comparison with the other members of the matrilin family, expression of matrilin-3a is more restricted to cartilage. Matrilin-3b was identified only recently and a specific antibody was already generated. However, due to time limitations, a detailed characterization of matrilin-3b has not yet been performed. Nevertheless, RT-PCR results indicate that matrilin-3b is clearly expressed, with the earliest detection of mRNA at 24 hpf.

Similar to its mammalian counterpart (Klatt et al., 2001), zebrafish matrilin-4 is the most widely expressed member of the matrilin family. It is also expressed very early in development. By RT-PCR a strong signal can be detected already at 24 hpf and protein expression is found not only in skeletal tissues but also in myosepta, in tissues surrounding the eyes and in the brain cortex. Uniquely, matrilin-4 is strongly expressed in the adenohypophysis in adult fish. The expression of matrilin-4 here may indicate a function of matrilin-4 in glandular function. Matrilin-4 expression in the adenohypophysis of mammals has not yet been studied.

The large number of splice variants is characteristic for zebrafish matrilins. Nearly all splice variants can be detected by RT-PCR at the embryonic stage but not in adult fish. It is not clear whether those splice variants have distinct expression patterns or unique functions during embryonic development. As specific antibodies were raised against the matrilin VWA1 domains which are shared between splice variants, it is not possible to answer this question by immunostaining. The alternative splicing of matrilins in zebrafish predominately affects the number of EGF-like domains. Even zebrafish matrilin-1, -3a and -3b variants occur that completely lack EGF-like domains. Therefore, it is very likely that the VWA domains are the principal interaction modules of matrilins and that the EGF-like domains act mainly as spacers.

A zebrafish matrilin-3b splice variant contains a sequence rich in proline and threonine/serine residues. This sequence is unique among matrilins in all species studied and is encoded by a single exon (Ko et al., 2005). Sequences rich in threonine/serine residues are often targets for a mucin-type N-acetyl-galactosamine O-glycosylation, and if such modification really takes place it may drastically influence the physical properties of this matrilin domain and probably evolves a new function. Interestingly, the matrilin-3b splice variant containing this new domain is not present in adult fish (Fig. 3-23) which may indicate a specific and important function during the development.

In both zebrafish and mammals, matrilins are more highly expressed during development than in adults with matrilin-4 showing the earliest onset. All zebrafish matrilins are present in cartilage, but their distributions are only partially overlapping (Fig. 3-25), which is again reminiscent of the zonal expression of mouse matrilins in the growth plate and the articular cartilage (Klatt et al., 2002).

4.3. Morpholino knockdowns of zebrafish matrilins

4.3.1. Matrilin knockdown phenotypes

Specificity is always crucial when using antisense oligonucleotides for gene-targeting experiments. In this dissertation, translation-inhibiting morpholinos directed against the members of the zebrafish matrilin family were employed. The amount of matrilin protein was therefore evaluated to determine whether the gene of interest has been specifically targeted. Indeed, whole mount antibody staining of matrilin-4 knockdown embryos at 24 hpf revealed that matrilin-4 was lost from the myosepta (Fig. 3-26), even though embryos did not show any apparent abnormality in body shape. The lack of an obvious phenotype in the embryos injected with low dose of matrilin-4 morpholino could be due to a dose-dependency which will be discussed later in detail. Nevertheless, knockdown embryos injected with a high dose of matrilin-4 specific morpholino showed a curled body and sometimes truncated body as well as a small head with

poorly developed eyes (Fig. 3-26, 27 and 31). These phenotypes may be due to the lack of expression of matrilin-4 in the skeleton, the myosepta and the eyes. In addition, a higher mortality was observed for matrilin-4 knockdown embryos as compared to controls, which may correlate to its early and wide expression.

The matrilin-1 knockdown phenotypes perfectly match the expression pattern. In addition to in skeletal tissues, zebrafish matrilin-1 is also expressed in the notochord. Matrilin-1 knockdown embryos present a curled body and alcian blue staining showed an abnormal skeletal phenotype. A retinal expression of matrilin-1 has been reported for human embryos (Mundlos and Zabel, 1994). In the matrilin-1 knockdown embryos the eyes were poorly developed which may indicate a role of matrilin-1 in zebrafish eye development.

As the antibody against matrilin-1 shows high cross-reactivity to matrilin-3b, it was not yet possible to demonstrate the loss of matrilin-1 protein in morpholino injected embryos. The cross-reactivity has to be eliminated prior to using this antibody in immunostaining. It was excluded that the cross-reactivity is due to the His₆ epitope, which is included in the recombinant protein to enable affinity purification (results not shown). Even though the cross-activity could be reduced by preincubation of matrilin-1 antibody with matrilin-3b protein, the optimal condition for immunostaining application still has to be determined.

The matrilin-3a knockdown showed serious defects in skeletal development in agreement with the restricted expression in cartilage. The embryos display a curled body axis and small heads. However, a more detailed analysis has to be performed to elucidate the role of matrilin-3a in the skeletal development of zebrafish.

4.3.2. Dose dependency of morpholino knockdown effects

It is important that consistent results are obtained when a fixed morpholino dose is injected into a group of embryos. The optimal dose varies for each gene specific morpholino and must therefore be determined separately. At the time of writing this

dissertation, the optimal doses of morpholinos have not yet determined for each matrilin. Nevertheless, it could be shown that skeletal malformations occur in all matrilin knockdown embryos at all the doses used and not with control morpholinos at similar dosage. Interestingly, the severity of malformations depended on the amount of morpholino injected. At low doses, matrilin-1 knockdown embryos show a curled body shape and abnormal caudal fin, while at high doses, the body axis no longer develops (Fig. 3-28). Similarly, at low doses the expression of matrilin-4 in myoseptum disappears even though the embryos do not show any apparent abnormality. However, at a higher doses, a curled body shape along with poor eye development could be observed paralleling the absence of the expression in myoseptum (Fig. 3-26). The coexpression of matrilin-1 and -4 may explain the lack of phenotype in the eyes when low doses of matrilin-4 morpholino were injected, while at high dose, the defect in the eyes may be too serious to be compensated by matrilin-1. Such dose dependent knockdown phenotypes are consistent with observations made for *bmp7* and *chordin* (Heasman, 2002; Imai and Talbot, 2001; Nasevicius and Ekker, 2000).

4.3.3. Strength and limitations of morpholinos

The morpholinos used in these studies function through an RNase H independent mechanism by hindering translational initiation. This approach makes the morpholino targeting highly predictable and significantly reduces non-specific effects. In contrast, RNAi, which is effective and can give reproducible results in nematode and *Drosophila*, yields highly variable and controversial results in zebrafish (Li et al., 2000; Oates et al., 2000). Morpholinos have been shown to be very effective in tissue culture and in several model organisms. They are completely resistant to nucleases and also to a broad range of other degradative factors occurring in biological systems (Hudziak et al., 1996). Therefore, the use of morpholinos avoids complications which could rise from toxic degradation products and also are effective even in long-term experiments. The efficacy is related to the effective concentration of morpholinos in the organism. When transcriptional rates are very high, morpholinos may be too dilute to be effective. In a cell-free system, it has been shown that morpholinos can achieve a high efficacy at concentrations above about 10 nM, and maintain their high sequence specificity up to

10,000 nM, the highest concentration tested (Summerton and Weller, 1997). However, the effective time scheme has not been well studied. It has been reported that morpholinos are extremely potent in all cells through the first 50 hours of development (Nasevicius and Ekker, 2000). In a receptor protein-tyrosine phosphatase knockdown zebrafish, it was shown that the lamination of the retina starts to be restored from 5 dpf (van der Sar et al., 2002).

The temporal expression of zebrafish matrilins was characterized by RT-PCR from 24 to 72 hpf. Matrilin-1, for example, gives a strong band at 72 hpf. However, in situ hybridization of 56 hpf embryos showed staining of matrilin-1 in pectoral fins (B. Kobbe, pers. communication). Therefore, it is possible that a weak matrilin-1 expression starts earlier than 72 hpf. In contrast matrilin-4 is strongly expressed already at 24 hpf. The early expression of matrilins, at stages when only a limited number of cells are present, enhances the chance for a morpholino to be effective when delivered already at the 1-cell stage. The early expression of matrilins enables the morpholinos to bind to all mRNAs and results in complete absence of protein. In addition, the turnover rate of extracellular matrix proteins is relatively slow and it is possible that matrilins cannot be restored later on. Therefore, it would be interesting to monitor also the later development and adult fish. However, the embryos with serious malformations often die before 5 dpf, indicating that matrilins play a vital and fundamental role during embryonic development of zebrafish.

4.3.4. Proper controls in morpholino experiments

The specificity is always the major concern in such gene-targeting experiments. In most publications which make use of the morpholino approach, critical controls and statistical data on phenotype frequency and survival rate are missing.

Mistargeting was defined as the fraction of unexpected phenotypes due to inhibition of a second gene and results in embryos with a composite phenotype (Ekker and Larson, 2001) and was shown to occur in 18% of fish even under rather stringent morpholino conditions (Ekker, 2000). An example is represented by the *bozozok/dharma*

morpholino, in which embryos additionally display a unwanted neural degeneration phenotype resulting in a high mortality (Nasevicius and Ekker, 2000). Such limitations lead to difficulties in phenotype interpretation and proper controls hence become critical. The probability of erroneous interpretation can be decreased by targeting one gene with two morpholinos of independent sequence and comparison of phenotypes from two independent knockdown embryos. Rescue experiments may also be performed by injecting mRNA of the gene of interest to confirm the specificity of morpholino (Amali et al., 2004; Yan et al., 2005). It must still be kept in mind that the toxicity, diffusion and penetration of mRNA and morpholino differ.

Another type of control frequently used is to inject either a nonsense or a mismatched morpholino. Of course, antibody analysis is a direct and powerful way to demonstrate whether the gene of interest has been successfully targeted. However, those controls still do not show whether a second gene is simultaneously targeted.

Often not all embryos present phenotypes and the phenotypes vary in severity. The differences in the degree of depletion may be due to the amount of protein present at the time of morpholino injection, the rate of diffusion, the localization of targeted mRNA and the rate of new transcription (Heasman, 2002). Therefore, calculation of phenotype frequency is important to correctly interpret the knockdown effect.

4.4. The difference in phenotype between knockout mice and knockdown zebrafish

Even though slight molecular changes are present in matrilin-1/-3 double knockout mice, single knockout matrilin-1, -2 and -3 mice have no obvious phenotype, possibly due to a redundancy in matrilin function in mice. The presence of highly conserved zebrafish orthologues, showing similar spatial and temporal expression, points to an important biological function of this gene family. In contrast to in mice, knockdown of each of the matrilins in zebrafish alone causes marked skeletal malformations. The reproducible results and significant difference of phenotype frequency between embryos injected with nonsense morpholinos and embryos injected with matrilin-1 morpholinos

strongly indicate that the skeletal abnormalities in the knockdown embryos are caused by matrilin depletion.

The contrary results between two different model organisms may be due to the degree of complexity in protein interaction and regulation. Even though the information on matrilin interactions is increasing, it is still not clear to what extent this role is static or dynamic *in vivo*. Extracellular matrix proteins and their interactions are even less characterized in zebrafish. It is possible that zebrafish express fewer extracellular matrix proteins and/or that the interactions between them are less complex, resulting in more pronounced phenotypes in this model organism.

5. Perspectives

Studies in zebrafish will provide a better insight into matrilin function. Morpholinos, potent antisense oligonucleotides, provide a fast, specific and less elaborate means to screen multiple genes for function. Much time and effort can be saved by investigating the function of a novel gene first in zebrafish by morpholino knockdown approach before going on to a higher model organism.

Beyond a more detailed analysis of the single knockdowns, double or triple knockdowns of zebrafish matrilins will be conducted to show a potential cooperative effect on the skeletal development. This will provide an indication of which of the possible double/triple mouse matrilin knockout should be performed first.

6. Bibliography

- Amali, A.A., C.J. Lin, Y.H. Chen, W.L. Wang, H.Y. Gong, C.Y. Lee, Y.L. Ko, J.K. Lu, G.M. Her, T.T. Chen, and J.L. Wu. 2004. Up-regulation of muscle-specific transcription factors during embryonic somitogenesis of zebrafish (*Danio rerio*) by knock-down of myostatin-1. *Dev. Dyn.* 229:847-856.
- Ameye, L., and M.F. Young. 2002. Mice deficient in small leucine-rich proteoglycans: novel *in vivo* models for osteoporosis, osteoarthritis, Ehlers-Danlos syndrome, muscular dystrophy, and corneal diseases. *Glycobiology.* 12:107R-116R.
- Anonymous. 2003. Whither RNAi? *Nat. Cell Biol.* 5:489-490.
- Aszodi, A., J.F. Bateman, E. Hirsch, M. Baranyi, E.B. Hunziker, N. Hauser, Z. Bosze, and R. Fassler. 1999. Normal skeletal development of mice lacking matrilin 1: redundant function of matrilins in cartilage? *Mol. Cell. Biol.* 19:7841-7845.
- Aszodi, A., D. Chan, E. Hunziker, J.F. Bateman, and R. Fassler. 1998. Collagen II is essential for the removal of the notochord and the formation of intervertebral discs. *J. Cell Biol.* 143:1399-1412.
- Aszodi, A., N. Hauser, D. Studer, M. Paulsson, L. Hiripi, and Z. Bosze. 1996. Cloning, sequencing and expression analysis of mouse cartilage matrix protein cDNA. *Eur. J. Biochem.* 236:970-977.
- Aszodi, A., L. Modis, A. Paldi, A. Rencendorj, I. Kiss, and Z. Bosze. 1994. The zonal expression of chicken cartilage matrix protein gene in the developing skeleton of transgenic mice. *Matrix Biol.* 14:181-190.
- Bartel, D.P. 2004. MicroRNAs: genomics, biogenesis, mechanism, and function. *Cell.* 116:281-297.
- Borochowitz, Z.U., D. Scheffer, V. Adir, N. Dagoneau, A. Munnich, and V. Cormier-Daire. 2004. Spondylo-epi-metaphyseal dysplasia (SEMD) matrilin 3 type: homozygote matrilin 3 mutation in a novel form of SEMD. *J. Med. Genet.* 41:366-372.
- Braasch, D.A., and D.R. Corey. 2002. Novel antisense and peptide nucleic acid strategies for controlling gene expression. *Biochemistry.* 41:4503-4510.
- Brachtendorf, G., A. Kuhn, U. Samulowitz, R. Knorr, E. Gustafsson, A.J. Potocnik, R. Fassler, and D. Vestweber. 2001. Early expression of endomucin on endothelium of the mouse embryo and on putative hematopoietic clusters in the dorsal aorta.

Dev. Dyn. 222:410-419.

- Brandau, O., A. Aszodi, E.B. Hunziker, P.J. Neame, D. Vestweber, and R. Fassler. 2002. Chondromodulin I is dispensable during enchondral ossification and eye development. *Mol. Cell. Biol.* 22:6627-6635.
- Briggs, M.D., and K.L. Chapman. 2002. Pseudoachondroplasia and multiple epiphyseal dysplasia: mutation review, molecular interactions, and genotype to phenotype correlations. *Hum. Mutat.* 19:465-478.
- Briggs, M.D., S.M. Hoffman, L.M. King, A.S. Olsen, H. Mohrenweiser, J.G. Leroy, G.R. Mortier, D.L. Rimoin, R.S. Lachman, E.S. Gaines, and et al. 1995. Pseudoachondroplasia and multiple epiphyseal dysplasia due to mutations in the cartilage oligomeric matrix protein gene. *Nat. Genet.* 10:330-336.
- Buckner, J.H., J.J. Wu, R.A. Reife, K. Terato, and D.R. Eyre. 2000. Autoreactivity against matrilin-1 in a patient with relapsing polychondritis. *Arthritis Rheum.* 43:939-943.
- Chapman, K.L., G.R. Mortier, K. Chapman, J. Loughlin, M.E. Grant, and M.D. Briggs. 2001. Mutations in the region encoding the von Willebrand factor A domain of matrilin-3 are associated with multiple epiphyseal dysplasia. *Nat. Genet.* 28:393-396.
- Chen, Q., D.M. Johnson, D.R. Haudenschild, M.M. Tondravi, and P.F. Goetinck. 1995. Cartilage matrix protein forms a type II collagen-independent filamentous network: analysis in primary cell cultures with a retrovirus expression system. *Mol. Biol. Cell.* 6:1743-1753.
- Chen, Q., Y. Zhang, D.M. Johnson, and P.F. Goetinck. 1999. Assembly of a novel cartilage matrix protein filamentous network: molecular basis of differential requirement of von Willebrand factor A domains. *Mol. Biol. Cell.* 10:2149-2162.
- Chen, X.D., S. Shi, T. Xu, P.G. Robey, and M.F. Young. 2002. Age-related osteoporosis in biglycan-deficient mice is related to defects in bone marrow stromal cells. *J. Bone Miner. Res.* 17:331-340.
- Chiu, Y.L., and T.M. Rana. 2002. RNAi in human cells: basic structural and functional features of small interfering RNA. *Mol. Cell.* 10:549-561.
- Coonrod, S.A., L.C. Bolling, P.W. Wright, P.E. Visconti, and J.C. Herr. 2001. A morpholino phenocopy of the mouse *mos* mutation. *Genesis.* 30:198-200.
- Corey, D.R., and J.M. Abrams. 2001. Morpholino antisense oligonucleotides: tools for investigating vertebrate development. *Genome Biol.* 2:reviews1015.

- Czarny-Ratajczak, M., J. Lohiniva, P. Rogala, K. Kozlowski, M. Perala, L. Carter, T.D. Spector, L. Kolodziej, U. Seppanen, R. Glazar, J. Krolewski, A. Latos-Bielenska, and L. Ala-Kokko. 2001. A mutation in COL9A1 causes multiple epiphyseal dysplasia: further evidence for locus heterogeneity. *Am. J. Hum. Genet.* 69:969-980.
- Dames, S.A., R.A. Kammerer, R. Wiltscheck, J. Engel, and A.T. Alexandrescu. 1998. NMR structure of a parallel homotrimeric coiled coil. *Nat. Struct. Biol.* 5:687-691.
- Danielson, K.G., H. Baribault, D.F. Holmes, H. Graham, K.E. Kadler, and R.V. Iozzo. 1997. Targeted disruption of decorin leads to abnormal collagen fibril morphology and skin fragility. *J. Cell Biol.* 136:729-743.
- Deak, F., D. Piecha, C. Bachrati, M. Paulsson, and I. Kiss. 1997. Primary structure and expression of matrilin-2, the closest relative of cartilage matrix protein within the von Willebrand factor type A-like module superfamily. *J. Biol. Chem.* 272:9268-9274.
- Deak, F., R. Wagener, I. Kiss, and M. Paulsson. 1999. The matrilins: a novel family of oligomeric extracellular matrix proteins. *Matrix Biol.* 18:55-64.
- Denli, A.M., and G.J. Hannon. 2003. RNAi: an ever-growing puzzle. *Trends Biochem. Sci.* 28:196-201.
- Dinser, R., F. Zaucke, F. Kreppel, K. Hultenby, S. Kochanek, M. Paulsson, and P. Maurer. 2002. Pseudoachondroplasia is caused through both intra- and extracellular pathogenic pathways. *J. Clin. Invest.* 110:505-513.
- Doege, K., K. Garrison, S. Coulter, and Y. Yamada. 1994. The structure of the rat aggrecan gene and preliminary characterization of its promoter. *J. Biol. Chem.* 269:29232-29240.
- Draper, B.W., P.A. Morcos, and C.B. Kimmel. 2001. Inhibition of zebrafish fgf8 pre-mRNA splicing with morpholino oligos: a quantifiable method for gene knockdown. *Genesis.* 30:154-156.
- Ekker, S.C. 2000. Morphants: a new systematic vertebrate functional genomics approach. *Yeast.* 17:302-306.
- Ekker, S.C., and J.D. Larson. 2001. Morphant technology in model developmental systems. *Genesis.* 30:89-93.
- Enobakhare, B.O., D.L. Bader, and D.A. Lee. 1996. Quantification of sulfated glycosaminoglycans in chondrocyte/Alginate cultures, by use of

- 1,9-dimethylmethylene blue. *Anal. Biochem.* 243:189-191.
- Fire, A., S. Xu, M.K. Montgomery, S.A. Kostas, S.E. Driver, and C.C. Mello. 1998. Potent and specific genetic interference by double-stranded RNA in *Caenorhabditis elegans*. *Nature.* 391:806-811.
- Fleming, A., R. Keynes, and D. Tannahill. 2004. A central role for the notochord in vertebral patterning. *Development.* 131:873-880.
- Frank, S., T. Schulthess, R. Landwehr, A. Lustig, T. Mini, P. Jenö, J. Engel, and R.A. Kammerer. 2002. Characterization of the matrilin coiled-coil domains reveals seven novel isoforms. *J. Biol. Chem.* 277:19071-19079.
- George, E., E. Georges-Labouesse, R. Patel-King, H. Rayburn, and R. Hynes. 1993. Defects in mesoderm, neural tube and vascular development in mouse embryos lacking fibronectin. *Development.* 119:1079-1091.
- Goetinck, P.F., I.A. Kiss, F. Deak, and N.S. Stürpe. 1990. Macromolecular organization of the extracellular matrix of cartilage. *Ann. N. Y. Acad. Sci.* 599:29-38.
- Haffter, P., M. Granato, M. Brand, M.C. Mullins, M. Hammerschmidt, D.A. Kane, J. Odenthal, F.J. van Eeden, Y.J. Jiang, C.P. Heisenberg, R.N. Kelsh, M. Furutani-Seiki, E. Vogelsang, D. Beuchle, U. Schach, C. Fabian, and C. Nusslein-Volhard. 1996. The identification of genes with unique and essential functions in the development of the zebrafish, *Danio rerio*. *Development.* 123:1-36.
- Hamilton, A., O. Voinnet, L. Chappell, and D. Baulcombe. 2002. Two classes of short interfering RNA in RNA silencing. *EMBO J.* 21:4671-4679.
- Hamilton, A.J., and D.C. Baulcombe. 1999. A species of small antisense RNA in posttranscriptional gene silencing in plants. *Science.* 286:950-952.
- Hammond, S.M., E. Bernstein, D. Beach, and G.J. Hannon. 2000. An RNA-directed nuclease mediates post-transcriptional gene silencing in *Drosophila* cells. *Nature.* 404:293-296.
- Handford, P.A., M. Mayhew, M. Baron, P.R. Winship, I.D. Campbell, and G.G. Brownlee. 1991. Key residues involved in calcium-binding motifs in EGF-like domains. *Nature.* 351:164-167.
- Hannon, G.J. 2002. RNA interference. *Nature.* 418:244-251.
- Hansson, A.S., D. Heinegard, and R. Holmdahl. 1999. A new animal model for relapsing chondritis, induced by cartilage matrix protein (matrilin-1). *J. Clin.*

Invest. 104:589-598.

- Hansson, A.S., D. Heinegard, J.C. Piette, H. Burkhardt, and R. Holmdahl. 2001. The occurrence of autoantibodies to matrilin 1 reflects a tissue-specific response to cartilage of the respiratory tract in patients with relapsing polychondritis. *Arthritis Rheum.* 44:2402-2412.
- Hansson, A.S., and R. Holmdahl. 2002. Cartilage-specific autoimmunity in animal models and clinical aspects in patients - focus on relapsing polychondritis. *Arthritis Res.* 4:296-301.
- Hauser, N., and M. Paulsson. 1994. Native cartilage matrix protein (CMP). A compact trimer of subunits assembled via a coiled-coil alpha-helix. *J. Biol. Chem.* 269:25747-25753.
- Hauser, N., M. Paulsson, D. Heinegard, and M. Morgelin. 1996. Interaction of cartilage matrix protein with aggrecan. Increased covalent cross-linking with tissue maturation. *J. Biol. Chem.* 271:32247-32252.
- Heasman, J. 2002. Morpholino oligos: making sense of antisense? *Dev. Biol.* 243:209-214.
- Heasman, J., M. Kofron, and C. Wylie. 2000. Beta-catenin signaling activity dissected in the early *Xenopus* embryo: a novel antisense approach. *Dev. Biol.* 222:124-134.
- Howard, E.W., L.A. Newman, D.W. Oleksyn, R.C. Angerer, and L.M. Angerer. 2001. SpKrl: a direct target of beta-catenin regulation required for endoderm differentiation in sea urchin embryos. *Development.* 128:365-375.
- Huang, X., D.E. Birk, and P.F. Goetinck. 1999. Mice lacking matrilin-1 (cartilage matrix protein) have alterations in type II collagen fibrillogenesis and fibril organization. *Dev. Dyn.* 216:434-441.
- Hudziak, R.M., E. Barofsky, D.F. Barofsky, D.L. Weller, S.B. Huang, and D.D. Weller. 1996. Resistance of morpholino phosphorodiamidate oligomers to enzymatic degradation. *Antisense Nucleic Acid Drug Dev.* 6:267-272.
- Hynes, R.O., and K.M. Yamada. 1982. Fibronectins: multifunctional modular glycoproteins. *J. Cell. Biol.* 95:369-377.
- Imai, Y., and W.S. Talbot. 2001. Morpholino phenocopies of the *bmp2b/swirl* and *bmp7/snailhouse* mutations. *Genesis.* 30:160-163.
- Iozzo, R.V. 1999. The biology of the small leucine-rich proteoglycans. *Functional*

network of interactive proteins. *J. Biol. Chem.* 274:18843-18846.

- Jackson, G.C., F.S. Barker, E. Jakkula, M. Czarny-Ratajczak, O. Makitie, W.G. Cole, M.J. Wright, S.F. Smithson, M. Suri, P. Rogala, G.R. Mortier, C. Baldock, A. Wallace, R. Elles, L. Ala-Kokko, and M.D. Briggs. 2004. Missense mutations in the beta strands of the single A-domain of matrilin-3 result in multiple epiphyseal dysplasia. *J. Med. Genet.* 41:52-59.
- Karcagi, I., T. Rauch, L. Hiripi, O. Rentsendorj, A. Nagy, Z. Bosze, and I. Kiss. 2004. Functional analysis of the regulatory regions of the matrilin-1 gene in transgenic mice reveals modular arrangement of tissue-specific control elements. *Matrix Biol.* 22:605-618.
- Kimmel, C.B., W.W. Ballard, S.R. Kimmel, B. Ullmann, and T.F. Schilling. 1995. Stages of embryonic development of the zebrafish. *Dev. Dyn.* 203:253-310.
- Klatt, A.R., D.P. Nitsche, B. Kobbe, M. Macht, M. Paulsson, and R. Wagener. 2001. Molecular structure, processing, and tissue distribution of matrilin-4. *J. Biol. Chem.* 276:17267-17275.
- Klatt, A.R., D.P. Nitsche, B. Kobbe, M. Morgelin, M. Paulsson, and R. Wagener. 2000. Molecular structure and tissue distribution of matrilin-3, a filament-forming extracellular matrix protein expressed during skeletal development. *J. Biol. Chem.* 275:3999-4006.
- Klatt, A.R., M. Paulsson, and R. Wagener. 2002. Expression of matrilins during maturation of mouse skeletal tissues. *Matrix Biol.* 21:289-296.
- Kleemann-Fischer, D., G.R. Kleemann, D. Engel, I. Yates, John R., J.-J. Wu, and D.R. Eyre. 2001. Molecular Properties of Matrilin-3 Isolated from Human Growth Cartilage. *Arch. Biochem. Biophys.* 387:209-215.
- Ko, Y., B. Kobbe, C. Nicolae, N. Miosge, M. Paulsson, R. Wagener, and A. Aszodi. 2004. Matrilin-3 is dispensable for mouse skeletal growth and development. *Mol. Cell. Biol.* 24:1691-1699.
- Ko, Y.P., B. Kobbe, M. Paulsson, and R. Wagener. 2005. Zebrafish (*Danio rerio*) matrilins: shared and divergent characteristics with their mammalian counterparts. *Biochem. J.* 386:367-379.
- Kobe, B., and J. Deisenhofer. 1994. The leucine-rich repeat: a versatile binding motif. *Trends Biochem. Sci.* 19:415-421.
- Kohfeldt, E., P. Maurer, C. Vannahme, and R. Timpl. 1997. Properties of the extracellular calcium binding module of the proteoglycan testican. *FEBS Lett.*

414:557-561.

- Kos, R., M.V. Reedy, R.L. Johnson, and C.A. Erickson. 2001. The winged-helix transcription factor FoxD3 is important for establishing the neural crest lineage and repressing melanogenesis in avian embryos. *Development*. 128:1467-1479.
- Laemmli, U.K. 1970. Cleavage of structural proteins during the assembly of the head of bacteriophage T4. *Nature*. 227:680-685.
- Leitinger, B. 2003. Molecular analysis of collagen binding by the human discoidin domain receptors, DDR1 and DDR2. Identification of collagen binding sites in DDR2. *J. Biol. Chem.* 278:16761-16769.
- Leitinger, B., A. Steplewski, and A. Fertala. 2004. The D2 period of collagen II contains a specific binding site for the human discoidin domain receptor, DDR2. *J. Mol. Biol.* 344:993-1003.
- Li, Y.X., M.J. Farrell, R. Liu, N. Mohanty, and M.L. Kirby. 2000. Double-stranded RNA injection produces null phenotypes in zebrafish. *Dev. Biol.* 217:394-405.
- Lupas, A., M. Van Dyke, and J. Stock. 1991. Predicting coiled coils from protein sequences. *Science*. 252:1162-1164.
- Mabuchi, A., N. Haga, K. Maeda, E. Nakashima, N. Manabe, H. Hiraoka, H. Kitoh, R. Kosaki, G. Nishimura, H. Ohashi, and S. Ikegawa. 2004. Novel and recurrent mutations clustered in the von Willebrand factor A domain of MATN3 in multiple epiphyseal dysplasia. *Hum. Mutat.* 24:439-440.
- Makihira, S., W. Yan, S. Ohno, T. Kawamoto, K. Fujimoto, A. Okimura, E. Yoshida, M. Noshiro, T. Hamada, and Y. Kato. 1999. Enhancement of cell adhesion and spreading by a cartilage-specific noncollagenous protein, cartilage matrix protein (CMP/Matrilin-1), via integrin alpha1beta1. *J. Biol. Chem.* 274:11417-11423.
- Malby, S., R. Pickering, S. Saha, R. Smallridge, S. Linse, and A.K. Downing. 2001. The first epidermal growth factor-like domain of the low-density lipoprotein receptor contains a noncanonical calcium binding site. *Biochemistry*. 40:2555-2563.
- Mann, H.H., S. Ozbek, J. Engel, M. Paulsson, and R. Wagener. 2004. Interactions between the cartilage oligomeric matrix protein and matrilins. Implications for matrix assembly and the pathogenesis of chondrodysplasias. *J. Biol. Chem.* 279:25294-25298.
- Marchler-Bauer, A., J.B. Anderson, P.F. Cherukuri, C. DeWeese-Scott, L.Y. Geer, M. Gwadz, S. He, D.I. Hurwitz, J.D. Jackson, Z. Ke, C.J. Lanczycki, C.A. Liebert, C. Liu, F. Lu, G.H. Marchler, M. Mullokandov, B.A. Shoemaker, V. Simonyan,

- J.S. Song, P.A. Thiessen, R.A. Yamashita, J.J. Yin, D. Zhang, and S.H. Bryant. 2005. CDD: a Conserved Domain Database for protein classification. *Nucleic Acids Res.* 33 Database Issue:D192-196.
- Mates, L., C. Nicolae, M. Morgelin, F. Deak, I. Kiss, and A. Aszodi. 2004. Mice lacking the extracellular matrix adaptor protein matrilin-2 develop without obvious abnormalities. *Matrix Biol.* 23:195-204.
- Morcos, P.A. 2001. Achieving efficient delivery of morpholino oligos in cultured cells. *Genesis.* 30:94-102.
- Morton, L.F., A.R. Peachey, L.S. Zijenah, A.H. Goodall, M.J. Humphries, and M.J. Barnes. 1994. Conformation-dependent platelet adhesion to collagen involving integrin alpha 2 beta 1-mediated and other mechanisms: multiple alpha 2 beta 1-recognition sites in collagen type I. *Biochem. J.* 299 (Pt 3):791-797.
- Mostert, A.K., P.F. Dijkstra, B.R. Jansen, J.R. van Horn, B. de Graaf, P. Heutink, and D. Lindhout. 2003. Familial multiple epiphyseal dysplasia due to a matrilin-3 mutation: further delineation of the phenotype including 40 years follow-up. *Am. J. Med. Genet. A.* 120:490-497.
- Mundlos, S., and B. Zabel. 1994. Developmental expression of human cartilage matrix protein. *Dev. Dyn.* 199:241-252.
- Muragaki, Y., E.C. Mariman, S.E. van Beersum, M. Perala, J.B. van Mourik, M.L. Warman, B.R. Olsen, and B.C. Hamel. 1996. A mutation in the gene encoding the alpha 2 chain of the fibril-associated collagen IX, COL9A2, causes multiple epiphyseal dysplasia (EDM2). *Nat. Genet.* 12:103-105.
- Muratoglu, S., C. Bachrati, M. Malpeli, P. Szabo, M. Neri, B. Dozin, F. Deak, R. Cancedda, and I. Kiss. 1995. Expression of the cartilage matrix protein gene at different chondrocyte developmental stages. *Eur. J. Cell Biol.* 68:411-418.
- Myllyharju, J., and K.I. Kivirikko. 2001. Collagens and collagen-related diseases. *Ann. Med.* 33:7-21.
- Myllyharju, J., and K.I. Kivirikko. 2004. Collagens, modifying enzymes and their mutations in humans, flies and worms. *Trends Genet.* 20:33-43.
- Nasevicius, A., and S.C. Ekker. 2000. Effective targeted gene 'knockdown' in zebrafish. *Nat. Genet.* 26:216-220.
- Oates, A.C., A.E. Bruce, and R.K. Ho. 2000. Too much interference: injection of double-stranded RNA has nonspecific effects in the zebrafish embryo. *Dev. Biol.* 224:20-28.

- Ohno, S., K. Murakami, K. Tanimoto, H. Sugiyama, S. Makihira, T. Shibata, K. Yoneno, Y. Kato, and K. Tanne. 2003. Immunohistochemical study of matrilin-1 in arthritic articular cartilage of the mandibular condyle. *J. Oral Pathol. Med.* 32:237-242.
- Okimura, A., Y. Okada, S. Makihira, H. Pan, L. Yu, K. Tanne, K. Imai, H. Yamada, T. Kawamoto, M. Noshiro, W. Yan, and Y. Kato. 1997. Enhancement of cartilage matrix protein synthesis in arthritic cartilage. *Arthritis Rheum.* 40:1029-1036.
- Otten, C., Wagener, R., Paulsson, M. and Zaucke, F. (2005). Matrilin-3 mutations that cause chondrodysplasias interfere with protein trafficking while a mutation associated with hand osteoarthritis does not. *J. Med. Gene.* in press.
- Paasilta, P., J. Lohiniva, S. Annunen, J. Bonaventure, M. Le Merrer, L. Pai, and L. Ala-Kokko. 1999. COL9A3: A third locus for multiple epiphyseal dysplasia. *Am. J. Hum. Genet.* 64:1036-1044.
- Paroo, Z., and D.R. Corey. 2004. Challenges for RNAi *in vivo*. *Trends Biotechnol.* 22:390-394.
- Paulsson, M., and D. Heinegard. 1979. Matrix proteins bound to associatively prepared proteoglycans from bovine cartilage. *Biochem. J.* 183:539-545.
- Paulsson, M., and D. Heinegard. 1981. Purification and structural characterization of a cartilage matrix protein. *Biochem. J.* 197:367-375.
- Paulsson, M., and D. Heinegard. 1982. Radioimmunoassay of the 148-kilodalton cartilage protein. Distribution of the protein among bovine tissues. *Biochem. J.* 207:207-213.
- Piecha, D., S. Muratoglu, M. Morgelin, N. Hauser, D. Studer, I. Kiss, M. Paulsson, and F. Deak. 1999. Matrilin-2, a large, oligomeric matrix protein, is expressed by a great variety of cells and forms fibrillar networks. *J. Biol. Chem.* 274:13353-13361.
- Piotrowski, T., T.F. Schilling, M. Brand, Y.J. Jiang, C.P. Heisenberg, D. Beuchle, H. Grandel, F.J. van Eeden, M. Furutani-Seiki, M. Granato, P. Haffter, M. Hammerschmidt, D.A. Kane, R.N. Kelsh, M.C. Mullins, J. Odenthal, R.M. Warga, and C. Nusslein-Volhard. 1996. Jaw and branchial arch mutants in zebrafish II: anterior arches and cartilage differentiation. *Development.* 123:345-356.
- Posey, K.L., E. Hayes, R. Haynes, and J.T. Hecht. 2004. Role of TSP-5/COMP in pseudoachondroplasia. *Int. J. Biochem. Cell Biol.* 36:1005-1012.
- Rao, Z., P. Handford, M. Mayhew, V. Knott, G.G. Brownlee, and D. Stuart. 1995. The

structure of a Ca(2+)-binding epidermal growth factor-like domain: its role in protein-protein interactions. *Cell*. 82:131-141.

Reed, C.C., and R.V. Iozzo. 2002. The role of decorin in collagen fibrillogenesis and skin homeostasis. *Glycoconj. J.* 19:249-255.

Rittenhouse, E., L.C. Dunn, J. Cookingham, C. Calo, M. Spiegelman, G.B. Doohar, and D. Bennett. 1978. Cartilage matrix deficiency (cmd): a new autosomal recessive lethal mutation in the mouse. *J. Embryol. Exp. Morphol.* 43:71-84.

Rucklidge, G.J., G. Milne, and S.P. Robins. 1996. Collagen type X: a component of the surface of normal human, pig, and rat articular cartilage. *Biochem. Biophys. Res. Commun.* 224:297-302.

Saxne, T., and D. Heinegard. 1989. Involvement of nonarticular cartilage, as demonstrated by release of a cartilage-specific protein, in rheumatoid arthritis. *Arthritis Rheum.* 32:1080-1086.

Schilling, T., T. Piotrowski, H. Grandel, M. Brand, C. Heisenberg, Y. Jiang, D. Beuchle, M. Hammerschmidt, D. Kane, M. Mullins, F. van Eeden, R. Kelsh, M. Furutani-Seiki, M. Granato, P. Haffter, J. Odenthal, R. Warga, T. Trowe, and C. Nusslein-Volhard. 1996. Jaw and branchial arch mutants in zebrafish I: branchial arches. *Development.* 123:329-344.

Schwarz, D.S., G. Hutvagner, B. Haley, and P.D. Zamore. 2002. Evidence that siRNAs function as guides, not primers, in the *Drosophila* and human RNAi pathways. *Mol. Cell.* 10:537-548.

Segat, D., C. Frie, P.D. Nitsche, A.R. Klatt, D. Piecha, E. Korpos, F. Deak, R. Wagener, M. Paulsson, and N. Smyth. 2000. Expression of matrilin-1, -2 and -3 in developing mouse limbs and heart. *Matrix Biol.* 19:649-655.

Shin, J.T., and M.C. Fishman. 2002. From zebrafish to human: Modular medical models. *Annu. Rev. Genomics Hum. Genet.* 3:311-340.

Smyth, N., U. Odenthal, B. Merkl, and M. Paulsson. 2000. Eukaryotic expression and purification of recombinant extracellular matrix proteins carrying the Strep II tag. *Methods Mol. Biol.* 139:49-57.

Staatz, W.D., K.F. Fok, M.M. Zutter, S.P. Adams, B.A. Rodriguez, and S.A. Santoro. 1991. Identification of a tetrapeptide recognition sequence for the alpha 2 beta 1 integrin in collagen. *J. Biol. Chem.* 266:7363-7367.

Stefansson, S.E., H. Jonsson, T. Ingvarsson, I. Manolescu, H.H. Jonsson, G. Olafsdottir, E. Palsdottir, G. Stefansdottir, G. Sveinbjornsdottir, M.L. Frigge, A. Kong, J.R. Gulcher, and K. Stefansson. 2003. Genomewide scan for hand osteoarthritis: a

- novel mutation in matrilin-3. *Am. J. Hum. Genet.* 72:1448-1459.
- Summerton, J. 1999. Morpholino antisense oligomers: the case for an RNase H-independent structural type. *Biochim. Biophys. Acta.* 1489:141-158.
- Summerton, J., and D. Weller. 1997. Morpholino antisense oligomers: design, preparation, and properties. *Antisense Nucleic Acid Drug Dev.* 7:187-195.
- Svensson, L., A. Aszodi, D. Heinegard, E.B. Hunziker, F.P. Reinholt, R. Fassler, and A. Oldberg. 2002. Cartilage oligomeric matrix protein-deficient mice have normal skeletal development. *Mol. Cell. Biol.* 22:4366-4371.
- Tomsig, J.L., and C.E. Creutz. 2002. Copines: a ubiquitous family of Ca(2+)-dependent phospholipid-binding proteins. *Cell. Mol. Life Sci.* 59:1467-1477.
- van der Sar, A.M., D. Zivkovic, and J. den Hertog. 2002. Eye defects in receptor protein-tyrosine phosphatase alpha knock-down zebrafish. *Dev. Dyn.* 223:292-297.
- Vogel, W., G.D. Gish, F. Alves, and T. Pawson. 1997. The discoidin domain receptor tyrosine kinases are activated by collagen. *Mol. Cell.* 1:13-23.
- Wagener, R., B. Kobbe, and M. Paulsson. 1997. Primary structure of matrilin-3, a new member of a family of extracellular matrix proteins related to cartilage matrix protein (matrilin-1) and von Willebrand factor. *FEBS Lett.* 413:129-134.
- Wagener, R., B. Kobbe, and M. Paulsson. 1998. Matrilin-4, a new member of the matrilin family of extracellular matrix proteins. *FEBS Lett.* 436:123-127.
- Wagener, R., H.W. Ehlen, Y.P. Ko, B. Kobbe, H.H. Mann, G. Sengle, and M. Paulsson. 2005. The matrilins--adaptor proteins in the extracellular matrix. *FEBS Lett.* 579:3323-3329.
- Watanabe, H., K. Kimata, S. Line, D. Strong, L.-y. Gao, C.A. Kozak, and Y. Yamada. 1994. Mouse cartilage matrix deficiency (cmd) caused by a 7 bp deletion in the aggrecan gene. *Nat. Genet.* 7:154-157.
- Watanabe, H., K. Nakata, K. Kimata, I. Nakanishi, and Y. Yamada. 1997. Dwarfism and age-associated spinal degeneration of heterozygote cmd mice defective in aggrecan. *PNAS.* 94:6943-6947.
- Watanabe, H., and Y. Yamada. 2002. Chondrodysplasia of gene knockout mice for aggrecan and link protein. *Glycoconj. J.* 19:269-273.
- Whittaker, C.A., and R.O. Hynes. 2002. Distribution and Evolution of von

Willebrand/Integrin A Domains: Widely Dispersed Domains with Roles in Cell Adhesion and Elsewhere. *Mol. Biol. Cell.* 13:3369-3387.

- Wiberg, C., A.R. Klatt, R. Wagener, M. Paulsson, J.F. Bateman, D. Heinegard, and M. Morgelin. 2003. Complexes of matrilin-1 and biglycan or decorin connect collagen VI microfibrils to both collagen II and aggrecan. *J. Biol. Chem.* 278:37698-37704.
- Winterbottom, N., M.M. Tondravi, T.L. Harrington, F.G. Klier, B.M. Vertel, and P.F. Goetinck. 1992. Cartilage matrix protein is a component of the collagen fibril of cartilage. *Dev. Dyn.* 193:266-276.
- Wu, J.J., and D.R. Eyre. 1998. Matrilin-3 forms disulfide-linked oligomers with matrilin-1 in bovine epiphyseal cartilage. *J. Biol. Chem.* 273:17433-17438.
- Yan, Y.L., C.T. Miller, R.M. Nissen, A. Singer, D. Liu, A. Kim, B. Draper, J. Willoughby, P.A. Morcos, A. Amsterdam, B.C. Chung, M. Westerfield, P. Haffter, N. Hopkins, C. Kimmel, J.H. Postlethwait, and R. Nissen. 2002. A zebrafish *sox9* gene required for cartilage morphogenesis. *Development.* 129:5065-5079.
- Yan, Y.-L., J. Willoughby, D. Liu, J.G. Crump, C. Wilson, C.T. Miller, A. Singer, C. Kimmel, M. Westerfield, and J.H. Postlethwait. 2005. A pair of Sox: distinct and overlapping functions of zebrafish *sox9* co-orthologs in craniofacial and pectoral fin development. *Development.* 132:1069-1083.
- Zamore, P.D., T. Tuschl, P.A. Sharp, and D.P. Bartel. 2000. RNAi: double-stranded RNA directs the ATP-dependent cleavage of mRNA at 21 to 23 nucleotide intervals. *Cell.* 101:25-33.

Abbreviations

BHMED	Bilateral hereditary micro-epiphyseal dysplasia
BSA	Bovine serum albumin
COMP	Cartilage oligomeric matrix protein
DAB	Diaminobenzidine
DDR	Discoidin domain receptor
DMB	Dimethylmethylene blue
dsRNA	Double-strand RNA
EBNA	Epstein–Barr nuclear antigen
ECM	Extracellular matrix
EDTA	Ethylenediaminetetraacetic acid
EGF	Epidermal growth factor
EtOH	Ethanol
GAG	Glycosaminoglycan
GAPDH	Glyseraldehyde-3-phosphate dehydrogenase
HE	Hematoxylin-eosin
HEK-293	Human embryonic kidney cell clone 293
hpf	Hour post fertilization
ihh	Indian hedgehog
kDa	Kilodalton
LRR	Leucine-rich repeat
MALDI-TOF	Matrix-assisted laser desorption ionization- time of flight

MED	Multiple epiphyseal dysplasia
MIDAS	Metal ion dependent adhesion site
mRNA	Messenger ribonucleic acid
NMR	Nuclear magnetic resonance
PBS	Phosphate buffered salts
p.c.	Post coitus
PFA	Paraformaldehyde
pNPP	4-nitrophenylphosphate disodium salt hexahydrate
Ppr	Parathyroid hormone/ parathyroid hormone-related peptide receptor
PSACH	Pseudoachondroplasia
RISC	RNA-induced silencing complex
RNAi	RNA interference
RT-PCR	Reverse-transcriptase polymerase chain reaction
siRNA	Small-interference RNA
SDS-PAGE	Sodium dodecyl sulfate polyacrylamide gel electrophoresis
SEMD	Spondylo-epi-metaphyseal dysplasia
SLRP	Small leucine-rich proteoglycan
TRAP	Tartrate-resistant alkaline phosphatase
VWA	Von Willebrand factor A

Erklärung

Hiermit erkläre ich, dass ich die vorliegende Dissertation selbstständig und ohne unzulässige Hilfe angefertigt, die benutzten Quellen und Hilfsmittel vollständig angegeben und die Stellen der Arbeit, die anderen Werken in Wortlaut oder dem Sinn nach entnommen sind, in jedem Einzelfall als Entlehnung kenntlich gemacht habe; dass die Dissertation noch keiner anderen Fakultät oder Universität vorgelegt und noch nicht veröffentlicht worden ist sowie, dass ich eine solche Veröffentlichung vor Ablauf des Promotionsverfahrens nicht vornehmen werde. Die Bestimmungen der geltenden Promotionsordnung sind mir bekannt. Die von mir vorgelegte Dissertation ist von Herrn Prof. Dr. Mats Paulsson betreut worden.

Köln, 5. Mai 2005

Ya-Ping Ko

Teilpublikationen: (This dissertation is in part based on following publications)

Ko, Y., B. Kobbe, C. Nicolae, N. Miosge, M. Paulsson, R. Wagener, and A. Aszodi. 2004. Matrilin-3 is dispensable for mouse skeletal growth and development. *Mol. Cell. Biol.* 24:1691-1699.

Ko, Y.P., B. Kobbe, M. Paulsson, and R. Wagener. 2005. Zebrafish (*Danio rerio*) matrilins: shared and divergent characteristics with their mammalian counterparts. *Biochem. J.* 386:367-379.

Wagener, R., Ehlen, H. W.A., **Ko, Y.P.**, Kobbe, B., Mann, H. H., Sengle, G., Paulsson, M. 2005. The matrilins-adaptor proteins in the extracellular matrix. *FEBS Lett.* 579:3323-3329.

Acknowledgements

First, I would like to express my earnest gratitude to Prof. Mats Paulsson for providing me with the opportunity to study in his department, for teaching me clarity of thought in scientific discussions and for giving me lots of support and encouragement.

I am also very grateful to Dr. Raimund Wagener for supervising me, for always being a ready listener, for the critical reading of my thesis, for helping me in solving any problems I encounter in life and for his support and encouragement.

I want to acknowledge Prof. Thomas Langer for tutoring, for important ideas on experimental design and for reading of my dissertation.

Further, I am deeply appreciative of the support of and collaboration with Dr. Attila Aszodi and Claudia Nicolae.

I am very much obliged to Prof. Dr. Sigrun Korsching, Dr. Alexander Reugels, Mehmet Saltürk and Aswani Kumar Kotagiri for all the information on how to set up a fish facility and to Oliver and Christina for their construction of the beautiful fish tanks.

Many thanks go to Birgit and Christian for their technical help, for answering my numerous questions and Birgit also for sharing her wonderful and interesting journey with me.

I am indebted to all the people in the lab, especially Harry, Henning, Christiane and Jan for providing a warm and friendly environment in which to study and for their patience and tolerance of my poor German.

I feel thankful to my colleagues from the graduate school for continuous encouragement and good company. Lots of thanks also go to Dr. Sebastian Granderath and Dr. Brigitte von Wilcken-Bergmann for helping me solving many problems in life.

I also wish to thank Prof. Maria Leptin just as all the professors of the graduate program for inviting me to Cologne and for their stimulating comments during my study.

In addition, I am so grateful to my wonderful friends, Chien-Fung, Chiu-Larn,

Shu-Feng, Cho-Chun, Hung and Sophie, for sending me delicious foods from Taiwan, for persistent inspiration and for good company.

Last, and most heartfelt, I would like to thank my beloved parents for their endless love and infinite support.

Lebenslauf

Persönliche Daten

Name Ya-Ping Ko
Geburtsdatum/-ort 12.07.1975, Ping-Tung, Taiwan
Staatsangehörigkeit taiwanesisch
Anschrift Bernkasteler Str. 52, 50969 Köln

Schulbildung

1981-1987 Primary school
1987-1990 Junior high school
1990-1993 Senior high school

Hochschulbildung

Sep. 1993 - Juli 1997 Bachelor of Science in Krankenpflege,
National Taiwan University, Taipeh, Taiwan
Sep. 1997 – Juni 1999 Master of Science in Physiologie,
National Taiwan University, Taipeh, Taiwan.
Thema: Die Effekte von pH_o und $[\text{K}^+]_o$ auf den
intrazellulären pH in der granulären Zellen des Kleinhirns
der Ratte.
Betreuer: Prof. Dr. Mei-Lin Wu.
Aug. 99 – Aug. 01 Wissenschaftliche Mitarbeiterin in der Arbeitsgruppe von
Dr. Steve Roffler im Institut für Biomedical Sciences,
Academia Sinica, Taipeh, Taiwan.

Doktorarbeit

Okt. 2001 -März 2002 Mitglied in der „International Graduate School in
Genetics and Functional Genomics“. Rotationsperiode in
den Arbeitsgruppen von Prof. Dr. U.I. Flügge, Prof. Dr.
M. Paulsson und Prof. Dr. S. Korsching.
Beginn: 01.04.2002 Promotion an der Mathematisch–Naturwissenschaftlichen
Fakultät der Universität zu Köln im Fach Physiologische
Chemie (biologische Richtung) am Institut für Biochemie
II der medizinischen Fakultät bei Prof. Dr. Mats Paulsson.
Thema: Analysis of matrilin function in knockout mice
and knockdown zebrafish